AN EXPERIMENTAL INVESTIGATION AND MODELLING OF BIO COMPATIBLE MATERIALUSING POWDER MIXED ELECTRO DISCHARGEMACHINE

Thesis

Submitted for the award of
Degree of Doctor of
Philosophy in Mechanical
Engineering

By

Diwaker Tiwari

Enrollment No: MUIT0120038255

Under the Supervision

Of

Dr. Ashok Kumar Srivastava

Professor

Department of Mechanical Engineering

Under the Maharishi School of Engineering & Technology
Session 2020-21 (Phase-I)

Maharishi University of Information Technology

Sitapur Road, P.O. Maharishi Vidya Mandir
Lucknow, 226013

Sept, 2024

MAHARISHI UNIVERSITY OF INFORMATION TECHNOLGY
LUCKNOW- 226013, INDIA

Date.....

SUPERVISOR'S CERTIFICATE

This is to certify that Diwaker Tiwari has completed the necessary academic turn and the swirl presented by him/her is a faithful record of bonafide original work under the guidance and supervision of **Prof. (Dr.) Ashok Kumar Srivastava**. He has worked on **"An Experimental Investigation and Modelling of Bio-Compatible Material Using Powder Mixed Electro Discharge Machine"**. Under the School of Engineering and Technology, Maharishi University of Information Technology, Lucknow. No part of this thesis has been submitted by the candidate for the award of any other degree or diploma in this or any other University around the globe.

Prof.(Dr.) Ashok Kumar Srivastava
(Supervisor)

IAHARISHI UNIVERSITY OF INFORMATION TECHNOLGY
LUCKNOW- 226013, INDIA

DECLARATION BY THE SCHOLAR

I hereby declare that the work presented in this thesis entitled **"An Experimental Investigation And Modelling Of Bio Compatible Material Using Powder Mixed Electro Discharge Machine"** in fulfillment of the requirements for the award of Degree of Doctor of Philosophy, submitted in the school of Engineering and Technology, Maharishi University of Information Technology, Lucknow is an authentic record of my own research work carried out under the supervision of **Dr. Ashok Kumar Srivastava,** Professor Department of Mechanical engineering Maharshi University Of Information Technology, Lucknow. I also declare that the work embodied in the present thesis-

i) **is my original work and has not been copied from any journal/ thesis/book; and**

ii) has not been submitted by me for any other Degree or Diploma inany University/ Institution.

Date:
Place: MUIT, Lucknow

(DiwakerTiwari)

ACKNOWLEDGEMENT

The present work will remain incomplete unless I express my feelings of gratitude towards a number of persons who delightfully co-operated with me in this work.

I am highly thankful and want to express my sincere gratitude to my respected supervisor **Prof. (Dr.) Ashok Kumar Srivastava** for his valuable guidance, keen interest, constructive counseling and critical appreciation throughout the course of dissertation.

I convey my deepest gratitude to **Prof. Bhanu Pratap Singh**, Vice Chancellor, Maharishi University of Information Technology, Lucknow for providing the necessary facilities to work. Sir, I am very thankful to your constant support, encouragement and supreme guidance.

I also express my gratitude to **Mr. Girish Chhimwal**, Deputy Registrar, Maharishi University of Information Technology, Lucknow, whose affectionate behaviour has supported me through the course of this investigation.

I also express my gratitude to **Prof. V.K Singh**, Dean Research and **Dr. Hitendra Singh** Incharge- Of research cell Maharishi University of Information Technology, Lucknow, for always extending his unconditional support and encouragement during my journey of doctoral research.

I also want to express my gratitude to **faculty and workshop staff of Hindustan College of Science and Technology** for his unconditional support for experimental work.

Lastly but not least, I acknowledge my indebtedness to my parents and other family members for their constant cooperation, their patience and forbearance.

Date: (Diwaker Tiwari)

Abstract

This study examines how various process parameters affect the machining properties of a bio-compatible Ti-6Al-4V alloy using PMEDM with silicon carbide (SiC) powder. The parameters investigated include peak current, pulse on/off time, powder concentration, and voltage gap. The study analyzed their effects on material removal rate (MRR), tool wear rate (TWR), surface roughness (SR), and surface morphology. A central composite design was used in the tests to make empirical models that use response surface methods to link the process parameters to the machining results. It is found that the Pulse current and Ton influence the material removal rate and the surface roughness significantly. The powder concentration also impacts PMEDM's machining performance. The Scanning electron microscopic images reveal the effect of powder seen in the machined components. The crater, micro cracks and machining marks can be seen in the SEM images. The surface integrity is correlated with the output parameters of surface roughness. The developed mathematical models effectively predict and optimize the machining properties of Ti-6Al-4V alloy using PMEDM with SiC powder. The relevance and importance of the parameters, as well as the impact and interaction effects of the parameters, have been determined by ANOVA analysis of the experimental results. Regression models have been created to predict the performance characteristics. The PMEDM process responses were analyzed for the simultaneous influence of many process parameters using Grey Relational Analysis (Multi-objective optimization), and the optimal set of process (input) parameters were identified. Samples (machined with the best possible settings) were analyzed for surface integrity and surface change by scanning electron microscopy. Machining using a dielectric composed of Al2O3 and SiC Powder showed considerable improvements in performance parameters during the experiments. The powder substance (combined with dielectric) and its concentration determine the enhancement of the properties.

Keywords: PMEDM; Process Parameter; RSM, Peak Current; Peak Voltage

CONTENTS

LIST OF FIGURES

List of Tables

List of Abbreviations

EDM - Electric Discharge Machine
PMEDM - Powder Electric Discharge Machine
EDMed - Electric Discharge machined
RSM - Response Surface Methodology
MRR - Material Removal Rate
TWR - Tool Wear Rate
SR - Surface Roughness
ANOVA- Analysis of Variance
GRA - Grey Relational Analysis
GRC - Grey Relational Coefficient GRG - Grey Relational Grade
SEM - Scanning Electron Microscope
EDS - Electron Dispersive Microscopy
EDAX - Element energy Dispersive X- Ray
DOF - Degree of Freedom
Seq SS - Sequential Sums of Squares
Adj SS - Adjusted Sums of Squares
Adj MS - Adjusted Mean Squares
F - F value or F ratio
P - Probability

List of Symbols

C_p	powder concentration, g/l
I_p	peak current, A
T_{on}	pulse-on time, μs
T_{off}	pulse-off time, μs
T_{mach}	machining time, s
T_{up}	tool lift time, μs
T_w	working time, μs
τ	duty cycle, %
V_g	gap voltage, V
E_i	initial voltatage for concentration N_i
E_{br}	breakdown voltage for final concentration N_i
o	Boltzmann constant
ε_1	permittivity of dielectric
ε_p	permittivity of powder particle
α	field enhancement factor for small protrusion
g_d	distance between bottom of the particle and micro-peak
h_p	height of the protrusion
d_1	spark gap without powder suspension
d_2	spark gap during PMEDM
ρ	density, g/cm^3
C	specific heat, J/kg-K
θ	Bragg angle in X-ray diffraction
β	integral breadth of the peak, rad
κ	constant (0.9)
λ	wave length of the X-ray radiation (0.15418 nm)
W_b	weight of workpiece before machining, g
W_a	weight of workpiece after machining, g
t	time, s
R_a	center line average surface roughness, μm
D_h	diameter of machined hole, mm
D_t	diameter of tool, mm
L	average crystallite size, Å
l	sampling length, mm
e	strain
C	specific heat, J/kg-K

T	temperature, K
T_0	initial or room temperature, K
R_w	fraction of heat transferred to workpiece, %
R	radius of crater, μm
h	convective heat transfer coefficient, W/m^2-K
C_v	crater volume, mm^3
d	crater depth, μm

Chapter 1

Introduction

1.1 Introduction

In the past several years, the usage of bio-compatible materials in the medical sector has grown significantly. Due to their outstanding biocompatibility, high strength, and resistance to corrosion, bio-compatible materials like titanium alloys have gained popularity. These materials are employed in a variety of applications, such as surgical equipment, dental implants, and implantable medical devices. However, because of their great strength and poor heat conductivity, these materials are difficult to machine. New machining methods are being created as a result to address these issues.

A technique called the Powder Mixed Electro Discharge Machine (PMEDM) has attracted a lot of attention lately. The hybrid machining process known as powder metal electrical discharge machining (PMEDM) is based on electro discharge machining (EDM) and powder metallurgy. The process asks for mixing conductive powder with the dielectric fluid used in electro-diathermic melting. The powder is added into the gap that is created during the machining process between the electrode and the workpiece, where it acts as a heat conductor and improves the efficiency of the machining operation.

The goal of this study is to find out if PMEDM can be used to make parts out of safe materials like titanium metals. The study looks at how different process factors, such as current, pulse on time, powder concentration, and electrode material, affect the ability to machine and surface features of the parts that are machined.

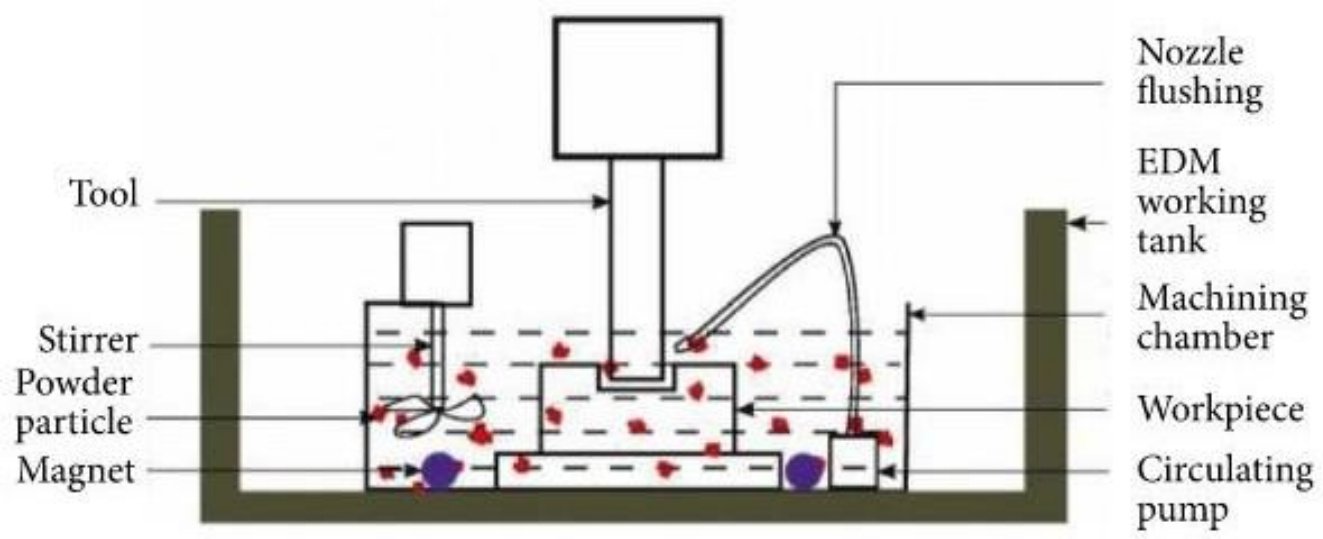

Fig 1.1- PMEDM Setup

1.2 Titanium Alloy Ti-6Al-4V

Alloy titanium One of the most popular and well-known titanium alloys is Ti-6Al-4V. It is also referred to as Grade 5 titanium and contains 6% aluminium, 4% vanadium, and 90% titanium. Due to its remarkable mix of qualities, which makes it appropriate for a wide range of applications, this alloy is widely employed in several industries.

The following are some of the essential features of titanium alloy Ti-6Al-4V:

High Strength: Ti-6Al-4V is known for its excellent strength-to-weight ratio, making it stronger than many steels while being significantly lighter.

Corrosion Resistance: Titanium alloys, including Ti-6Al-4V, possess excellent corrosion resistance, especially in environments like seawater and many chemical environments.

High Temperature Stability: Ti-6Al-4V retains its strength and stability at elevated temperatures, making it suitable for high-temperature applications.

Low Density: Titanium alloys have a low density, approximately half that of steel, making them ideal for weight-sensitive applications.

Biocompatibility: Ti-6Al-4V is biocompatible, meaning it is compatible with human tissues and is commonly used in medical implants and surgical instruments.

Good Fatigue Resistance: The alloy exhibits good fatigue resistance, making it suitable for applications subjected to cyclic loading.

Low Modulus of Elasticity: Ti-6Al-4V has a lower modulus of elasticity compared to other metals like steel, which can be advantageous in certain applications.

Due to its unique combination of properties, Ti-6Al-4V finds applications in various industries, including aerospace, medical, automotive, marine, and sporting goods. Some common applications include aircraft components, gas turbine engine parts, orthopedic implants, bicycle frames, and marine components.

The fourth most expensive structural metal is titanium, which is also the ninth most common element in the crust of the planet [1]. William Gregor, a Britisher, made the discovery of the metal in 1791.

The scientist discovered a mysterious chemical in the mineral menachanite, which he called menachite. German scientist Martin H. Klaproth, who discovered the same element in the mineral rutile and was inspired by the moniker of the Titans—the mighty Greek Rulers—gave the metal its name in 1795. American scientist Matthew A. Hunter created the first pure Titanium (99.9%) from titanium tetrachloride in 1910.

The Kroll Process was created by Luxembourgian metallurgist William Justin Kroll in the 1930s and allows for the mass manufacturing of titanium. After a protracted mellowing process, industrial production of titanium began in 1948.

Titanium is a material that is strong for how light it is and can stand up to high temperatures. The material also has great resistance to rust. Titanium is a low-density element that can be made stronger by combining it with other elements and then deforming it. Titanium metal and its alloys have great strength-to-density ratios, great corrosion and wear resistance, amazing biocompatibility, surprising mechanical abilities, and enormous stress strength. The aerospace industry uses titanium and titanium alloys extensively to create engine parts, aircraft frames, and missiles [2]. Additionally, titanium is utilized in the petrochemical and chemical process industries, maritime (offshore deep-sea) industries, hydrocarbon processing and production sectors, power generation, nuclear waste storage, desalination, ore leaching, and metal recovery applications [3]. Due to its exceptional specific strength, titanium is also utilized to produce sporting goods like golf clubs, tennis racquets, and bicycles. Because titanium and its alloys are non-toxic and have great biocompatibility, they are frequently employed in applications requiring direct contact with bone or tissue. Titanium is used in the manufacture of surgical staples, orthopedic pins and screws, orthodontic products, and ligament clips, among other things [4,5].

The element titanium has the chemical symbol Ti and the atomic weights 22 [6] and 47.9, respectively. Titanium frequently appears in either the HCP crystal structure, also known as the Alpha () phase, or the BCC crystal structure, also known as the Beta () phase (Phase at High Temperature). At 882 °C, pure titanium passes through an allotropic transition, transitioning from the Alpha phase to the Beta phase. Up to its melting point, which is over 882 °C, titanium's Beta () phase remains stable. By introducing particular components, the temperature of transition may be recovered. For instance, stabilizers such as oxygen, nitrogen, and aluminum boost the temperature of transformation, whereas stabilizers such as molybdenum, niobium, and vanadium reduce the temperature of transformation. Because they seldom affect the temperature of transition, silicon, tin, and zirconium are regarded as neutral elements [7]. At high temperatures (up to 550°C), aluminium is used as a reinforcing substance. There are numerous distinct types of commercially available pure titanium grades where oxygen acts as a strengthening agent [8,9]. Figure 1.2 shows how temperature and phase affect titanium alloy.

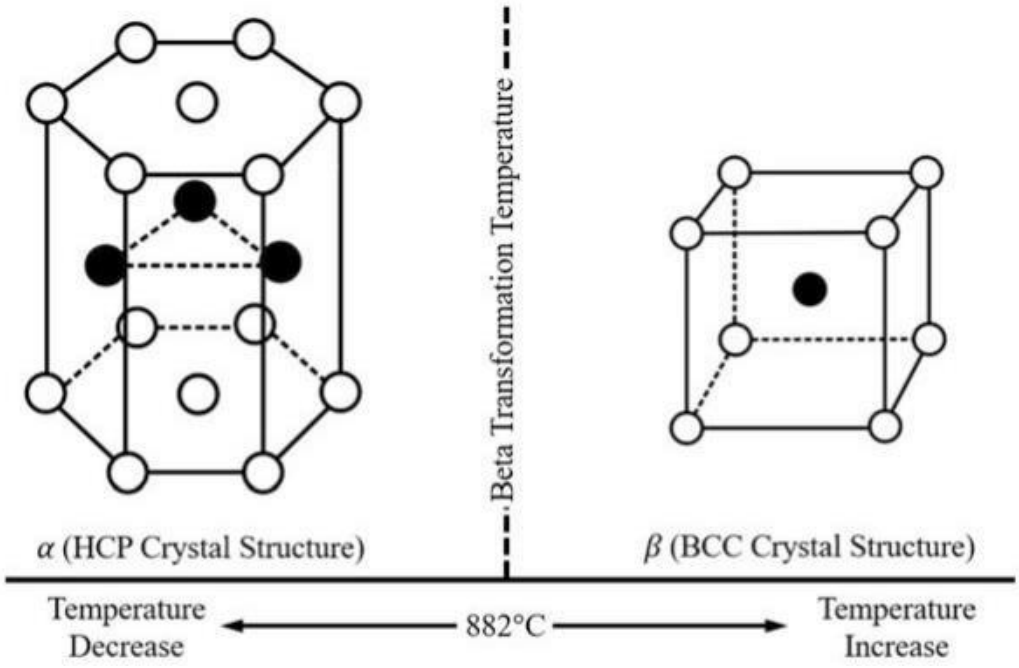

FIGURE 1.2 Two allotropic forms of titanium

1.3 Machinability of Titanium and its Alloys

Machinability is a measure of how easily a material can be machined efficiently and effectively. It is an important consideration in material selection for various applications, as it impacts the ease of manufacturing and the cost of producing finished parts. Machinability is influenced by various factors, including cutting forces, power consumption, cutting temperature, chip size, and surface integrity.[12]

Titanium and its alloys are known to have relatively low machinability compared to other metals like steel or aluminum. Several factors contribute to the challenges of machining titanium and its alloys.

Low Thermal Conductivity: Titanium and its alloys have low thermal conductivity, which means that the heat generated during machining is not dissipated quickly. This leads to heat concentration at the cutting edge and face of the tool, resulting in tool failure and increased wear.

Chemical Reactivity: Titanium readily reacts with gases like hydrogen, nitrogen, and oxygen, forming hydrides, nitrides, and oxides, respectively. These reactions can reduce the fatigue strength and cause embrittlement of the alloy.

Chemical Affinity: At temperatures above 500°C, titanium and its alloys have a strong chemical affinity with most materials, leading to the welding of chips with the tool and resulting in diffusion-dissolution wear.

Low Elastic Modulus: Titanium alloys have a low elastic modulus, which can cause deflection, chatter, and tolerance issues during machining. The low elastic modulus, combined with the formation of built-up edge on the tool wear-land, increases thrust force and deflection of slender workpieces.

High Forces for Plastic Deformation: Titanium alloys have high strength even at elevated temperatures, requiring higher forces for plastic deformation. This increased force affects tool life negatively.

Dynamic Shear Strength: Titanium alloys have great dynamic shear strength, leading to abrasive cutting edges that notch the tool and increase tool wear.

1.4 Application of Titanium Alloys

Titanium alloys find numerous applications across various industries due to their exceptional properties. Some of the typical applications of various grades of titanium alloys are as follows:

- **Ti Grade 1 (Unalloyed Titanium):**

  Medical Implants: Titanium Grade 1, with its good weldability, high ductility, and formability, is commonly used for medical implants like joint replacements, bone plates, and dental implants.
- **Ti-5Al-2.5Sn (Annealed condition):**

  Cryogenic and Aerospace Applications: This alloy with good ductility and toughness is widely used in aerospace components, aircraft structures, and cryogenic storage tanks.
- **Ti-8Al-1Mo-1V:**

  Fan Blades: Ti-8Al-1Mo-1V, known for its high weldability and strength, is used in the manufacturing of fan blades.
- **Ti-6Al-2Sn-4Zr-2Mo:**

  Flat Rolling and Forging: This titanium alloy offers high strength, creep resistance, and good temperature stability, making it suitable for flat rolling and forging applications.
- **Ti-2.25Al-11Sn-5Zr-2Mo:**

  Jet Engine Blades, Bulkhead Forging: This alloy is known for its high strength and creep resistance, making it ideal for applications in jet engine blades and bulkhead forging.
- **Ti-5.8Al-4Sn-3.5Zr-0.7Nb-0.5Mo-0.35Si:**

  Compressor Blades: This titanium alloy exhibits very good service temperature characteristics, making it suitable for compressor blades in aircraft engines.
- **Ti-6Al-4V:**

  Aerospace Components, Prosthetic Implants: Ti-6Al-4V is one of the most widely used titanium alloys. Its average strength, temperature resistance, and good

corrosion resistance make it suitable for aerospace components, such as aircraft structural components and engine parts. It is also used in prosthetic implants.[14]

- **Ti-10V-2Fe-3Al:**

  Airframes, Landing Gear: This titanium alloy with high strength and toughness is used in airframes and landing gear components.

- **Ti-15Mo-3Al-2.7Nb-0.2Si:**

  Exhaust Systems of Commercial Aircraft: This alloy offers high oxidation resistance and creep resistance, making it suitable for exhaust systems in commercial aircraft.[15]

These applications showcase the versatility of titanium alloys in various industries, including aerospace, medical, automotive, and chemical processing, where their unique combination of properties is highly valued.

FIGURE 1.3 Titanium Alloys Ti-6Al-4V Applications

1.5 Electric Discharge Machining (EDM)

A non-traditional machining technique called electric discharge machining (EDM) employs electrical energy to remove material from a workpiece. It is frequently used to machine complex forms and challenging materials. According to the electrical discharge theory, material is removed from a workpiece by localised melting and vaporisation when regulated sparks are created between an electrode (tool) and the workpiece.[16]

The following essential elements and phases are part of the EDM process:

- **Electrode and Workpiece:** The EDM machine consists of an electrode (usually made of copper, graphite, or other conductive materials) and a workpiece (the material to be machined). The electrode is connected to the negative terminal of the power supply, while the workpiece is connected to the positive terminal.
- **Dielectric Medium:** The electrode and workpiece are immersed in a dielectric medium, which is usually a non-conductive fluid (such as deionized water or kerosene). The dielectric medium serves multiple purposes, including cooling the sparking area, flushing away debris, and preventing arcing between the electrode and workpiece.
- **Electrical Discharge:** A controlled electrical discharge is generated between the electrode and workpiece by applying a high voltage across them. This creates a spark, and intense heat is generated at the point of contact, causing the material to melt and vaporize.
- **Material Removal:** As the sparks occur repeatedly, small craters are formed on the workpiece's surface due to material removal. The sparks also create a recast layer and heat-affected zone on the machined surface.
- **Flushing and Debris Removal:** The dielectric fluid is continuously circulated and used to flush away the eroded particles and debris from the machining area.
- **Shape Replication:** The electrode and workpiece do not physically contact each other during the process. The shape of the electrode is replicated on the workpiece as material is removed, resulting in the desired shape.

EDM is widely used in industries where high precision and intricate shapes are required, such as aerospace, medical, mold and die making, and automotive. It is particularly useful for machining hard materials, complex contours, and delicate or fragile components.

However, the process is relatively slow compared to traditional machining methods and is more suitable for small-scale production or prototyping[16].

1.6 Principle of EDM Process

Electric discharge machining (EDM) is a way to carefully remove material from a workpiece by sending electrical discharges or sparks between an electrode (the tool) and the object. The EDM method is based on electric breakdown and the creation of a plasma path that can carry electricity.[17]

The EDM process is based on the following main ideas:

- **Electrical Breakdown:** To start the EDM process, a strong voltage is applied between the electrode and the material. When the voltage is turned up, the electric field between the electrode and the workpiece gets strong enough to ionise the insulating fluid (usually deionized water or oil) around the electrode and the workpiece.
- **Forming a Plasma Channel:** The ionised dielectric fluid makes a plasma channel between the electrode and the workpiece that is electrically conductive. This plasma tunnel lets the current pass, making the circuit complete.
- **Electrical Discharges:** When the electric current flows through the plasma channel, it heats up a small area of the workpiece very quickly. This heat makes the material in the item melt and evaporate, leaving behind a small hole or pit.
- **Erosion and removal of material:** The sparks from the electrical shocks wear away the material on the surface of the workpiece. The dielectric fluid carries away the degraded material, and the process keeps taking away material in the form of tiny chips or waste.
- **Non-Contact Machining:** During the EDM process, the tool and the material do not touch each other. Instead, the material is taken away by repeatedly building up and breaking down the plasma channel.
- **Controlling factors:** The EDM process can be managed by a number of factors, such as the voltage, current, pulse length (on-time), pulse interval (off-time), flushing rate, and electrode shape. These settings are changed to get the material removal rate, surface finish, and accuracy that are needed.

The EDM process is especially good for working with hard and hard-to-work-with materials, making complex and detailed shapes, and making sure the end product is very accurate. It is used a lot in fields like aerospace, automobiles, medicine, and making tools and dies.

1.7 Powder Mixed Electric Discharge Machining (PMEDM)

In a process called Powder combined Electric Discharge Machining (PMEDM), small powder particles are mixed with the electrical fluid. This makes the Electric Discharge Machining (EDM) process work better and do more. Powder granules improve the surface finish, the rate at which material is removed, and how well the machine works.[18]

For PMEDM, the dielectric fluid is mixed with the right particles, such as graphite, metal, silicon, or chromium. During the machining process, the powder particles are pushed into the space between the electrode (tool) and the workpiece while they are floating in the dielectric. During the machining process, the contact between the powder granules and the electrical discharges makes the whole process more efficient.[19]

Powder Mixed Electric Discharge Machining (PMEDM) has a number of important benefits and features, such as:

- **Improved Material Removal Rate (MRR):** The addition of powder particles in the dielectric increases the discharge energy and sparks density. This results in higher material removal rates, making PMEDM more efficient than conventional EDM for certain applications.
- **Better Surface Finish:** PMEDM often provides improved surface finish compared to conventional EDM. The fine powder particles assist in flushing away the debris and molten material, leading to a smoother surface.
- **Reduced Electrode Wear:** The presence of powder particles in the dielectric reduces the contact area between the electrode and workpiece. This reduces electrode wear and prolongs the electrode's life, resulting in longer machining tool life.
- **Enhanced Flushing Efficiency:** The powder particles in the dielectric improve the flushing of the eroded material from the inter-electrode gap, preventing clogging and ensuring stable machining conditions.

- **Increased Machining Precision:** PMEDM can achieve higher machining precision and accuracy due to better control over the spark formation and distribution of electrical discharges.
- **Versatility**: PMEDM can be used for a wide range of materials, including hard-to-machine materials like titanium alloys and superalloys.

Overall, Powder Mixed Electric Discharge Machining (PMEDM) is a promising advancement in the EDM process, offering improved performance and broader applications, especially for materials with high hardness and low machinability.

1.8 Process Variables of PMEDM

PMEDM involves several process variables that can be controlled to optimize the machining performance and achieve desired results. These variables can be broadly classified into electrical parameters, non-electrical parameters, electrode-based parameters, and powder-based parameters. Here, we will focus on electrical parameters:

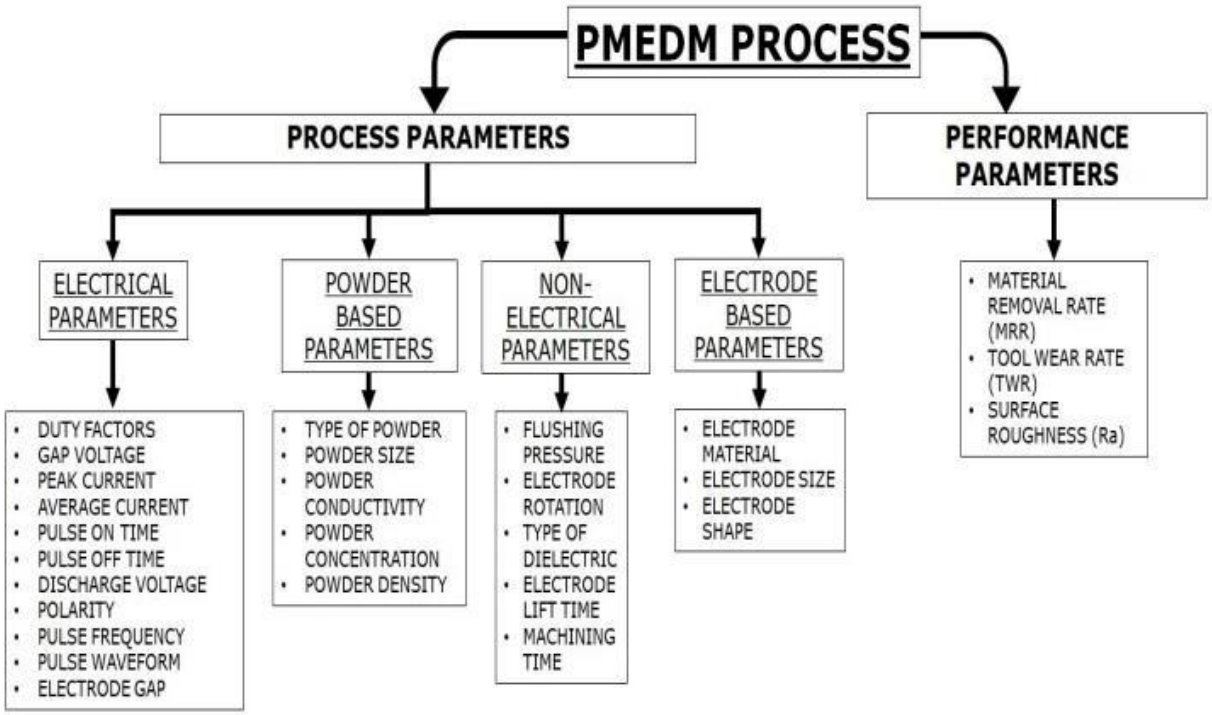

FIGURE 1.4 Parametric analysis of the PMEDM process

1.8.1 Electrical Parameters

1.8.1.1 Peak Current (Ip):

Peak current is the term used to describe the highest current level experienced during the electrical discharge machining process. It is an important parameter because it controls how much energy is given to the workpiece. While higher peak currents result in faster material removal rates, they can also worsen tool wear and surface polish. The material being cut and the required machining rate influence the choice of peak current.

1.8.1.2 Discharge Voltage (V):

During the EDM process, the voltage between the tool (the electrode) and the subject is called the discharge voltage. It's a big part of what starts and keeps the electrical spark between the electrodes going. The main things that affect the voltage setting are the breakdown voltage of the insulator and the distance between the electrodes. With wider gaps between the electrodes, you can use higher voltage settings, but the stronger electric field may cause the tool to wear out faster and make the surface harder to machine.

1.8.1.3 Pulse ON Time (TON):

The pulse ON time is the duration for which the current flows through the electrodes during one cycle of the EDM process. Dielectric ionization occurs during this period, and the amount of energy applied during TON determines the material removal rate. Longer pulse ON times results in more energy being absorbed by the workpiece, leading to deeper craters and increased material removal.

1.8.1.4 Pulse OFF Time (TOFF):

Pulse OFF time is the time during which the electrical supply is cut off, and the dielectric characteristics are restored by reionization. During TOFF, the removed molten material solidifies and is flushed out from the inter-electrode gap. The duration of TOFF should be minimized to ensure efficient machining and stable process conditions.

1.8.1.5 Duty Cycle:

The duty cycle is the ratio of the pulse ON time (TON) to the total cycle time. It represents the percentage of time the electrical discharge is active during one cycle. Higher duty cycle values indicate that more energy is being applied to the workpiece, resulting in higher material removal rates. However, excessively high duty cycles can lead to instability in the EDM process and insufficient flushing.

1.8.1.6 Polarity:

The orientation in PMEDM refers to how the tool electrode and the workpiece electrode are wired together. The tool electrode can be hooked to either the positive or negative pole of the power source. Positive polarity is when the tool is connected to the cathode (the negative pole) and the workpiece is connected to the anode (the positive pole). Positive polarity makes the subject (the anode) heat up the most, which removes a lot of material.

These electrical factors can be changed and optimized based on the specific needs of the machining process, the material being machined, and the desired surface finish and material removal rates. To make PMEDM work well and be reliable, these factors must be carefully chosen and controlled.

1.8.2 Non-electrical Parameters

In addition to the electrical parameters, Powder Mixed Electric Discharge Machining (PMEDM) is also affected by a number of non-electrical factors. Both of these factors are important for getting the machining speed and surface quality you want. Let's look at a few important non-electrical parameters:

1.8.2.1 Dielectric Fluid:

The dielectric fluid used in PMEDM serves several important functions. It acts as an electrical insulator until the voltage breakdown occurs, at which point dielectric breakdown must occur instantaneously to facilitate the electrical discharge. The dielectric fluid also plays a crucial role in flushing the inter-electrode gap and carrying away the excess heat generated during the discharges. It should have good fluidity, thermal conductivity, and dielectric strength to effectively remove debris and reduce thermal damage. Various dielectric fluids can be used, such as deionized water, kerosene, mineral oil, silicon oil, and others, each with its specific properties and advantages.

1.8.2.2 Dielectric Flushing:

Proper flushing is essential in PMEDM to remove the eroded molten material from the inter-electrode gap. Efficient flushing helps maintain stable machining conditions and improves the surface finish. Various flushing techniques can be employed, such as vacuum flushing, side flushing, and pressure through tool/workpiece flushing. The use of a servo- controlled tool head with cyclic up-down motion or vibrating tool head enhances the flushing efficiency.

1.8.2.3 Material Removal Rate (MRR):

Material removal rate is a critical parameter in PMEDM, representing the volume of material removed from the workpiece per unit time. It is influenced by the powder concentration, particle size, and electrical parameters. Higher material removal rates are desirable in certain applications, but they should be balanced with other considerations, such as surface finish and tool wear.

1.8.2.4 Surface Roughness (SR):

Surface roughness refers to the quality of the machined surface and is affected by various parameters, including the powder type, concentration, particle size, electrical parameters, and flushing efficiency. Controlling the surface roughness is essential to meet the required surface finish specifications.

1.8.2.5 Tool Wear: The wear of the electrode during PMEDM is a critical factor that affects the accuracy and precision of the machining process. Proper selection of electrode materials, tool shape, and electrical parameters can help minimize tool wear and prolong tool life.

1.8.2.6 Powder Concentration and Density:

The concentration and density of the powder particles in the dielectric fluid can significantly impact the machining performance. Optimal powder concentration ensures improved material removal rates and surface finish, but excessively high concentrations may lead to process instability and reduced flushing efficiency.

1.8.3 Electrode-Based Parameters

Electrode-based parameters in Powder Mixed Electric Discharge Machining (PMEDM) refer to the characteristics and properties of the electrodes used in the machining process. These parameters play a crucial role in determining the machining efficiency, accuracy, and surface quality. Let's delve into some important electrode-based parameters:

1.8.3.1 Electrode Material:

The choice of electrode material is critical in PMEDM as it directly influences tool wear, material removal rate, and surface finish. Commonly used electrode materials include copper, brass, tungsten, tungsten-copper alloy, carbon steel, zink-based alloy, graphite, and others. Each material offers different properties, such as electrical conductivity, thermal conductivity, and machinability, which impact the overall performance of the process.

Copper and brass electrodes are commonly used due to their good electrical and thermal conductivity, making them suitable for various applications.

Tungsten and tungsten-copper alloy electrodes are preferred when machining hard and high-temperature alloys due to their high melting point and wear resistance.

Graphite electrodes are popular for achieving high material removal rates and fine surface finishes.

1.8.3.2 Electrode Shape and Size:

The shape and size of the electrode determine the final shape and accuracy of the machined feature. Various electrode shapes, such as circular, rectangular, triangular, and square, can be used depending on the required geometry. The size of the electrode affects the spark gap and clearance between the electrode and workpiece, which, in turn, influence the machining efficiency and surface finish.

1.8.3.3 Electrode Clearance:

The electrode clearance refers to the distance between the tool electrode and the workpiece during the PMEDM process. An appropriate electrode clearance is necessary to create the desired cavity and facilitate efficient flushing of debris. The clearance should be adjusted based on the material being machined and the desired rate of material removal.

1.8.3.4 Tool Servo System:

A servo-controlled tool head can be employed in PMEDM to control the electrode movement and maintain stable machining conditions. The tool servo system helps control the gap between the electrode and workpiece, ensuring uniform machining and improved surface quality.

1.8.3.5 Electrode Wear:

Like in traditional EDM, electrode wear is a critical issue in PMEDM. Minimizing electrode wear is essential to maintain dimensional accuracy and prolong tool life. Proper selection of electrode material and tool wear compensation strategies can help mitigate electrode wear.

By optimizing the electrode-based parameters, PMEDM can achieve higher efficiency, precision, and surface quality in machining various materials, including titanium and its alloys. The selection of appropriate electrode materials, shapes, and sizes should be carefully considered based on the specific requirements of the machining operation.

1.8.4 Powder-Based Parameters

In Powder Mixed Electric Discharge Machining (PMEDM), powder-based factors refer to the qualities and traits of the powder materials added to the dielectric fluid. Adding powders to PMEDM can change the way it is machined and the quality of the surface it makes. Let's look at some important factors for powder:

1.8.4.1 Type of Powder:

Various types of powders can be added to the dielectric fluid to enhance the PMEDM process. These powders can include graphite, aluminum, silicon carbide, chromium, silicon, tungsten, alumina, boron carbide, carbon nanotubes, and more. Each powder type offers unique properties, such as thermal conductivity, electrical conductivity, hardness, and particle size distribution, which can influence the machining performance.

Graphite powder is commonly used due to its electrical conductivity and ability to reduce tool wear and improve surface finish.

Aluminum powder enhances material removal rate and reduces surface roughness by promoting energy transfer during sparking.

Silicon carbide powder improves the thermal conductivity of the dielectric fluid, leading to better flushing and reduced recast layer formation.

1.8.4.2 Powder Size and Conductivity:

The particle size of the added powder is an essential parameter that affects the machining efficiency and surface quality. Smaller powder particles can lead to a more uniform distribution in the dielectric fluid and result in improved machining characteristics. Additionally, the electrical conductivity of the powder impacts the sparking and energy transfer during machining.

Smaller powder particles can enhance flushing efficiency and reduce the recast layer thickness, resulting in better surface finish.

1.8.4.3 Powder Concentration and Density:

The concentration of the added powder in the dielectric fluid is a crucial parameter that influences the machining process. The concentration should be optimized to achieve the desired material removal rate, surface finish, and electrode wear.

An appropriate powder concentration can enhance material removal rate and surface finish while maintaining stable machining conditions.

Higher powder concentrations may lead to improved machining performance, but excessive concentrations can cause instability and arcing.

By controlling the powder-based parameters in PMEDM, manufacturers can tailor the machining process to achieve specific machining objectives for different materials. Optimization of powder type, size, concentration, and conductivity can help improve material removal rates, surface quality, and overall process efficiency.

1.9 EDM Surface Layers

During Electric Discharge Machining (EDM), the surface of the workpiece undergoes various transformations, resulting in the formation of distinct layers. These layers can significantly impact the properties and characteristics of the machined surface. The main surface layers formed during EDM are as follows:

- **Spattered EDM Surface Layer:**

  During the machining process, small molten metal droplets that are released from the workpiece and tool electrode cause splattering, which results in the formation of this layer. On the machined surface, these droplets harden, leaving a rough and irregular surface roughness. Microcracks and cavities in the spattered layer might compromise the surface's integrity.

- **Recast Layer:**

  The recast layer is a thin and hardened layer of material that forms on the surface of the workpiece during EDM. It is created as a result of the re-solidification of molten metal from the workpiece and tool electrode. The recast layer typically exhibits a different microstructure and hardness compared to the base material. It is often brittle and may contain defects, such as micro-cracks and voids, which can influence the mechanical properties of the machined surface.

- **Heat-Affected Zone (HAZ):**

  The area surrounding the recast layer that is significantly thermally influenced during EDM is known as the heat-affected zone. Despite not melting, the material in the HAZ experiences localised heating as a result of the tremendous heat produced during sparking. Without reaching its melting point, this might cause changes in the material's microstructure and hardness. The EDM settings and material qualities affect the depth and size of the HAZ.

A number of variables, such as EDM parameters (such as pulse length, current, voltage, and flushing), material properties, and the kind and state of the electrode utilised, affect the creation and attributes of these surface layers. The machined surface may experience both good and bad impacts from these layers. The recast layer can increase surface hardness and wear resistance, but it can also cause surface roughness and weaken fatigue resistance. The resulting machined component must thus have the appropriate surface quality and mechanical qualities, which requires optimizing EDM settings and utilizing the right electrode materials.

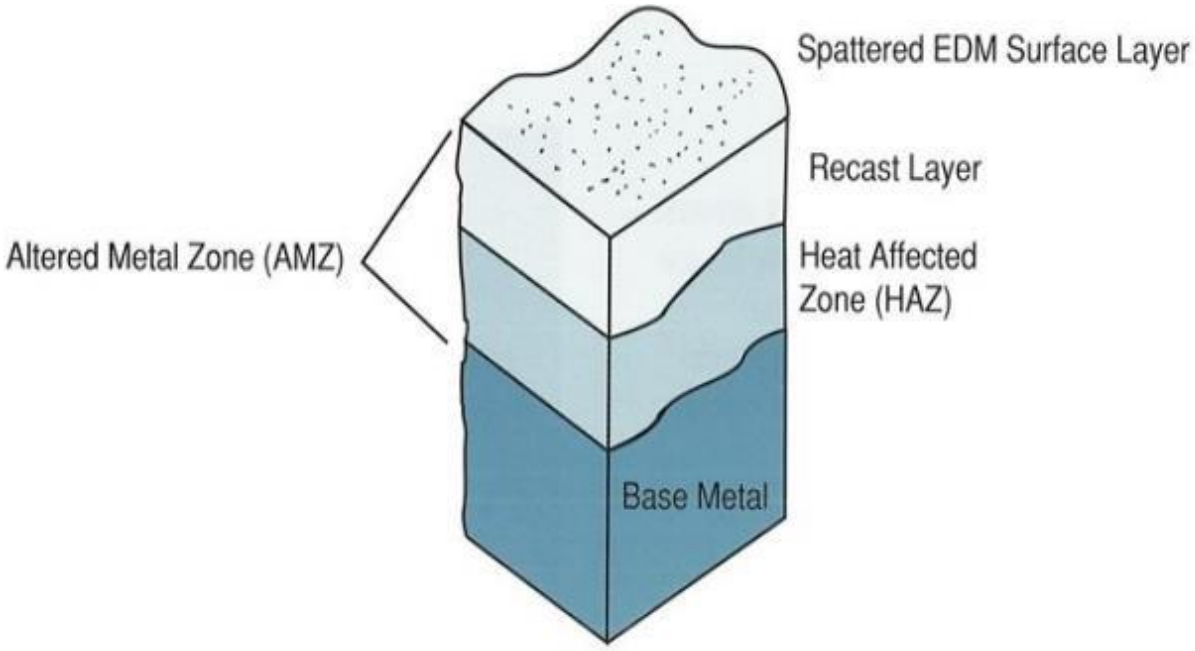

FIGURE 1.5 Layers formed on EDMed Surface

1.10. Research Objectives

The objectives of the present study are as follows:

- The following are the goals of the current study:
- To investigate the suitability of the PMEDM technique for the machining of difficult-to-cut materials.
- To determine if using deionized water, a low viscosity environmentally friendly die-electric fluid, in the EDM process is practical.

- To examine how Powder Particle Concentration and its makeup affect the efficiency of the process. To determine how Powder Mixed EDM affects Surface Integrity by analyzing the material (with an electron microscope).

The achievement of these objectives can provide valuable information on the use of PMEDM for machining bio-compatible materials and contribute to the development of new machining techniques for medical applications. Moreover, the study can provide useful data on the effect of various process parameters on the microstructure and surface morphology of the machined parts, thus improving our understanding of the machining process. Ultimately, the findings of the study can help in optimizing the machining parameters and improving the quality and efficiency of the machining process.

1.11 Research Questions

Based on the research objectives outlined in the introduction, the following research questions can be formulated:

1. How effective is the PMEDM process in machining bio-compatible materials, such as titanium alloys, compared to other machining techniques?
2. What is the influence of various process parameters, such as current, pulse on time, powder concentration, and electrode material, on the machinability and surface characteristics of the machined parts?
3. Can a mathematical model based on response surface methodology be developed to predict the material removal rate and surface roughness for different combinations of process parameters in the PMEDM process?
4. How does the concentration of the conductive powder affect the material removal rate and surface roughness of the machined parts?
5. What is the influence of different electrode materials, such as copper and graphite, on the machinability and surface characteristics of the machined parts?
6. What is the microstructure and surface morphology of the machined parts produced by the PMEDM process, and how does it compare to those produced by other machining techniques?
7. What is the mechanism of material removal in the PMEDM process, and how does it differ from other machining techniques?

Answering these research questions can provide a comprehensive understanding of the PMEDM process and its potential for machining bio-compatible materials. The findings can help in optimizing the process parameters and improving the quality and efficiency of the machining process.

1.12 Organization of the study

Chapter 1: Introduction

Chapter 2: Literature Review

Chapter 3: Methodology

Chapter 4: Results and Discussion

Chapter 5: Conclusion and Future Recommendation

Chapter 2 Literature Review

2.1 Titanium Alloy Ti-6Al-4V

Titanium alloys tender variety of applications like biomedical, space, defense and automotive sectors as they have inimitable characteristics. These may include excellent mechanical properties and tribological properties [20]. Machinability is expressed as the exertion to machine material with the specified-set of Parameters – DOC, Spindle Cutting velocity and feed rate, the same is appraised in rapports of reactive forces, surface finish, tools life and cost of machining. It is observed that Ti–6Al–4V cataracts under the class of hard – to – cut alloys and have very poor machinability when manufactured by conformist machining practices [21]. In spite of the wide range of tools accessible for conformist machining and metal cutting, there is a gap to ascertain the right tool or process by which the anticipated machining characteristics can be accomplished. Also, the diverse cutting environments like dry-cutting, flood-cooling, MQL, use of solid lubricants and HPS are available and can be used for machining of these alloys. Different graded tool materials like PVD, CVD, Carbide inserts, Ceramic etc. have been proved to have advantage in machining, which conventionally are not suitable for Dry Machining [22]. Young's Modulus is for these alloys is very low and it causes chatters and vibrations when machining is carried out. Moreover, heat concentration in the tool tip develops friction between tool and chip interface. This causes in a lower tool life and results in to poor surface integrity and finish. Cryogenic cooling of tool helps to overcome these issues and enhances the probability of proper machining of these alloys [23]. Beta (β) Titanium alloy - Ti555.3 has shown deprived machinability compared with Ti-6Al-4V alloys. At higher machining speed (90 m/mins), machining of beta alloy is much more difficult than Ti-6Al- 4V. A layer of titanium carbide (TiC) was formed on the tool surface when both alloys upon machining [24]. C. Veiga et al. [25] summarized machinability of Titanium alloy considering its properties. The parameters like temperature of cutting, formation of chips and the forces cutting as well as resisting the deformation have been considered while turning of Ti-6Al-4V. Rihoha Z. et al. [26] studied dry machining (turning) of Ti alloy Ti- 6Al-2Sn-4Zr6Mo using WC tool. They reported that due to low thermal conductivity of the alloy at higher values of cutting speed and DOC, the crater wear increases. The researches

also reported that due to stored elastic energy and low modulus of elasticity a rigid machining setup is mandatory to avoid the issues of chattering and vibrations. Alokesh Pramanik et al. [27] conducted a comprehensive research to link industrial performance (output-commercial) requirements with experimental (laboratory based) understandings emphasizing mechanism formation of chip. The researcher also reported that the cutting tools are cyclically loaded as the cutting forces varies due to formation of Sawtooth chips. Coromant S. reported that in most cases the chips generated by machining of titanium are segmental and thin [28]. The reasons for these institution of segmental chips are adiabatic shear band that is resulted by curbed shear deformation caused by straining, hardening and thermal unstiffening [29, 30] or enlargement of cracks from the outer chip surface [31, 32]. Fig. 2.1 describes the segmented chip formed during machining of Ti-6Al-4V [33]. Machado et al. [34] reported that under the action of all-pervading shearing serrated chips occurs, the mechanism is termed as ―Catastrophic Thermoplastic Shear - CTS‖. The rate of shearing occurring between the adjacent layers has value more than the work hardening rate. The CTS also occurs between the tool and formed chips.

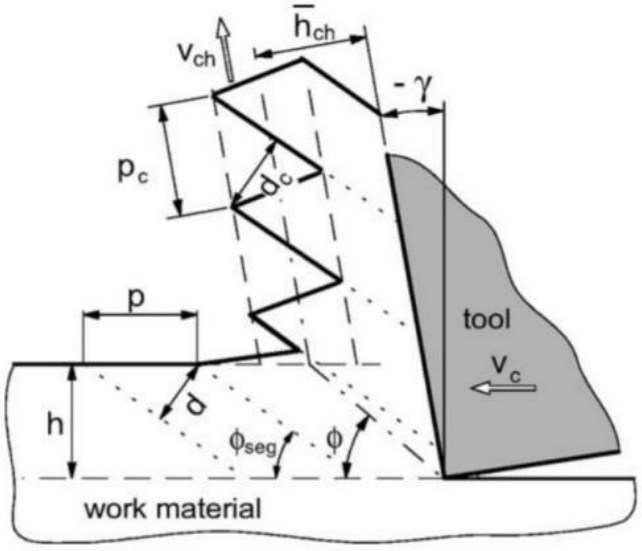

FIGURE 2.1 Segmented chip formed during machining of Ti-6Al-4V [33]

Ashwin Polishetty et al. [35] studied turning of Ti-6Al-4V (Selective lased melted) for investigating the influence of feed rate and cutting speed on the resultants surface finish and cutting forces. They reported increase in the cutting forces and deterioration in surface finish at high speed and feed rates. The SLM Ti-6Al-4V having high hardness and

brittleness demands higher cutting forces to deform and results lower surface finish. Patil Amit S et al. [36] reviewed the challenges of machining Ti-6Al-4V and reported that coated carbide tools offered maximum MRR when used with high pressure through spindle lubrication system. They also reported that use rigid clamping reduces chatters and lower DOC, maximum spindle RPM delivers better surface finish. L. Turnad Ginta et al. [37] investigated end milling of preheated Ti-6Al-4V using WC insert. The machining was done at various preheating temperature and the results revealed that preheating of the workpiece reduces the requirement of cutting forces and amplitude of accelerated vibration improving the tool life by 3.25 times. They also reported that preheating lessens the strain hardening characteristics. Fig. 2.2 graphically represents comparison of preheating temperature with tool life and cutting force.

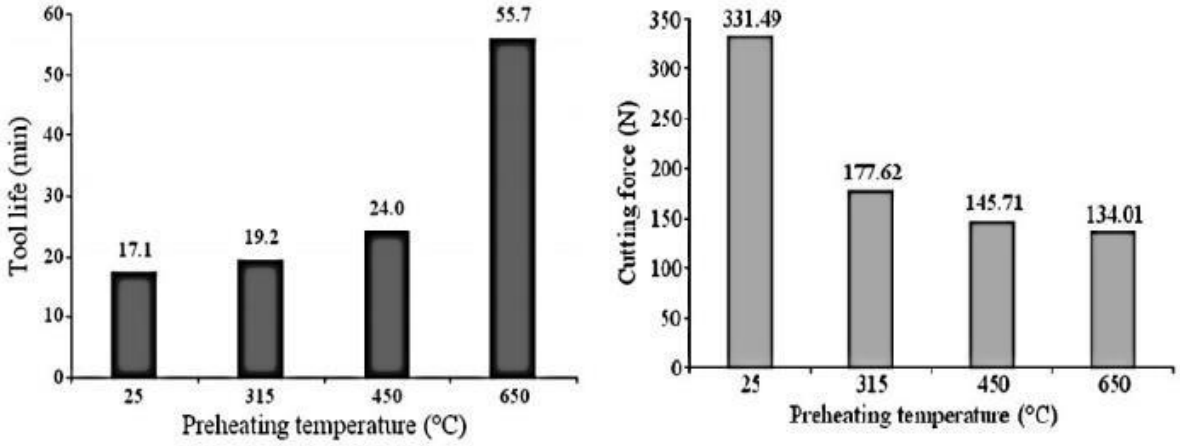

FIGURE 2.2 Comparison of Preheating Temperature with Tool Life and Cutting Force[37]

Che-Haron et al. [38] reported alteration in the surface microstructure while machining of Ti64 using 883 insert. The white layer surface microhardness found to have significant increase till a depth of 0.05mm (Fig. 2.3) because of change of microstructure and transformation of phase.

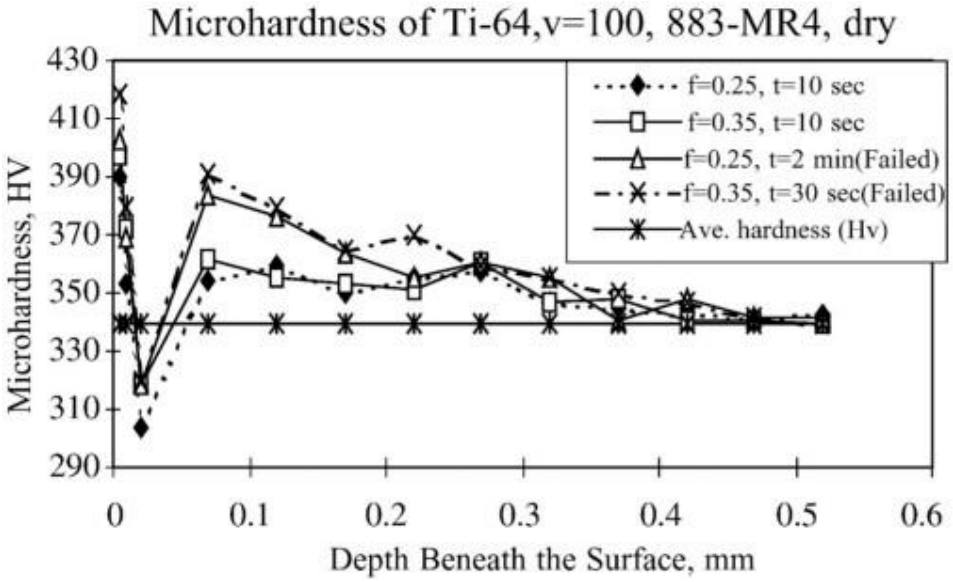

FIGURE 2.3 Subsurface microhardness – Dry machining of Ti64 [38]

Nouari et al. [39] experimented with uncoated and coated (CVD) carbide tools for dry milling of titanium alloy. They reported mechanism of delamination of coated (CVD) tool. They also reported that the arc engagement of 15% maximum delivers reasonable tool life with higher rate of material removal at higher speeds. Nabhani [40] and Nazmi [41] experimented machining of titanium alloy Ti64 with various tools – coated carbide tool, polycrystalline diamond tool and polycrystalline cubicboron nitride. It was concluded that use of polycrystalline diamond tool delivers the best figures for tool life compared to the other tool materials considered for study. A comparison of tool life for various materials is shown in Fig. 2.4

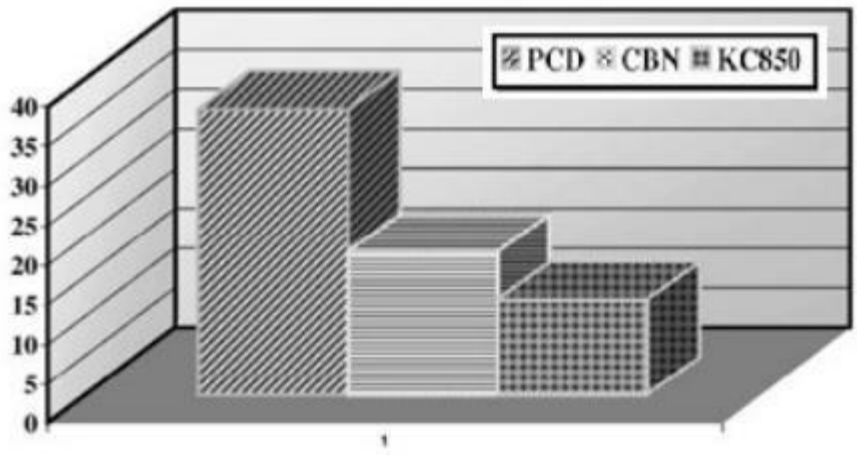

FIGURE 2.4 Tool life comparison – Machining of titanium alloy [41]

Sharif et al. [42] experimented face milling of Ti-6Al-4V using coated (PVD) Tin inserts to analyse the upshot of edge-geometry on failure characteristics of tool. They reported that under same machining conditions performance of sharp cutting edge tool is better compared to a tool having champhered edge due to unwarranted chipping of cutting edge and rake face. The comparison of cutting speed and tool life is shown in Fig. 2.5.

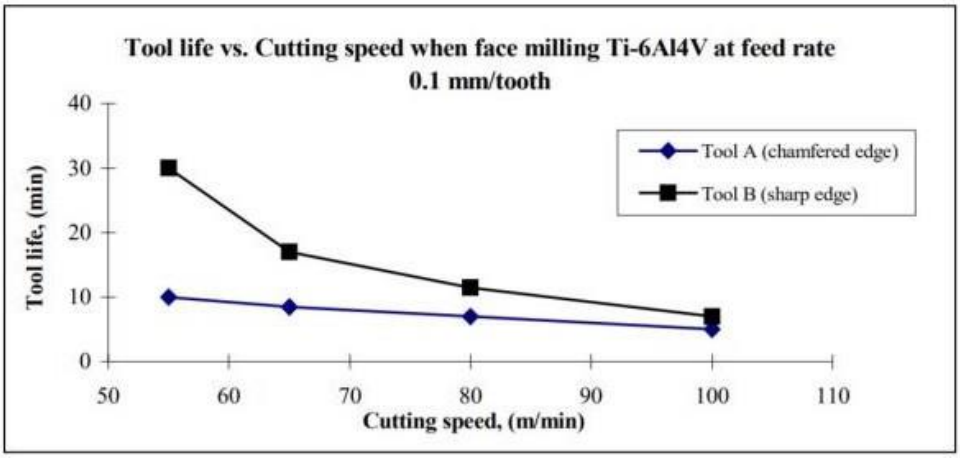

FIGURE 2.5 Comparison of Tool life - Milling with Sharp and Chamfered tool [42]

Zareena et al. [43] investigated the mechanism of tool wear using diamond (singlecrystal) tools for exactitude machining of commercial titanium alloys Ti–6Al-4V and CP–Ti. They conducted the experiments using Perfluoropolyether barrier and reported that the tool wear is most affected by high tool tip temperature, workpeice's chemical affinity and formation of builtup edge. Machado A. et al. [44] experimented turning of Inconel-901 and Ti-6Al-

4V using single point cemented carbide inserts (grade K20) with a setup of high pressure jet of cutting fluid targeting tool tip. The results showed significant reduction in diffusion wear and improved flushing of machining zone with abridged occurrence of welding between chip and tool.

2.2 Electric Discharge Machining

In late 1940s the EDM process was discovered [45]. The EDM process manufactured parts are mostly used in spacecraft, automotive and surgical industries. The process physics eliminates generation of vibrations and mechanical stresses being a non-contact process [46]. Ramasawmy H. [47] has reported that EDM can efficiently machine any material that can conduct electricity, regardless of its hardness. Thermal and Electrical conductivity and melting point of material are the factors that affects the quality of EDMed workpeice [48, 49]. Being a contactless process, the process is best used to machine materials that are very hard and thin and fragile [50 - 52]. In EDM process the material is removed by the incidence of consecutive distinct sparks. These sparks cause localized melting and evaporation of the materials from the electrodes [53, 54]. Some of the distinctive features of EDM process are – deformation free process, resultant surfaces are burr free and higher accuracy of machining 3D intricate geometries [55, 56]. Rajurkar [57, 58] detailed advancements in EDM processes like use of powder additive dielectrics, vibration assisted machining and automation of the process. F. Han et al. [59] investigated EDM process with high frequency response using a Chapter 2 - Literature Review 34 transistor-type pulse generator for increasing rate of erosion. The results of the experiments concluded that almost 24 times higher MRR was achieved using the modified pulse generator compared to RC pulse generator. R. Casanueva et al. [60] designed DC-DC series parallel resonance converter to generate high frequency impulse for EDM operation. They reported that the EDMing characteristics were modified due to the effective resistance and capacitance of an electric circuit. M. Ghoreishi et al. [61] investigated influence excitation of pre-ignition spark voltage on MRR, TWR and Surface finish. The results of the experiments showed clearly that the pulse excitation contributed to enhancement of erosion of material and results in higher surface roughness. Y. Tsai et al. [62] and T. Muthuramalingam et al. [63] investigated effect of impulse current on EDM of WC – SKD steel using copper tool electrode. The results revealed that the current impulse alters the energy density and has the

most effect on rate of material removal and tool wear. S. M. Son et al. [64] experimented EDM for investigating effect of pulse condition on process performance. They concluded that surface finish, MRR and TWR are significantly affected by pulse duration. For precision manufacturing application EDMing with short pulse duration results in better efficiency. K. Liu et al. [65] experimented with various pulse (discharge) shapes for the investigation of EDM process characterization. The mechanism of material removal of Si3N4–TiN during EDM has been discussed. Several discharge-pulse forms like ISO and relaxation have been experimented. The experimental results revealed that use of uniform energy discharge results in to reasonable surface quality. V. Janardhan and G. Samuel [66] investigated EDM process to analyse the influence of process parameters on the MRR and surface finish. MATLAB was used to assimilated the spark gap data. They reported that reduction in the pulse-off time during the process results in to increase of rate of material erosion. S.H. Yeo et al. [67] anticipated a technique for pulse discerning that helps to monitor EDM process. The technique considered pulse current as the most influencing factor as it represents the plasma channel intensity better compared to voltage. They reported that possibility of arcing should be eliminated ideally to achieve good surface integrities. M. Gostimirovic et al. [68] used RC-pulse generators to investigate effect of process variables (electrical) for EDM of Mn-V steel using Gr electrode. The experimental results reported that rate of material removal is most affected by pulse duration and pulse current. B. Nowicki et al. [69] investigated the effect of pulse discharge on surface finish in terms of formation of bulk craters. The investigation results revealed a strong relation between spark discharge and machined surface in the context of crater volume. Higher discharge current results into deeper craters. B. Mohan et al. [70] experimentally investigated effect of discharge current, electrode material and its polarity on MRR, TWR and SR. The experimental results concluded that increasing the discharging current the rate of removal of material and tool wear increases. Puertas el. al. [71] investigated the effect of pulse ON/OFF time and pulse intensity on dimensional accuracy and surface quality of the EDMed part using a factorial design. Researchers concluded that Pulse current intensity has utmost effect on surface roughness, that is at higher pulse intensities along with higher pulse ON times, the resultant surface roughness values are high.

T. A. El-Taweel [72] experimented CK-45 steel EDM with a powder metallurgy manufactured electrode Al-Cu-Si-TiC. The author investigated TWR, MRR by varying flushing pressure, discharge current and TON. Response Surface Method was used to analyse the Reponses. The results revealed that flushing pressure does not have much influence on rate of material removal and tool wear. S. H. Tomadi et. al. [73] conducted EDM of W-C material using Cu-W electrode. The experiments were designed using taguchi full factorial method and rate of material removal and tool wear were investigated. Discharge current, Voltage (supply), TON, TOFF were selected as process parameters. The supply voltage has utmost effect on rate of material removal compared to discharge current and TOFF. Herpreet Singh et. al. [74] studied EDM of steel using cryogenic copper tool electrode. The intention of the cryogenic treatment is to improve MRR and lower TWR. The experimental results indicated increase in TWR when operated with longer pulse off times. The higher pulse on time resulted in reduced rate of tool wear when operated with cryogenically treated tool. Ali Ozgedik and Can Cogun [75] experimented EDM of 1040 steel using copper electrode to analyse the effect of current, duration of pulse and flushing method on SR, rate of MR and TW. Several flushing conditions were experimented to analyse characteristic (geometric) of tool wear. Results of the experiments showed that the surface roughness, relative wear and tool wear increases with increase in discharge current. Injection and Suction flushing technique result in increased MRR. In static flushing condition the MRR founds to be low due to inefficient flushing of the inter electrodial gap. Hascalık and Caydas investigated EDM of Ti-6Al-4V using several electrode materials – Cu, Gr and Al. Surface integrity has been analysed through SEM, EDX and XRD analysis for several combination of pulse current and duration. The results showed an increase in tool wear, surface roughness and recast layer thickness hen operated with higher discharge current and duration. A hard thin layer of Ti24C15 (carbide) was also found on the surface when operated with copper electrode. The researchers also reported that use of Gr electrode results in higher MRR but the TWR and SR also increases [76].

J. Strasky et al. [77] investigated EDM of Ti-6Al-4V as a process of orthopaedic surface-treatment. In-vitro osteointegration, surface finish and modifications of surface chemical characteristics have been studied. They concluded that a carbon enriched layer is formed on the surface when EDM process is operated at high currents which helps improving

osteointegration. The experimental results also concluded that due to the formed microcracks, internal stresses (tensile) and the oxide layer (brittle), the fatigue strength deteriorates. Lin Gu et al. [78] investigated EDM (die-sink) of Ti-6Al-4V using bundled electrode. The experimental results of EDMing with bundled electrode were compared with the responses of conventional EDM. The comparison revealed that bundled electrode offers higher rate of MR and TW as it opens up the opportunity to operate at substantially high current discharges. Using a multihole inner flushing technique alongwith bundled electrode offers efficient flushing and hence opens up the spectrum for rough machining of large surface area. Ndaliman M. et al. [79] experimentally investigated EDM of Ti6Al4V alloy using electrode - Cu-TaC and dielectric – urea. The experimental results confirming formations of oxides (TiO), carbides (TiC) and nitrides (Ti2N and Ta2N) on the machined surface that alters the fatigue and wear resistant capacities of the alloy. D. Thesiya et al. [80] experimented Ti-6Al-4V EDM at high discharge currents using a taguchi method to analyse the effect on surface finish and thickness of recast layer. The experimental results revealed that the factors affecting the characteristics of recast layer are gap voltage and discharge current. Operating at lower values of discharge current and voltage results in thin recast layer and lesser surface finish when operated with copper tool. Y. C. Lin et al. [81] investigated Ti6Al4V machining characteristics using a hybrid EDM + USM process. Discharge current, TON and type of dielectric were selected as the parameters of study and performance was measured through MRR, TWR, REWR and surface finish. The experimental results showed an increase in MRR and reduction in recast layer thickness as the discharge efficacy improves due to the generated waveform during the hybrid process. Shabgard M. and Alenabi H. [82] investigated EDM of Ti alloy using vibration assisted tool. Pulse current, TON and frequency of vibration were considered process parameters and recast layer thickness was measured. Surface integrity was measured using SE micrography and XRD. In this research, an attempt was made to investigate the influence of copper tool vibration with ultrasonic frequency on output parameters in the electrical discharge machining of Ti–6Al–4V. The results of the experiments revealed that using vibrating (at ultrasonic frequency) tool the MRR increases and the crack density and TW reduces. Gaikwad S. et al. [83] investigated EDM of Ti-6Al-4V alloy using a core electrode. Grey Relational Analysis (GRA) method was adopted for optimizing the

responses – MRR, TWR and Ra. EDM was carried with electrodes having through holes (eccentric and central). The experimental results revealed that the electrical parameters pulse current and pulse on time has significant effect on EDM characteristics. GRA a multi objective optimization technique has been experimented to analyse effect of multiple parameters in the responses. Ghoreishi and Atkinson [84] experimented EDM with low/high frequency vibrating tool and rotary tool to considering the effect on TWR and MRR. The researchers concluded that for stated surface finish value the vibro-rotary motion improves the rate of material removal. G. S. Prihandana et al. [85] studied performance of EDM with a low frequency vibrated workpiece. The experimental set was designed with a vibrating work table to generate low frequency wave that practically improved the flushing efficiency. The researchers concluded MRR is majorly affected by frequency and amplitude of generated vibrations. Yoshida and Kunieda [86] studied the mechanism of electrode wear in dry electric discharge machining process. They reported that dry EDM results in to nearly trivial tool wear as the tool electrode surface is protected by the deposited workpeice molten material.

2.3 Dielectric Fluids in Electric Discharge Machining

For the environmental safely and promotion of better health alternate of kerosene is to be thought of as it decomposes in to CH4 and CO vapours that are harmful. Water (pure or additive mixed) serves as a good alternate of kerosene for EDMing operations [87]. Jeswani, M. [88] used distilled water and kerosene to investigate performance of EDM process. The experimental results concluded that at higher discharge energy rates the distilled water dielectric occasioned higher MR and lower TW compared to kerosene. The results also revealed that using distilled water dielectric results in reduction in accuracy of machining and better surface quality. Erden and Temel [89] experimented with brass electrode and deionized water dielectric for the performance characterization of EDM of steel. Brass electrode connected to negative polarity was used for the material erosion. The experimental results showed an increase in rate of material removal and reduction in rate of tool wear when operated with deionised water compared to hydrocarbon oil. Jilani and Pandey [90] performed EDM experiments with tap water, distilled water and 25-75 mixture of tap water and distilled water as dielectric using copper electrode. The experimental results revealed that the tap water dielectric used with a negatively charged copper

electrode results in best rate of machining with very trivial wear of tool electrode. They also concluded that at lower pulse rate (max. upto 50μs) compared to distilled water, tap water results in better surface qualities. Koenig and Joerres [91] investigated EDM operation using aqueous glycerine water solution as dielectric fluid. They reported that at high currents (discharge) and high duty cycle rates the aqueous glycerine water solution results in better performance compared to hydrocarbon fluids. An increase of approximately 40% was found when working with aqueous solution with a massive reduction in tool wear of approximately of 90%. Koenig and Siebers [92] explained the relationship between working medium – dielectric and process of material removal. Due to the higher thermal stability of water, EDM process can be done at higher discharge rates which intern results in improvement of rate of material removal. Specific boiling energy is the main significant difference amongst the hydrocarbon oil dielectrics and water based dielectrics. Low temperature boiling occurs in water based dielectrics as energy - specific boiling is eight times higher compared to hydrocarbon oils. Koenig et al [93] experimented EDM with water based dielectrics. The researchers concluded that for roughing and semi- finishing applications, glycerin-water solution dielectric results in improving the process capabilities with higher rate of removal of material.

Masuzawa T. [94] and Tanaka K. et al. [95] reported that organic compounds having larger molecular weights results in to better rate of material removal.The researchers insisted increased use of inflammable water based organic solutions to improve the performance characteristics. The experimental results of EDMing using polyethylene glycol-water dielectric are quite comparable with commercial EDMoil. Zhang Y. et al. [96] experimented with oxygen-mixed water emulsion. The experimental results revealed that oil-water emulsion (mixed with oxygen) improved the rate of machining significantly and has reduced the tool wear rate. Also the produced recast layer was having a lesser thickness. Liu Y. et al. [97] investigated EDM using oil-water emulsion dielectric – an environment friendly dielectric. The experimental results revealed that the amount of water in the oil-water emulsion and pulse discharge has noteworthy effect on EDM performance. The results also revealed that increasing the emulsion temperature results in reduction in rate of removal of material. Tsunekawa Y. et al. [98] performed EDM experiments using Ti-Al (64% and 36% respectively) electrodes to analyse the modification of surface in

EDM process. The experiments were conducted with kerosene dielectric and negative polarity tool electrode. The surface analysis revealed presence of TiC dendritic hastens on the machined surface. The elongated pulse discharges resulted in larger sized crated with increased depth of alloying. The pressure used to form the electrode has insignificant effect on rate of material transfer.

Kruth J. et al. [99] investigated the effect of type of dielectric fluid and material of electrode on metallographic phases and structure of formed recast layer during EDM process. The researchers concluded that dielectric - EDM oil promotes the formation of Fe3C hard layer on the machined surface while water when used as a dielectric resulted in surface decarbonisation. Chen S. et al. [100] investigated EDM of Ti6Al4V using distilled water and kerosene. The experimental results revealed that a hard layer of carbides forms on the machined surface while using kerosene as dielectric and a layer of oxides forms in case of water dielectric. Larger size debris are formed during EDMing titanium alloys using distilled water dielectric. In case of EDM with distilled water dielectric, the generated discharge impulse is small and stable Ekmekci B. et al. [101] conducted experiments with deionized water to analyse surface characteristics in EDM of mold-steel. The experimental results indicated that using deionized water dielectric reduces the microcracks intensity and results in reduction of austenitic phase. Sharma A. et al. [102] investigated feasibility analysis of micro EDM using CVD diamond electrode and different dielectrics – water and oil. The experimental results indicated an increase in MRR when operated with CVM diamond electrode (positive polarity) with kerosene. The results also revealed that use of copper electrode with CVD diamond workpeice results in admirable shape control and offers almost zero wear of tool. Leao and Pashby [103] presented a thorough literature review of use of several nonhydrocarbon dielectric fluids. They reported that looking to process improvements, the water based dielectric fluids have good capabilities to replace conventional hydrocarbon oils in die-sink EDM application.

2.4 Powder Mixed Electro Discharge Machining

The PMEDM process was invented in late 1970s. Erden and Bilgin [104] first experimented with Cu, Fe, C and AL powder mixed kerosene as dielectric for EDMing of steel. The researchers observed that powder addition to dielectric enhances the dielectric fluid breakdown characteristics and improves machining efficiency. They also reported that

excess concentration results in short-circuiting and hence reduces the stability of machining. In 1981, Jeswani M.L., et al. [105] investigated Gr powder (particle size 10 microns) mixed kerosene for EDM of mild steel using copper electrode. The researcher concluded 60% improvement of rate of removal of material when EDMing with Gr powder mixed kerosene (concentration 04 grms./ltrs.). The results also revealed improvement of rate of tool wear by 15%. Narumiya H. et al. [106] experimented EDM with Al, Si and Gr powder mixed dielectric with varying concentration powder from 02 to 40 grms./ltrs. The experimental results revealed increase in inter-electrodial gap and thereby improving flushing efficiency. Low concentrations of Si and Gr powder resulted in enhanced surface quality. Mohri N. et al. [107] investigated effect of addition of Si powder (to dielectric) on surface quality of EDMed part. The experiments were conducted on a confined area of 500 cm2 . The investigation results revealed a development of high quality surface – mirror like having smaller craters and lesser cracks.

Kobayashi K. et al. [108] experimented with Si, Al and Gr powder added dielectric for machining of tool steel SKD-61. The experimental results indicated an enhancement of surface finish when operated with powder added dielectric. The researchers also concluded that the surface quality of PMEDMed component is better with Al and Gr powder compared to Si powder. Singh and Yeh [109] investigated Al and Gr powder mixed EDM of Al-matrix composites. They designed a setup having a stirrer in an auxiliary machining tank. The results revealed that addition of Al powder in dielectric improved MRR and Gr powder addition resulted in improvement of surface finish. The researchers also stated that process efficiency has an effect of quality of dielectric – a fresh charge dielectric results in improving the EDM characteristics. Sanjeev K. and R. Singh [110] experimented with Mg powder added dielectric for investigating EDM of OHNS steel. The experimental results indicated improvement in machining surface quality. They also reported the issue of powder settlement in the corners of the tank due to which the process characteristics are slightly altered. A stirrer along with a dielectric recirculation system helps to resolve the issue.

Uno Y. et al. [111] experimented EDM with Ni powder blended dielectric for analyzing the surface modification. The experimental results revealed that the surface quality resulted by PMEDM was better than the conventional EDM. The surface was having layer on hard TiC

which increases the wear resistant characteristics of EDMed part. Pecas and Henriques [112] used Si powder added dielectric for EDMing of tool steel AISI H13. Different values of pulse discharge were experimented to analyze the effect on EDMed part's surface finish. The researchers reported that Si powder addition reduces the crater size and the recast layer thickness. Tzeng and Lee [113] experimented EDM with various powders – Al, Cr, SiC and Cu added dielectrics. The researchers developed a filtration device to retain the debris entering into the dielectric supply and circulation mechanism. The researchers concluded that powder particle's properties that affects EDM characteristics are powder concentration, particle size, particle's thermal and electrical conductivity. Wong Y. et al.
[114] used different powders to analyze EDM's capability to produce mirror like surface finish. The researchers concluded that addition of powder promises improvement in surface finish. Compared to several added powders the Al powder resulted in to better surface finish – near mirror like. Table 2.1 represents the powder characteristics and Table 2.2 suggests the value of spark gap distances for various powders.

TABLE 2.1 Powder characteristics - PMEDM

Material	Mesh Size	Particle Size (μm)	% of Purity
Silicon carbide	08	2.36 ± 0.08	-
Crushed glass	10	2.0 ± 0.07	-
Aluminum	325	45 ± 3	99.5%
Silicon	325	45 ± 3	99.5%
Graphite	400	38 ± 3	99% (Purum)

Ming Q. et al. [115] experimented with inorganic-oxide powder added dielectric for EDM of high carbon steel. They reported that the conductive and lipophilic characteristics of the powder added dielectric results in improvement in surface quality and reduces the

amplitude of cracks. The concern they reported was settlement of powder particles at the tank bottom and corners. Cogun C. et al. [116] investigated EDM process performance using Gr and H3BO3 powder added kerosene as dielectric. The results indicated that addition of Gr powder results in

improvement of surface characteristics. Okada A. et al. [117] investigated carbon powder mixed EDM using Cu electrode. The researcher concluded that the increasing powder concentration in dielectric and operating EDM at higher TON results in thicker and harder layer of solidifying materials.

TABLE 2.2 Spark Gap distances for various powders – PMEDM

Dielectric (Pure / Powder Mixed)	**Spark Gap Distance (µm)**
Aluminum	120 – 160
Silicon Carbide	80 – 90
Molybdenum sulphide	44 – 48
Graphite	45 – 50
Silicon	27 – 33
Crushed glass	10 – 15
Pure Dielectric	10 – 15

Chow et al. [118] conducted experiments with SiC powder and Al powder added dielectric kerosene for Ti alloy micro-slit machining. The researchers concluded that addition of the powder increased the inter-electrodial gap and hence enhanced the rate of removal of material. Furutani K. et al. [119] experimented with Ti powder mixed kerosene as dielectric for EDMing carbon steel using a copper electrode. The researchers found a hard layer (1600 HV) of TiC upon machining the steel. The analysis revealed that the carbon

deposition was because of the dielectric breakdown. Yan B. et al. [120] investigated performance of EDM using Al and Cr powder mixed kerosene as dielectric. The researchers reported that addition of powder expands the electrode gap that improves the spark stability and thereby improves the surface finish. They also reported that addition of powder increases the rate of MR and TW at higher values of discharge currents. The finer grain size of the powder particle eases the bridging and suspension resulting in to reasonable fine surface.

Kozak J. [121] compared EDM with different dielectrics – kerosene and powder blended deionized water. The researcher reported that the tool wear rate was significantly reduced when powder mixed deionized water was used, which also offers a better option for dielectric selection considering environmental aspects. Klocke F. et al. [122] examined the effect of powder mixed dielectric on resolidified layer using discharge energies of the range – micro-Joule. HSFC technique was used to investigate the formed plasma channel when operated with Al powder mixed EDM. It was concluded that the EDM process performance is affected by the type of powder used and its concentration. Yan, B.H et al.

[123] used urea mixed distilled water for EDMing of pure Ti metal. The experimental results reported a layer of TiN because of the migration of nitrogen to the machined surface from urea mixed water. The hard Tin layer improved the wear resistant capabilities. The researchers also reported that at higher discharge currents, the urea mixed dielectric resulted in to improved rate of MR and TW. Wu K. L. et al. [124] studied effect of Al powder and surfactant mixed dielectric on surface characteristics of EDM of SKD steel. The researchers reported that mixing of surfactant and powder into the dielectric improves the distribution of pulse discharge, which in-turn results in improvement of surface quality. Fig. 2.6 shows the effect of dielectric on resultant surface finish.

Anil Kumar et al. [125] investigated influence of Al powder mixed dielectric EDM of Inconel 718 by varying the powder size and concentration. They reported that addition of Al powder in EDM dielectric improves the machining characteristics. They also reported that using fine grain powder with a concentration of 06 grms./ltrs. results in better rate of material removal and good surface finish. Gurule N. B. et al. [126] experimented rotary EDM of die steel using with Al powder mixed dielectric to improve the rate of material removal. Experiments were designed and analyzed using Taguchi method. The researchers

reported that most influencing parameters are pulse current, TON, rotational speed of tool and concentration of powder in dielectric. The results indicated that best surface finish is achieved at powder concentration 04 grms./ltrs. and tools spindle speed of 900 RPM.

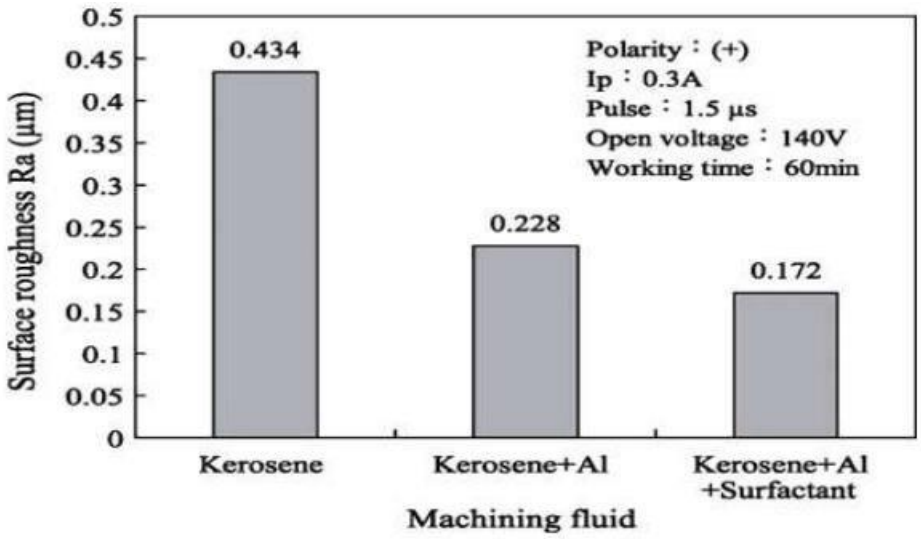

FIGURE 2.6 Effect of dielectric on Surface Finish

K. H. Syed et al. [127] experimented with Al powder added distilled water for EDMing of diesteel W300 using Cu electrode. The researchers followed taguchi method to design and analyse the experiments in terms of SR, MRR and TWR by varying pulse current, TON, concentration of powder in dielectric and electrode polarity. The experimental results concluded that Al powder mixed distilled water dielectric offers increased MRR and results into a better surface finish having thin layer of resolidified materials. Kuang Yuan Kung et al. [128] experimented Al powder mixed commercial grade mineral oil EDM-44 for EDM of WC-Co workpeice using copper electrode. The researchers reported that the efficiency of machining increases using Al powder mixed dielectric due to the dispersed energy dispersion. The increase in powder concentration results in to increase in rate of material removed. The higher particles sized PMEDM results in enhanced rate of material removal from workpeice and tool electrodes. Paramjit Singh et al. [129] investigated Al powder mixed EDM of Hastelloy using Cu electode. The powder concentration and grain size of powder were varied to analyse its effect on SR, MRR, TWR and RR. The experimental study revealed that the rate of MR and TW are affected by particle size and concentration.

The addition of powder to dielectric increases rate of material removal and resultant surface finish. S. Sood et al. [130] investigated the effect of discharge current, TON/TOFF and Gr and Cu mixed kerosene dielectric on produced surface microhardness and toughness for PMEDM of die steel EN-31 using Cu electrode. The experimental results revealed that powder addition has improved the surface characteristics. S. Singh et al. [131] designed a PMEDM setup with a dedicated tank with a stirrer for storage and circulation of Al2O3 and TiC powder mixed dielectric for machining of D3 die steel. Several compositions of dielectrics, spark-gap period and tool lift time were the selected parameters to analyse the effect on rate of MR and TW. The results indicated a strong effect of powder type and concentration on the responses. G. Singh et al. [132] conducted experiments with Al powder added EDM oil 125 CC SAE 40 for PMEDMing of steel H13 using Cu electrode. The researcher reported that addition of powder particles in dielectric helps to improve surface finish. They also reported that EDMing with negatively polarity tool helps to decrease the rate of tool wear. Mathapathi U. et al. [133] investigated PMEDM of ASI D3/HCHCR steel using Cr and Gr powder mixed dielectric and Cu electrode. They concluded that in PMEDM process the rate of MR is higher and TW is lower compared to conventional die-sink EDM. Increasing the TOFF the rate of removal of material reduces. Kumar et al. [134] studied the effect of Al powder mixed dielectric for EDMing of Inconel 718 alloy using Cu electrode. OVAT technique is adopted to analyze the process performance with negative polarity tool. The results of the experiments revealed that using 325 mesh size Al powder mixed dielectric improves the surface roughness by 17% and the tool wear is reduced by 80%. Fig. 2.7 represents the effect of power particle concentration on tool wear rate.

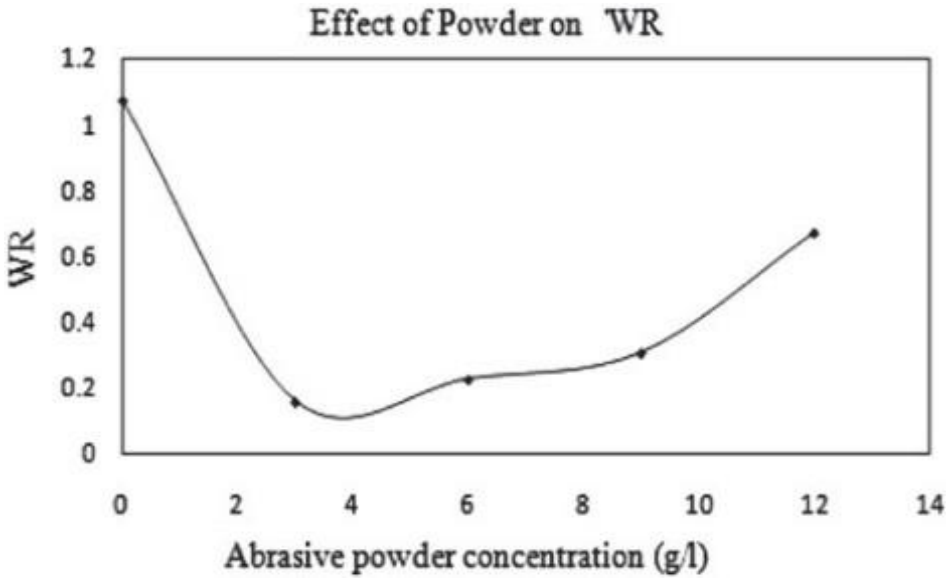

FIGURE 2.7 Effect of Powder Concentration Tool Wear [131]

Bhattacharya A. et al. [135] studied PMEDM of several grades of steel - H11, EN31 and HCHCr for rough machining and finish machining. ANOVA analysis has been done to analyse the main and interaction effects of process parameters. The experimental results revealed that the best MRR value was found for EN31 whereas HCHCr demanded higher values of discharge current and TON. The addition of Gr powder enhanced the surface finish of PMEDMed part. For the same machining conditions H11 exhibits higher rate of removal of material compared to HCHCr. Tan P. C. and Yeo S. H. [136] experimented with nanopowder-mixed dielectric for the analysis of surface integrity in case of µEDM. They concluded that the plasma channel expands due to the addition of powder in to dielectric and results in to reduced fractional heatflux to workpiece. Fig. 2.8 represents the microphotograph of the resolidified layers formed on the workpeice surface at different concentration of powder. Goyal S. and Singh R. [137] investigated PMEDM of steel - AISI 1045 using Gr powder added dielectric. During the experiments Voltage Gap, Pulse current and Duty cycle were kept constant and Gr powder size and its concentration were varied. The experimental results suggested that MRR and SR is influenced by grain size.

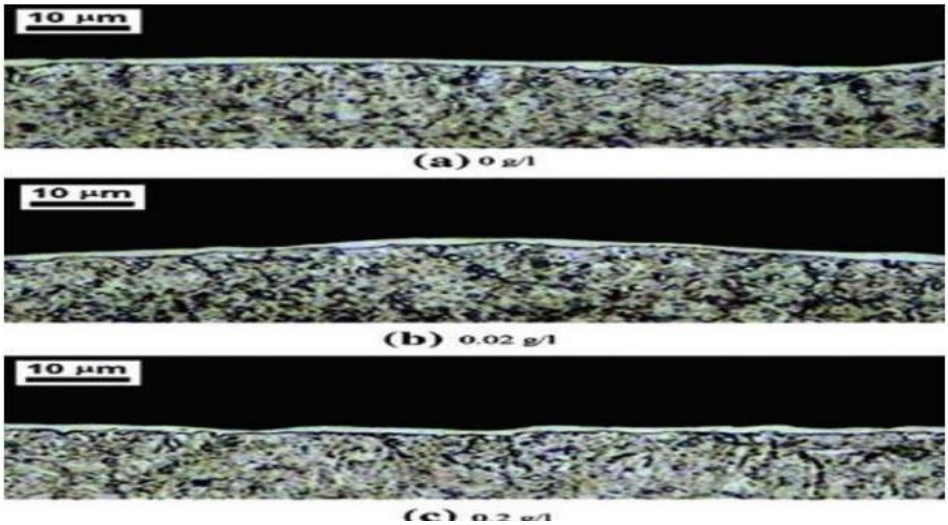

FIGURE 2.8 Recast Layers on µEDMed Surface [133]

Kucukturk and Cogun [138] experimented EDM process to generate holes in ceramic – non conducting material using Gr powder mixed dielectric. To initiate sparking the ceramic workpieces were coated with conductive layer. The discharge process continues to erode the material because of formed thin layer of decomposed carbons of dielectric and suspended Gr powder. Jahan M. et al. [139] investigated micro PMEDM of Wc-Co alloy using nano powder of Gr, Al2O3 and Al. The experimental results indicated no significant effect of Al2O3. But the addition of Al and Gr powder to dielectric showed a noteworthy improvement in surface finish. Chen S. et al. [140] investigated surface modification of titanium using µ-current EDM using Ti powder added deionized water as dielectric. The experimental results indicated that at lower pulse currents and powder concentration of 06 grms./ltrs. The surface finish achieved is commendable. They also concluded that addition of powder improves the surface wettability and reduces the formation of cracks.

Tsai and Chang [141] investigated EDM with polyaniline powder (polymer) suspended dielectric for the effect on surface roughness. The researchers concluded that use of low concentration polyaniline powder results in better surface finish even than the Si powder suspended EDM. They found out that surface finish can be improved further using a conductive powder PANI-SALT. Jabbaripour B. et al. [142] experimented PMEDM of ϒ-TiAl (intermetallic) using Cr, Al, SiC, Gr and Fe powder added dielectric. The material erosion is more at higher currents as the thermal energy produced will be more. The results of the experiments concluded that Al powder results in the best surface quality amongst all

the selected powder for the experiments. They also reported that upto certain level of powder concentration the erosion rate increases and after that it reduces due to the instable discharges. Fig. 2.9 indicates effects of various powder used on surface finish resulted.

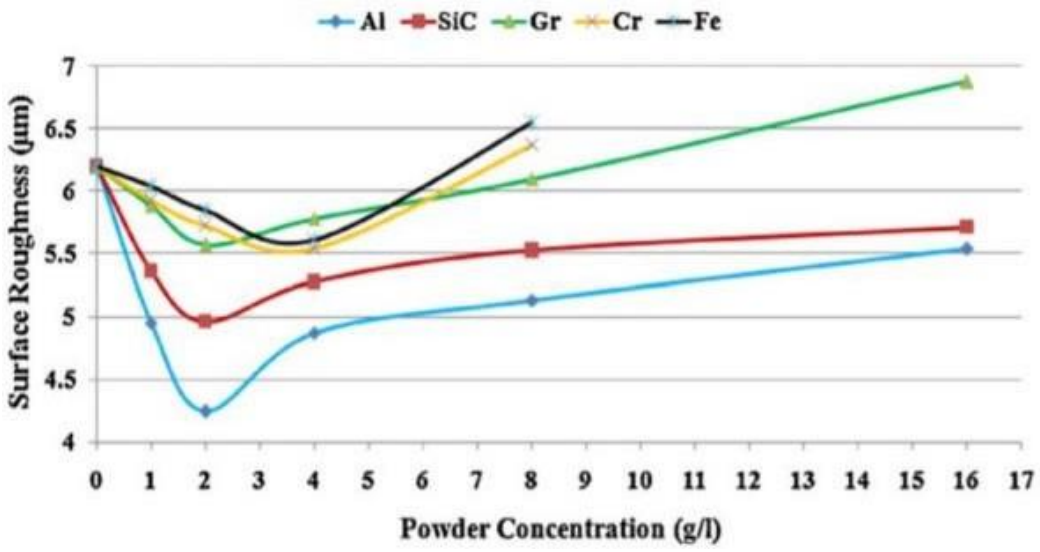

FIGURE 2.9 Effect of Various Powders and their Concentration on SR – PMEDM [139]

Ojha et al. [143] experimented with nickel powder mixed EDM of steel EN-19. Powder concentration, Electrode angle, pulse current and duty cycle were the considered process parameters. The results of the experiments were revealing that pulse current has the most significant effect of rate of material erosion. The rate of MR and TW increases with increase in powder concentration. Kolli and Kumar [144] investigated EDM of Titanium alloy using boron carbide powder mixed dielectric. Experiments were conducted with different levels of P.C and found that addition of B2C2 helps to improve the surface characteristics.

Shabgard and Behnam [145] experimented CNT added dielectric for EDMing of Ti6Al4V using Cu electrode. The surface characteristics of CNT added PMEDM of Ti alloy was analyzed using SEM. The results revealed that the CNT addition to dielectric reduces the formation of cracks alongwith an improved stability of machining. The addition of CNT particles improves the surface finish as the spark energy distributes evenly. Ramesh S. et al. [146] used Al, Sic and Al2O3 powders for analyzing EDM performance characteristics

for machining of steel AISI P20. The experimental results revealed that Al powder mixed dielectric alongwith copper electrode offered highest rate of MR. The combination of tungsten tool electrode and Al2O3 powder blended dielectric offers lowest radial overcut and alongwith lower rate of tool wear. Sugunakar A. et al. [147] investigated PMEDM of super alloy RENE 80. Gr and Al powder were added to dielectric in different levels to analyse the surface integrity and characteristics of recast layer. The experimental results indicated reduction in the thickness of recast layer upon using powder mixed dielectric.

S. K. Sahu et al. [148] investigated Gr powder mixed EDM of Inconel 718. The experimental results indicated that the rate of material removal increases with higher pulse currents. Amit Kumar et al. [149] used Al2O3 powder blended deionized water to analyse EDMing of Inconel alloy 825. The results of the experiments have shown that powder blending improves process performance compared to convention method. Divya Rana et al.

[150] conducted EDM experiments with various powder added dielectrics. The researcher experimented with metal powder added dielectric and concluded that the addition of metal powder increases the inter electrodial gap and reduces the insulating capacity of dielectric. The stability of the spark and rate of erosion of material improves consequently. Gudur S. et al. [151] investigated PMEDM of SiC powder blended dielectric for EDMing of steel SS-316L. Powder concentration, pulse intensity and pulse time has been studied to the performance analysis using RSM technique. The experimental results stated that the concentration of powder has significant effect on erosion rate of material. Kuriachen B. et al [152] experimentally investigated effect of SiC powder (Micro Sized) added dielectric for EDMing of Ti6Al4V using WC electrode. The effect of varying voltage and powder concentration were analyzed on rate of MR and TW. It was concluded that at moderate value of voltage and lower values of concentration of powder, the material erosion was found to be maximum. The rate of tool wear increases with current and voltage. Harmesh Kumar [153] reported the experimental investigation results using CNT powder for EDM of diesteel AISI D2. The surface characteristics were analyzed by varying pulse current, CNT concentration and duration of the pulse. The researcher reported that the duration of pulse is affecting the erosion rate and surface finish. They also concluded that rate of erosion is significantly affected by concentration of CNT in dielectric. Zakaria M. Z. et al.

[154] investigated TaC powder mixed EDM with an objective to analyse the surface

properties of stainless steel workpeice. Different concentration of TaC powder in kerosene were experimented for analyzing the effect on surface hardness and property of corrosion resistance. They reported that addition of TaC powder in kerosene for EDMing of SS workpeice improves that corrosion reactance characteristics.

Paul B. K. et al. [155] investigated Si powder added EDM of EN-31 steel using RSM technique. Powder concentration, pulse current and duty cycle were the considered parameters to analyse the effect on rate of material removal and surface finish. The results of the experiments revealed that the surface finish and MRR is most affected by concentration of dissolved powder and peak (discharge) current. Patel S. et al. [156] experimentally investigated PMEDM of Inconel alloy 718 using Al2O3 powder added dielectric and Cu-W electrode. The electrode was rotated at 300 RPTaguchi technique was employed to analyse the effect of parameters on SR, TWR and MRR. The researchers concluded that concentration of powder has insignificant effect on process performance. Khan A. A. et al. [157] reported PMEDM of SS AISI 304 using Cu electrode and Al2O3 powder suspended dielectric. The rate of removal of material and quality of surface were investigated using ANOVA method. The results of the experiments showed considerable improvement in surface quality by addition of Al2O3 powder. They also reported that a little improvement was notice in the rate of material removal when powder was added. TON has significant effect on SR and MRR. 2.5 Modelling and M and Ip, TON, Gap voltage and P.C were considered as process parameters

Taguchi technique was employed to analyse the effect of parameters on SR, TWR and MRR. The researchers concluded that concentration of powder has an insignificant effect on process performance. Khan A. A. et al. [157] reported PMEDM of SS AISI 304 using Cu electrode and Al2O3 powder suspended dielectric. The rate of removal of material and the quality of the surface were investigated using ANOVA method. The results of the experiments showed considerable improvement in surface quality by addition of Al2O3 powder. They also reported that a little improvement was notice in the rate of material removal when powder was added. TON has significant effect on SR and MRR.

2.5 Modeling and Optimization of EDM and PMEDM Process

Kansal H. K. et al. [158] developed a model for PMEDM process to demonstrate the temperature dispersals, material flow and residual stress distribution over workpeice. The

model was also capable to identify surface cracks on PMEDMed workpeice. The developed model was used to predict temperature distribution and compute the stresses generated while machining. Sethuramalingam and Vinayagam [159] experimented with SWCNT mixed kerosene for diesinking of AISI D2 steel for the development of higher surface finish. The surface roughness was modelled considering adaptive neuro-fuzzy interface approach. The developed model was used to predict responses like rate of material removal and surface roughness. Cogun and Savsar [160] investigated EDM for discharge pulse time holdup period using a γ distribution function. The γ variable model were developed for several machining conditions with changes in shape factor and scale factor. Trial for all the model were taken using error criteria.

Salah N. B. et al. [161] studied EDM process for the development of numerical model for temperature distribution during EDM process of steel AISI 316L. The model was used to infer the rate of material erosion and surface roughness. The Chapter 2 - Literature Review 54 modelled values were compared with experimental results for the validation of the model. Bhattacharyya B. [162] studied EDM of Inconel 625 for analyzing the effect of lattice strain and size of crystallite. The researcher reported that technique of williamson- Hall plot helps to segregate impact of lattice strain and crystallite size. The researcher reported that lattice strain and crystallite size have substantial influence on material microstructure. Jahan M. P. et al. [163] investigated μEDM of WC using Cr, Al and Al2O3 nano-powder mixed dielectric for improvement of surface quality. The researchers reported theoretical model to explain the mechanism of material removal using breakdown characteristics. Experiments were conducted to analyse the effect of powder addition on surface roughness and material removal rate. The results concluded that the addition of powder increases the sparkgap and helps enhancing surface finish

Prabhu S. et al. [164] experimented CNT powder mixed EDM of steel AISI D2 using ANFIS technique for development of surface roughness model. 1st order sugeno fuzzy interference model was used for prediction of Reponses. The model predicted values were compared with experimented values to find out error of prediction. R2 value was used to indicate that the predicted value that is very nearer to the experimental data. Pradhan M. K.

[165] investigated surface quality of EDMed part surface using tool steel AISI D2 and Cu electrode. Surface topography, thickness of resolified layer alongwith rate of TW and MR

were investigated. The researcher reported that pulse current and discharge time are the most swaying factors. Fuzzy based ANN model was developed for predicting responses – rate of material removal and tool wear. Reddy V. et al. [166] modelled EDM process parameters for optimizing rate of material erosion for steel EN-31 using RSM. Behrens A.
[167] investigated EDM process using a neurofuzzy based controller to control the inter electrodial gap to improve process capabilities. The results of the experiments have revealed that the controller helps to improve the surface finish and thereby enhances the process capabilities.
Popa M. S. et al. [168] experimented with various process parameters to improve the EDM process quality. The researchers formed an equation for discharge energy that models depth of generated crated in EDM. The results of the experiments were used to check the validity of the generated model and it was concluded that discharge current has the most influence of depth of crater generated. Fenggou C. et al. [169] experimented EDM to generate a model that predicts the performance of diesink EDM process using ANN. The results revealed that discharge current is the most influencing parameter and hence ANN model was developed to analyse-predict the current rating that optimizes the EDM process characteristics. Caydas and Hascalik [170] investigated WEDM process and developed a model to predict surface roughness. Gap voltage, duration of pulse and rate of wire feed was the parameters of selection to model the WEDM process that improves the process efficiency.
Muthukumara V. [171] experimented EDM of Inconel 800 using RSM and developed a mathematical model to predict radial overcut. The experiments were conducted to determine significant parameters using ANOVA analysis with a significance level of 5%. It was found that the generated models predicted the response with determination coefficient of 0.97 for radial overcut. Singh H. et al. [172] investigated powder mixed EDM and developed an FE model to predict the distribution of temperature that affects the size of crater produced on EDMed surface. The model was tested to predict rate of material removal using theory of single crater and multiple crates. Assarzadeh and Ghoreishi [173] analysed Al2O3 powder added EDM using a dual response surface (desirability) technique for machining of steel CK-45. PMEDM was experimented with several powder concentrations and the developed model technique was used to compare predicted and

experimental results. The test results showed that the developed model predicts the responses with and error of maximum 11%. Abdolahi A. et al [174] generated a model that predicts the responses that confers efficient machining of using function of Non- dimensional process evaluation.

Bhosle R. B. et al. [175] investigated μEDD of Inconel 600 using GRA for process optimization and W-C tool. ANOVA analysis was done to identify significant parameters that affects process response. The results of the experiments concluded that the most affecting parameters are voltage, capacitance and feedrate. Dhupal D. et al. [176] developed a regression (quadratic) model using MOPSO technique for optimizing EDM process. The developed algorithm helps to analyse the process model for EDM process optimization. Nagaraju N. et al. [177] optimized EDM process using the parameters – gap voltage, TON, inter-electrodial gap width and the responses – rate of material removal and SR. Fuzzy based multi-response optimization (MPCI) was experimented converting the multiple responses in to an index that categorizes multiple responses to enhance the performance of EDM process. Shao and Rajurkar [178] modelled μEDM for simulation of process of crater formation considering thermal aspect of machining. The model helps to represent of the actual machining conditions like distribution of heat flux, expansion of plasma channel and other temperature reliant properties. The generated model alongwith the experimental response – dimensions of crater are the representative of fraction energy distribution. Parsana S. et al. [179] investigated EDMing of Mg-REZn-Zr alloy using a multi objective optimization technique - passing vehicle search (PVS). RSM – BBD was used to generate model the responses – rate of MR, TW and hole roundness. The model was developed using the experimental responses. The researchers also concluded that pulse current and pulse time are most governing parameters.

Prakash C. et al. [180] investigated EDM with HA powder mixed dielectric to machine biodegradable alloy Mg–Zn–Mn. MO-PSO method was used to optimize the process parameters and identify the best concentration level of powder – HA, pulse current and TON. Ramanan and Dhas [181] conducted WEDM of AA7075- PAC composite. The process was optimized using GRA – fuzzy techniques for rate of material removal and tool wear respectively. The experimental results were used to model the fuzzy model. The method was used to predict the optimal value of material erosion rate and surface finish.

Aharwal K. et al. [182] conducted EDM of Al-SiC workpiece using Cu electrode with an objective to optimize material removal rate and surface finish. Voltage, TON, TOFF and duty factor were the considered parameter for process optimization. Sengottuvel. Pa et al. [183] optimized EDM process characteristics for multi-objective optimization of Inconel 718 using fuzzy approach.

Cu was selected as tool material with various geometries – circle, triangle, rectangle and square. The experimental results concluded that higher flushing equipped with high current offer improved process and the geometry of tool does not have significant effect on responses. to model the fuzzy model. The method was used to predict the optimal value of material erosion rate and surface finish. Aharwal K. et al. [182] conducted EDM of Al-SiC workpiece using Cu electrode with an objective to optimize material removal rate and surface finish. Voltage, TON, TOFF and duty factor were the considered parameter for process optimization. Sengottuvel. Pa et al. [183] optimized EDM process characteristics for multi-objective optimization of Inconel 718 using fuzzy approach. Cu was selected as tool material with various geometries – circle, triangle, rectangle and square. The experimental results concluded that higher flushing equipped with high current offer improved process and the geometry of tool does not have significant effect on responses.

Dewangan S. et al. [184] optimized the surface characteristics of EDM process using grey-fuzzy logic approach. The technique was implemented to improve surface quality of EDMing of tool steel AISI P20. A fuzzy grey relational grade was generated to optimize the process parameters. The ANOVA analysis results concluded that input current was the most significant parameters that affects the performance characteristics. Tripathy S. et al.

[185] investigated hybrid EDM process wherein Taguchi-TOPSIS-GRA method was used to optimize EDMing of die-steel H11 using Cu electrode. Ip, TON, TOFF, duty cycle and gap voltage were selected as the parameters of study and rate of tool wear, material erosion and surface finish were the selected responses. Results of ANOVA tests were used to identify the significant parameters with a confidence level of 95%.

A model was generated to predict the responses using GRA and TOPSIS methods. Manohara M. et al. [186] used Taguchi-Grey method for optimization of EDM of Inconel 718 alloy. The optimization of the parameters was done to improve the responses – MRR and TWR. The parameters selected were pulse current, TON, TOFF and Gap (spark).

Tantra N. et al. [187] developed a theoretical model to predict EDM tool wear characteristics. The generated model was used to predict the parameters that results in the lowest wear and improves the process efficiency for the process of making holes in blades of turbines. The developed model was compared with Heuvelman model and the researcher concluded that the generated model was not having any direct relation with it. Huu and Nguyen [188] experimented Ti powder mixed PMEDM of die steel with an intent to optimize productivity, cost and quality of PMEDM process. Effect of TON, TOFF and pulse current were analyzed for the responses surface finish and rate of tool wear and material removal. Multi-objective optimization was done to set optimum levels of parameters that results in fine surface quality at reasonable cost. The developed models could be used to analyse the machine limits that yields maximum productivity. Niamat and Misbah [189] conducted experiments with Ti powder mixed dielectric for accomplishing multiobjective optimization of PMEDM process using Gr electrode. The method used to optimize was Taguchi-AHP-Deng and the responses selected were rate of material removal, tool wear, surface hardness and thickness of resolidified layer. The experimental results concluded that Gr electrode with positive polarity results in process improvement. The researchers also concluded that addition of Ti powder in dielectric reduces the thickness of resolidified material. The reported results also confirmed that Deng's method also helps in multi-response optimization.

2.6 Research Gap

While there has been extensive research on electrical discharge machining (EDM) of titanium alloys like Ti-6Al-4V, several key gaps remain in the literature that warrant further investigation:

Limited studies on powder-mixed EDM of Ti-6Al-4V: Most previous research on EDM of Ti-6Al-4V has focused on conventional EDM without powder additives in the dielectric fluid. There is a lack of comprehensive studies examining the effects of different powder types, concentrations, and particle sizes specifically for powder-mixed EDM of Ti-6Al-4V. A systematic evaluation of how various powder additives impact the machining performance and surface integrity is needed.

- **Insufficient understanding of powder mechanisms:** The fundamental mechanisms by which powder particles enhance the EDM process for titanium

alloys are not fully understood. More in-depth analysis is required to elucidate how different powder materials interact with the plasma channel, affect debris removal, and influence the formation of the recast layer during machining of Ti-6Al-4V. Advanced characterization of the powder effects at the microscale could provide valuable insights.

- **Limited optimization of powder-mixed EDM parameters:** While some studies have examined the effects of individual EDM parameters, there is a lack of comprehensive multi-parameter optimization specifically for powder-mixed EDM of Ti-6Al-4V. Systematic optimization of powder concentration, particle size, and EDM electrical parameters in combination is needed to determine ideal operating conditions.
- **Inadequate surface integrity analysis:** Most previous research has focused primarily on material removal rate and surface roughness as the key outputs. A more thorough examination of surface integrity aspects like recast layer thickness, heat affected zone, surface crack formation, and microhardness changes is needed, especially for powder-mixed EDM of Ti-6Al-4V. The effects of different powder additives on these surface integrity characteristics have not been adequately explored.
- **Lack of predictive modeling:** There is a lack of comprehensive predictive models for powder-mixed EDM of titanium alloys that can accurately estimate machining performance and surface quality based on input parameters. Development of physics-based or data-driven models that can predict outputs like material removal rate, tool wear, surface roughness, and recast layer thickness would be highly valuable for process planning and optimization.
- **Limited studies on alternative dielectric fluids:** Most EDM research on Ti-6Al-4V has utilized hydrocarbon-based dielectric oils. There is a need to explore more environmentally-friendly alternatives like deionized water or water-based dielectrics for powder-mixed EDM of titanium alloys. The impacts of different dielectric fluids in combination with powder additives have not been adequately investigated.

- **Insufficient analysis of electrode materials:** The effects of different electrode materials in combination with powder additives for machining Ti-6Al-4V have not been thoroughly examined. Systematic evaluation of how electrode material choice impacts machining performance and surface quality in powder-mixed EDM is lacking.
- **Lack of micro-EDM studies:** While some research has examined conventional EDM of Ti-6Al-4V, there is very limited work on micro-EDM of this alloy, especially with powder additives. The unique challenges and opportunities of using powder-mixed dielectrics for micro-scale machining of titanium alloys need further exploration.
- **Inadequate comparison to other processes:** There is insufficient comparative analysis between powder-mixed EDM and other advanced machining processes for titanium alloys like laser machining, electrochemical machining, or ultrasonic machining. A thorough comparison of capabilities, limitations, and resulting surface integrity between different processes would be valuable.
- **Limited studies on complex geometries:** Most EDM research on Ti-6Al-4V has focused on simple geometries like flat surfaces or drilled holes. There is a lack of studies examining the machining of complex 3D geometries in titanium alloys using powder-mixed EDM. The unique challenges of flushing, debris removal, and dimensional accuracy for intricate shapes need further investigation.
- **Insufficient analysis of powder circulation and filtration:** The practical aspects of powder circulation, settling, filtration, and reuse in an industrial EDM setup have not been adequately addressed for titanium alloy machining. Optimizing the powder handling system for long-term stable operation requires further study.
- **Lack of sustainability analysis:** There is very limited work examining the overall sustainability and environmental impact of powder-mixed EDM for titanium alloys compared to conventional EDM or other processes. A holistic life cycle assessment considering factors like energy consumption, waste generation, and environmental effects of different powder additives is lacking.
- **Inadequate investigation of hybrid processes:** The combination of powder-mixed EDM with other assistive techniques like ultrasonic vibration, magnetic field

application, or cryogenic cooling has not been thoroughly explored for machining of Ti-6Al-4V. Such hybrid approaches may offer unique capabilities that warrant further research.

- **Limited studies on economics and industrial viability:** While much research has focused on the technical aspects, there is insufficient analysis of the economic viability and practical implementation challenges for industrial-scale powder-mixed EDM of titanium alloys. Cost-benefit analysis and identification of key barriers to adoption in production environments is needed.

Addressing these research gaps through systematic experimental studies, advanced modeling and simulation, and holistic analysis of technical and practical aspects would significantly advance the field of powder-mixed EDM for titanium alloys. This could enable more effective and efficient machining of Ti-6Al-4V and similar difficult-to-cut materials for critical aerospace, biomedical, and other advanced applications.

2.7 Methodology of Present Research

The research objectives have been achieved by developing the detailed research framework. This research work is mainly concerned with process parameter optimization and experimental investigation of surface characteristics for PMEDM of Ti6Al4V. The methodology adopted (Fig. 2.10) to address the objectives is as follows;

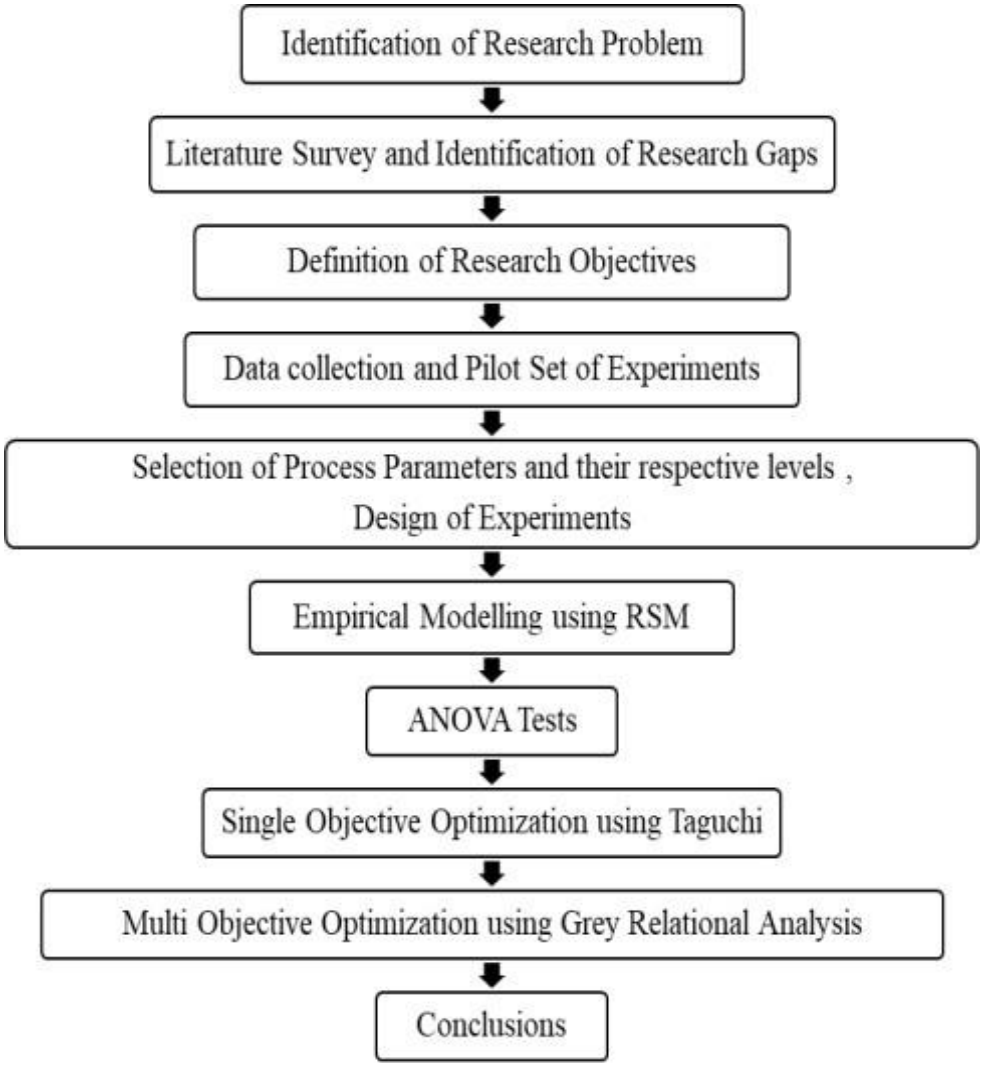

FIGURE 2.10 Flow Diagram of Present Research

CHAPTER-3
METHODOLOGY AND EXPERIMENTATIONS

3.1 Introduction

The goal of the current research is to examine the viability of using deionized water as a dielectric medium and to examine the impact of discharge current, pulse-ON-time, pulse-OFF-time, and powder consternation on the rate of material removal, the rate of tool wear, and the integrity of the surface for PMEDM of titanium alloy Ti6Al4V using Al2O3 and SiC powder mixed with deionized water dielectric and copper electrode. This chapter discusses about selection of materials for experimentation, design of experiments, experimental setup and measurement of responses in detail.

3.2 EDM Machine Setup

In the present research, experiments are performed on Die-sink EDM machine (Joemars AZ Series, Model : JM 320) with servo controlled fuzzy equipped head (Joemars AZ 50) and dielectric storage tank (Joemars D 320). Electrolyte copper was considered as tool material having size 08 mm diameter and positive polarity. The EDM machine is equipped with a fuzzy based servo controller for experimenting EDMing with various parameters at different levels. Technical specification of EDM are given in Table 3.1

Table 3.1 Technical Specifications of EDM Machine (Joemars AZ Series - JM 320)

Specifications	Details
Work Table Size	600 mm x 300 mm
X, Y Travel	300 mm x 200 mm
Ram Servo Travel	200 mm
Max. Electrode Weight	60 Kg
Max. Workpiece Weight	550 Kg
Work Tank	800 mm x 500 mm x 300 mm

Machine Unit Weight	1000 Kg
Outside Dimensions	1530 mm x 1590 mm x 1955 mm
Controller (Joemars AZ 50)	(Fuzzy Equipped)
Max. Machining Current	50 Amps
Total Power Input	4.5 KVA
Max. MRR	390 (mm^3/min)
Best Surface Finish	0.25 µm (Ra)
Net Weight	180 Kg
Outside Dimensions (Dielectric Tank - Joemars D 320)	580 mm x 500 mm x 1720 mm
Dielectric Tank Capacity	240 Ltrs.
Recirculation Pump	0.5 HP
Filtering Method	Filtering Paper Method

3.2.1 Development of PMEDM Setup

The working tank of EDM machine (Joemars AZ Series, Model : JM 320) has capacity of 240 Ltrs. In the current research the objective is to analyze effect of powder added dielectric on performance characteristics of PMEDM process. Keeping the objective in mind, fine power was to be added to the dielectric in different concentrations. For each set of experiments fresh charge of powder mixed dielectric have to be used. The process of changing the powder mixed dielectric and cleaning the tank and the dielectric circulation system from powder particles was very difficult and even not economically justifiable. So,

considering the economy of machining and to reduce the waste of dielectric (powder mixed) an auxiliary machining setup was designed having a secondary machining tank, dielectric storage tank and dielectric pumping and circulation system. Fig. 3.1 shows the developed experimental PMEDM setup.

The designed setup has a secondary machining tank. The tank was placed on machine table in the main machining tank. Fig. 3.2 shows the secondary machining tank. A fixture assembly was placed in the secondary machining tank to hold the workpeice during the experiments. The tank was filled with the dielectric (powder mixed) till the workpeice and tool (partly) submerges in to the fluid fully – principle of Die-sink EDM. A dielectric storage tank having a capacity of 10 ltrs. was designed and fabricated to handle sufficient quantity of powder mixed fluid (Fig. 3.3). A dielectric pumping and recirculation system was fabricated with a nozzle considering side flushing technique. In order to prevent powder particles from congregating and settling in the tank's bottom and corners, a motorized stirrer mechanism was also included.

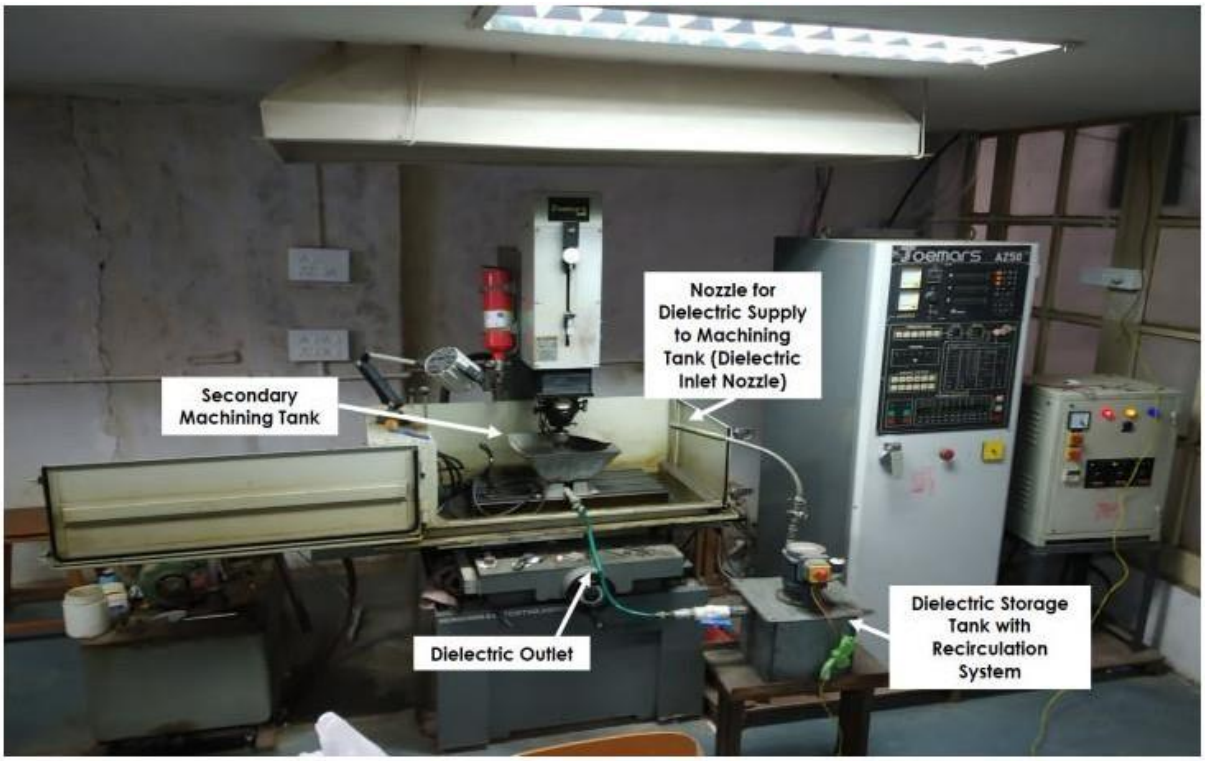

FIGURE 3.1 Experimental Setup of PMEDM

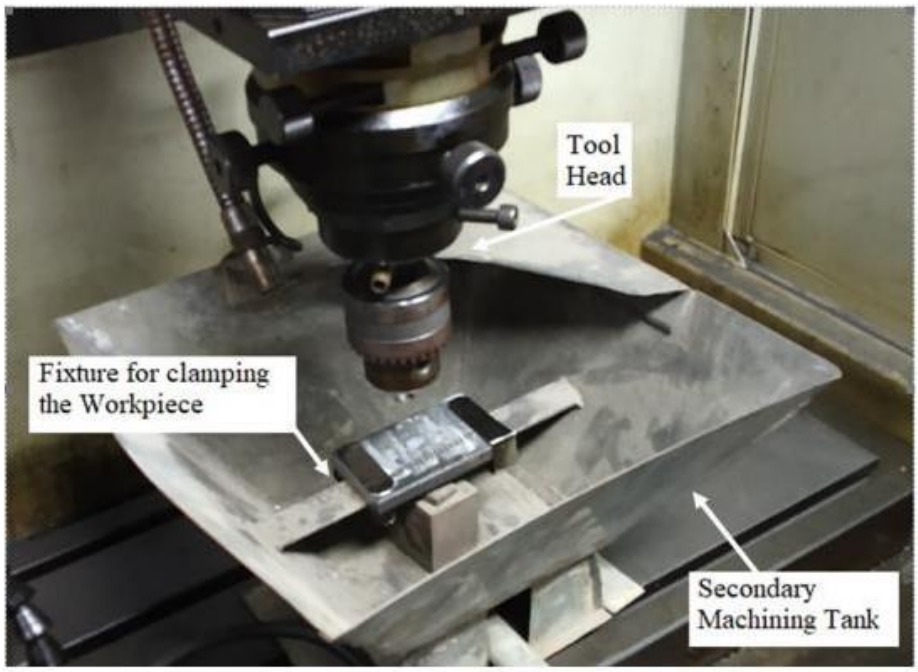

FIGURE 3.2 Secondary Machining Tank

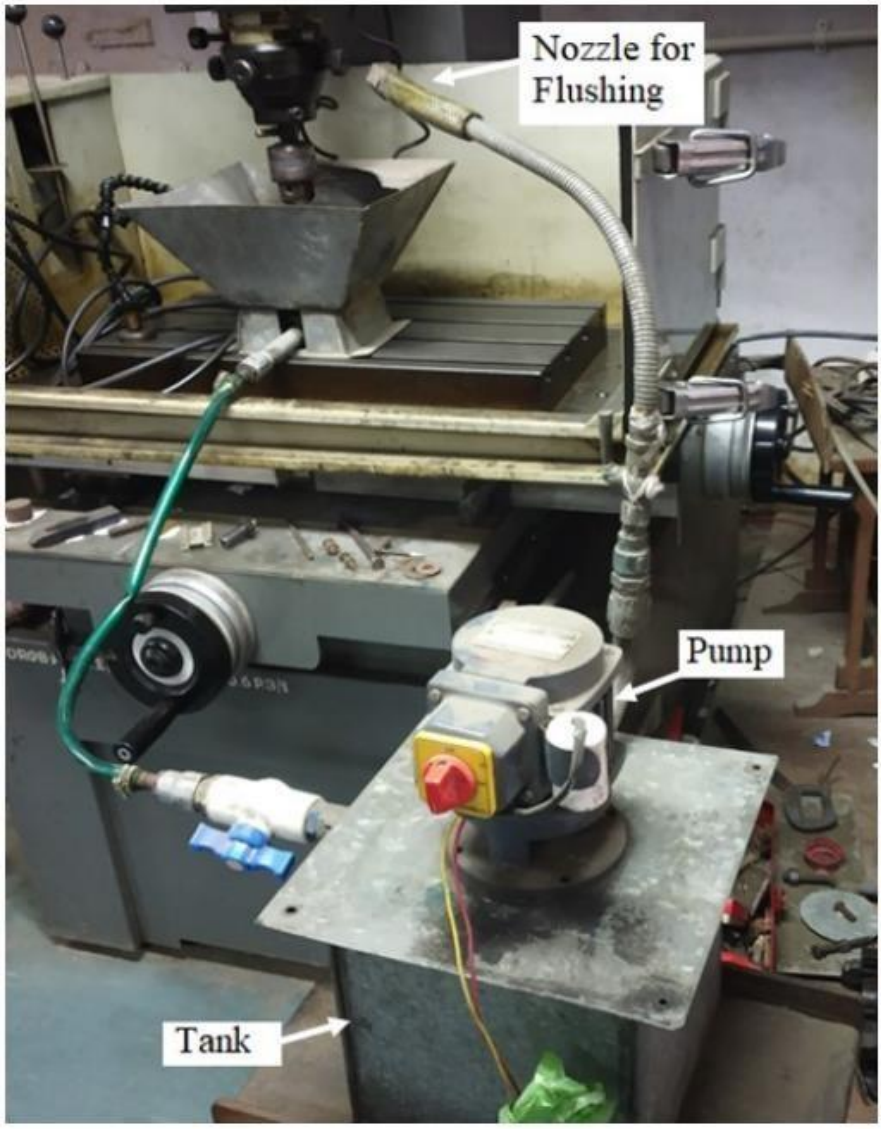

FIGURE 3.3 Dielectric Storage tank with recirculation mechanism

3.3 Selection of Materials

3.3.1 Workpeice Material

Titanium Alloy Grade 05 – Ti-6Al-4V is selected as the workpeice material in the present investigation. The alloys exhibit an exceptional strength to weight ratio, commendable creep and corrosion resistance, and deserving biocompatibility. The alloy is used for the applications that demands high fatigue-strength and high temperature-high strength. The chemical compositional analysis is given in Table 3.2. The alloy possesses low thermal conductivity, chemical affinity, low modulus of elasticity and work hardenability. Owing to

these properties conventional machining of these alloy is challenging. Thin plates of annealed Ti-6Al-4V with dimensions 100mm x 50mm x 2.5mm have been used for the experiments. The properties of Ti-6Al-4V alloy are presented in Table 3.3.

Table 3.2 Chemical Composition of Titanium Alloy Ti-6Al-4V

Element	% Weight
Titanium	89.36
Aluminium	5.98
Vanadium	3.99
Oxygen	0.20
Carbon	0.08
Nitrogen	0.5
Hydrogen	0.015

3.3.2 Tool Material

An Electrolytic copper (99.9%) tool (size – 08 mm diameter and 50 mm length) was used as the tool electrode material. Diepolishing (with emery paper) on the order of 0.1 to 0.15 microns was used to complete the tool's face. The electrode was mounted the three jaw chuck (of the machine spindle – Fig. 3.2) and was tightened adequately. To ensure the perpendicularity of the electrode with reference to the workpeice, the ―carbon paper method‖ was practiced. In the method a carbon paper is kept between the electrode and the workpeice and the electrode is pressed against the workpeice. This gives an impression of the tool in form of carbon imprint. Depending upon the imprint results the corresponding reorientation of the tool is to be done using the adjustment screws of the spindle head. The procedure is to be practiced till a full circle imprint is achieved.

Table 3.3 Properties of Ti-6Al-4V

Property	Value
Density	4.42 g/cm³
Young's Modulus	110 GPa
Poisson's Ratio	0.31
Thermal Conductivity	7.2 W/m·K
Volume Electrical Resistivity	170 ohm·cm
Melting Temperature	1649 °C ± 15°C
Specific Heat	560 J/kg·°C

3.3.3 Dielectric Fluid:

Deionized water is selected as dielectric fluid for the present research experiments. The deionized water is an environmental friendly alternate to the hydrocarbon based fluids/oils (example: kerosene, EDM oils) The literature analysis led to the conclusion that the erosion process therein possessed stronger thermal stability and, as a result, substantially higher power inputs could be employed to enhance MRR. Additionally, it is found that using deionized water as the dielectric minimizes the rate of tool wear. Whereas these hydrocarbons based oils decomposes in time and releases harmful vapors of CH4 and CO. The literature analysis led to the conclusion that the erosion process therein possessed stronger thermal stability and, as a result, substantially higher power inputs could be employed to enhance MRR. Additionally, it is found that using deionized water as the dielectric minimizes the rate of tool wear. Table 3.4 shows the values of typical properties of deionized water.

Table 3.4 Properties of Deionized Water

Property	Value
Breakdown Strength	65 – 70 kV/mm
Specific Heat	4200 J/kg·K
Thermal Conductivity	0.62 W/m·K

3.3.4 Powder Material

Aluminium Oxide (Al2O3) and Silicon Carbide (SiC) powders having noteworthy characteristics (thermos-physical) have been mixed with deionized water for the current research .Table 3.5 lists these powders' characteristics.

Table 3.5 Properties of Powder Materials

Properties	Aluminium Oxide (Al2O3)	Silicon Carbide (SiC)
Electrical resistivity (μΩ-cm)	1 × 10^8	1 × 10^9
Thermal conductivity (W $cm^{-1}°C^{-1}$)	0.35	1.0–5.0
Specific heat (J/kg-K)	990	460.54
Melting temperature (ºC)	2054	2987
Density (g/cm^2)	3.89	3.21
Heat of fusion (kJ/kg)	620	360

3.4 Process Parameters

A comprehensive literature survey for EDM and PMEDM process has been presented in Chapter 02. The parameters chosen for the current study project are Pulse Current (Ip), Pulse ON Time (TON), Pulse OFF Time (TOFF), and Powder Concentration in light of the results of the literature review. Surface Roughness (Ra), Tool Wear Rate (TWR), and Material Removal Rate (MRR) have all been studied in relation to the responses.

3.4.1 Selection of range of parameters

Pilot experiments were carried out to investigate the impact of the chosen process parameters on the PMEDM process responses. The outcomes of the pilot studies made it easier to define the set of parameters for the experiment. The process parameters MRR, TWR, and Ra for various combinations of the Ip, TON, TOFF, Gap voltage, and powder concentration in the dielectric were examined during the pilot tests. Table 3.6 displays the process parameters and their corresponding range-levels.

Table 3.6 Process Parameters and Their Levels

Parameters	Levels
Pulse Current (Amps)	6, 9, 13
Pulse ON Time (μSec)	5, 10, 15
Pulse OFF Time (μSec)	72, 82, 96
Powder Concentration (grms./ltrs.)	0.00, 0.25, 0.50

3.5 Design of Experiments

Design of experiments (DOE) is a technique for determining the interrelationships between the variables influencing the performance characteristics of the process. In essence, the information aids in the process parameter optimization that results in improved performance characteristics. The experiments in the current study were designed using the Response Surface Methodology (RSM)-Central Composite Design (CCD) technique..

3.5.1 Response Surface Method-Central Composite Design

A statistical-mathematical method known as the Response Surface Methodology (RSM)-Central Composite Design (CCD) is used to model and evaluate the relationship between process parameters and process responses [190, 191]. The RSM-CCD aids in determining the number of experiments needed for process analysis and improvement. The method aids in understanding how the chosen parameters interact with answers. The produced response surface empirical model explains the impact of the parameters of the sovereign process. RSM-CCD is a model that is often used to plan experiments, develop models, assess the impact of parameters on responses, and optimize parameters to improve process responses with the fewest possible experiments [192–194]. The technique is frequently used to issues with process characterization and/or optimization. The traditional Response Surface Methodology Approach is shown in Fig. 3.4.

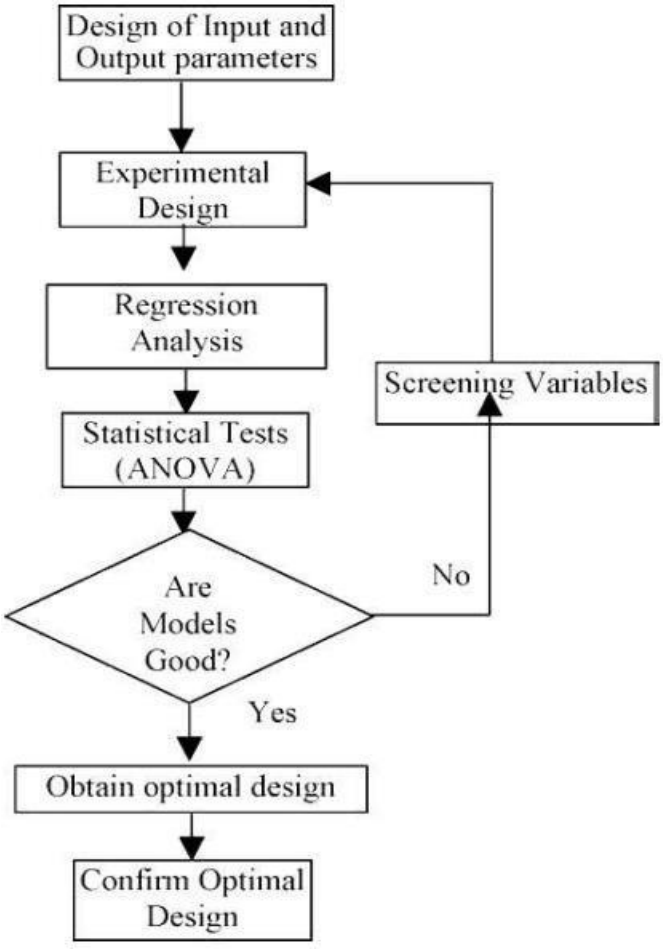

FIGURE 3.4 Set of Procedure for Response Surface Methodology

3.6 Measurement of Responses

The impact of adding powder to the dielectric, varying the powder concentration, and other process variables have all been examined in the current study effort. EDM and/or PMEDM process performance is characterized by the rate of material removal and tool wear. The surface finish or roughness of the process identifies its dimensional accuracy. The current experimental investigation's goals are to determine whether employing deionized water as a dielectric medium is feasible and to examine the impact of powder (in various concentrations) and other process factors on the integrity of the surface and the rate of MR and TWR**.** The methodology experimented for the characterizing performance analysis is deliberated underneath.

3.6.1 Material Removal Rate

For any machining process the rate of removal of material is of prime importance as it directly affects the productivity. In the present research, after every successful set of operation (machining), the workpeice was unclamped and weighed to know the weight loss - intern the amount of material removed. An electronic precision weighing scale (A&D HR-200 having least count 0.1µgrams.) was used to measure the weight of the workpeice before and after the machining. The weighing scale is shown in Fig. 3.5. Duration (time) for each successful experiment was recorded using a stopwatch (digital). The rate of removal of material was calculated using the value of weight loss – measured after every experiment. Eqn. 3.4 was used to calculate the MRR considering the volumetric loss of workpeice material (mm3 /min).

FIGURE 3.5 Precision Weighing Scale - A&D HR-200

3.6.2 Tool Wear Rate

For any production system the objective is to improve the MRR with the minimum possible tool wear. Lower electrical resistance and higher melting point are the typical characteristics of tool material. The tool is weighed after every successful machining operation and the value of difference in the weight of the tool is used to calculate TWR.

FIGURE 3.6 Surface Roughness Tester – SJ 201

3.7 Surface Characterization

3.7.1 Scanning Electron Microscopy (SEM)

Scanning electron microscope (SEM) is the most adaptable methods for analyzing (imaging) chemical composition, microstructure and the surface morphology of materials. The SEM results reveal the composition, topography (surface) and material's crystallographic details [195]. In the SEM, an electron pillar is created in high vacuum by electron weapon, and this bar is then quickened towards the example with the assistance of positive electric field, and afterward centered around to the example with the assistance of attractive focal points. This engaged electron shaft communicates with the example surface, and the cooperation is changed in to a picture of the example. The goal of the SEM picture differs relying on the capacity of the electron spot delivered by the attractive focal points. The electron bar communicates with certain volume of the example which is under scrutiny, and the profundity of this connection is an element of the organization of the example, vitality and edge of the occurrence electron bar [196].

3.7.2 Energy Dispersive Spectroscopy (EDAX)

Energy Dispersive X-ray Analysis (EDAX) is used for observing the compositional analysis. The X-beam signals delivered because of the association of the electron shaft with the example during the SEM investigation are utilized for the Vitality Dispersive X-beam spectroscopic (EDX) considers, which is commonly called miniature examination. The barrage of the essential electrons on the example surface offers ascend to the launch of the inward shell electrons of the example, and the change of the external electrons to top off the opening in the internal shell causes the creation of x-beams: the fingerprints of the components present in the example. The EDX spectrometer gathers these x-beams and the natural examination is conceivable utilizing the x-beam top force and position data with the assistance of the product related with the framework [197]. In the present research surface morphology analysis is done using SEM (Make : Philips, Netherlands, Model : ESEM EDAX XL-30) at Sophisticated Instrumentation Centre for Applied Research and Testing – SICART, V. V. Nagar, Gujarat. Fig 3.7 shows the SEM setup.

FIGURE 3.7 SEM Machine - ESEM EDAX XL-30

CHAPTER-4
RESULTS AND DISCUSSIONS

4.1 Introduction

The effects of the process variables pulse current (Ip), pulse ON time (TON), pulse OFF time (TOFF), and powder concentration in the dielectric on the responses material removal rate (MRR), tool wear rate (TWR), and surface roughness (Ra) have been discussed for PMEDM of Ti6Al4V using Al2O3 and SiC mixed Deionized water as the dielectric fluid. The Response Surface Method-Central Composite Design methodology was used to develop the tests. In order to prevent any systematic mistake from seeping into the system, a total of 30 experimental runs have been completed in triplicate. Table 4.1 lists the experimental findings, including the measured response values for MRR, TWR, and Ra.

4.2 ANOVA (Analysis of Variance) Analysis

ANOVA is a common statistical method for interpreting experimental data. ANOVA aids in identifying the significance of a process parameter's impact on performance metrics. This makes it possible to learn how much of an impact each regulated parameter has on the desired quality attribute. By examining the main outcomes of each of the aspects, it is possible to identify the pattern illustrating the influence of various components on the process. The ANOVA based on the raw data identifies the variables that affect the average response as opposed to decreasing variation [198]. The MINITAB 16 program was used to examine the relative importance of the factors in relation to the output responses in order to determine the optimum parameter combinations from the ANOVA analysis. The following steps are included in the ANOVA analysis: (Eqn. 4.1 to 4.10);

Total of Results $(T) = \sum_{i=1}^{n} \sum_{j=1}^{R} Yij$ (4.1)

Where Yij represents the value of the characteristics in the ith trial jth repetition

Correction Factor $(C.F) = T^2/N$ (4.2)

Where N is the total number of Experiments.

Total sum of squares $(SST) = \sum_{i=1}^{n} \sum_{j=1}^{R} Yij - C.F$ (4.3)

The degree of variance in the response is measured by the sequential Sum of squares for each term in the model.

Sum of Squares of Parameter

$$(SSA) = [\ A\ (1)^2/NA1 + A\ (2)^2/NA2 + \ldots + A\ (N)^2/NAN\ ] - C.F \qquad (4.4)$$

Where N_{A1}, N_{A2} and N_{An} are the number of experiments with parameter A at respective levels 1,2…, n. The sums of squares for all the factors are calculated similarly.

Error sum of squares $(SSe) = (SST) = (SSA)$ (4.5)

The degree of freedom describes how much information can be extracted from a given collection of data and be uniquely identifiable. The DOF of a factor is one less than the levels of data for that factor. The degree of freedom quantifies the amount of independent information required to calculate each squared sum.

Degrees of Freedom $(DOF) = (\text{Total No. of Trial}) - 1$

(4.6) DOF of each Parameters = $(\text{Number of levels of each parameter} - 1)$

(4.7) Variance due to Parameter $(VA) = SSA / fA$ (4.8)

Perecentage contribution of parameter A towards mean of the response

$$(PA) = [SSA/SST]\ X\ 100 \qquad (4.9)$$

The variance ratio (F-ratio) compares the variation brought on by an error term to the variance brought on by the impact of a factor. This ratio is used to determine the significance of the component under investigation in proportion to the variance of all the elements contained in the error term. The F value from the study is compared to a value from a standard F-table for a certain degree of significance. When the computed F value is less than the value obtained from the F tables at the selected level of significance, the factor does not contribute to the sum of squares within the confidence level.

$$FA = VA/VE \qquad (4.10)$$

An analysis of variance (ANOVA) assists in formally evaluating the relevance of the key components and their interactions by comparing the mean square against an estimate of the experimental errors at specific confidence levels. Analyzing the ANOVA table for a particular investigation enables one to decide which components require control and which do not. Analysis of variance (ANOVA) was used in the current study to assess the model's significance and lack of fit. If the probability (P) value in this case is less than 0.05, it is statistically significant at a 95% confidence level.

4.2.1 Analysis of Material Removal Rate (MRR)

ANOVA was used to examine the MRR findings and find the important variables influencing the performance metrics. The ANOVA table for the mean MRR with a 95% confidence interval is shown in Table 4.2. The basic idea behind the F-test is that a process parameter's (input) bigger F value indicates a stronger impact on the response parameter. Each factor's variance data has been F-tested to determine its significance. The probability (P) value used in the current study is less than 0.05, which denotes that all parameters with P values below 0.05 are significant parameters. Input Current (F value: 12.97), Pulse ON Time (F value: 23.38), and Powder Concentration (F value: 2.19) were shown to be significant under the experimental circumstances. MRR is not significantly affected by pulse OFF time. Pulse ON Time, input current, and powder concentration are shown to have the greatest effects on MRR.

TABLE 4.1 Analysis of Variance (General Linear Model) for MRR

Source	DOF	Seq SS	Adj SS	Adj MS	F	P
Ip	2	8.5652	8.6841	4.3420	12.97	0.000
TON	2	16.1218	15.6473	7.8236	23.38	0.000
TOFF	2	0.2035	0.4142	0.2071	0.62	0.548
P.C.	2	3.4725	3.4725	1.7363	5.19	0.015
Error	21	7.0278	7.0278	0.3347		
Total	29	35.3909				
S				0.578497		
R^2				80.14%		
R^2 (Adj.)				72.58%		

Different residual plots for the ANOVA of Material Removal Rate are shown in Fig. 4.1. The Normal Probability curve for residuals is shown in Fig. 4.1 (a). The shown residual

values show that the error terms have a normal distribution. Residuals versus fits plot is shown in Fig. 4.1 (b). The residuals' assumption of random distribution and constant variance is confirmed by the figure. The distribution of the residuals for all experimental observations may be seen in the residuals histogram. The residuals' histogram, shown in Fig. 4.1(c), indicates that the residuals (and consequently the error terms) are regularly distributed. A plot of residuals vs order of data collection is shown in Fig. 4.1 (d). The premise that the residuals are independent of one another is verified using the figure. The residuals are dispersed randomly around the middle line and the plot displays no discernible pattern. Fig. 4.2 presents the MRR principal effect plot. The graph shows that as the pulse current, pulse ON time, and powder concentration rise, so does the MRR. While a longer pulse OFF time causes the MRR to decrease.

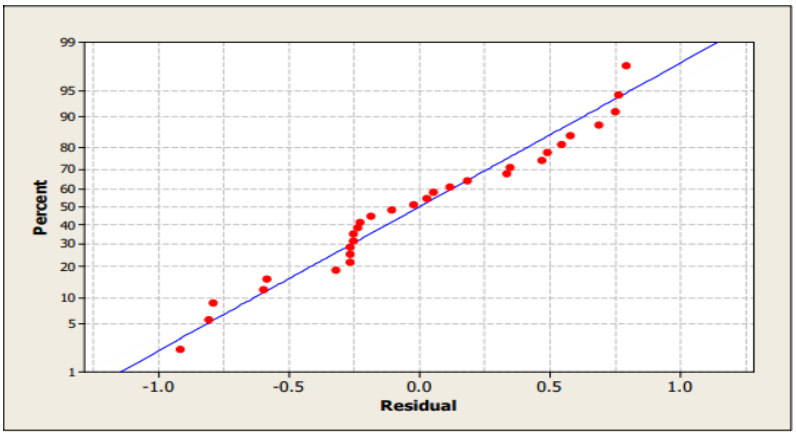

FIGURE 4.1 (a) Normal Probability Plot for Residuals – MRR

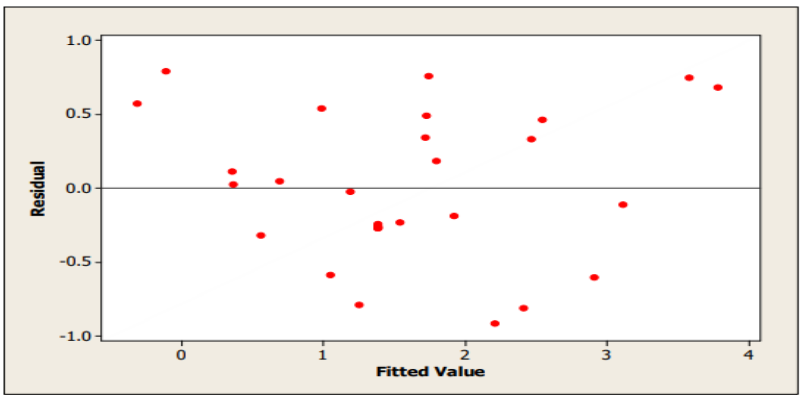

FIGURE 4.1 (b) Residuals Vs Fitted Values – MRR

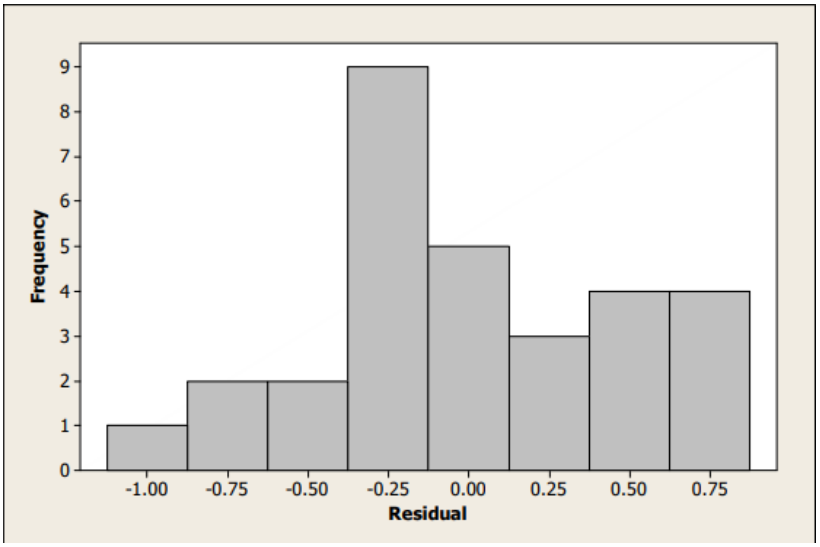

FIGURE 4.1 (c) Histogram of Residuals – MRR

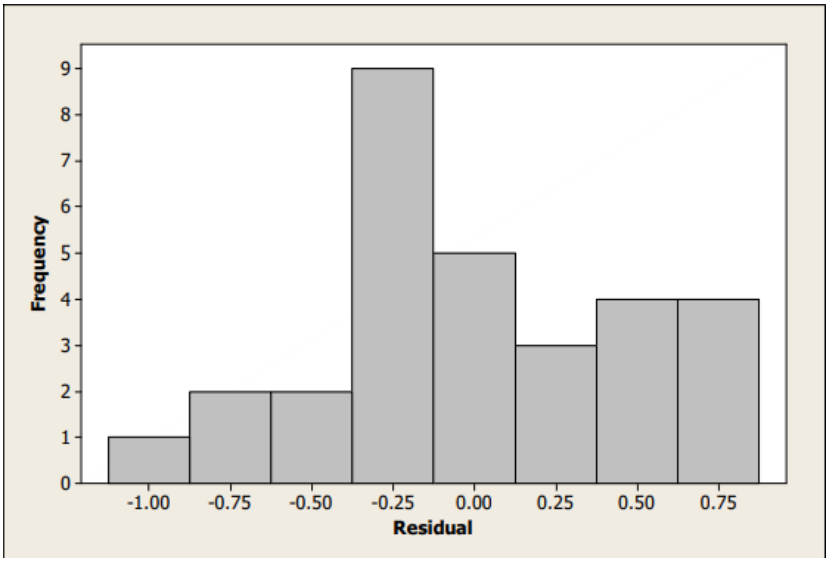

FIGURE 4.1 (d) Residuals Vs Order of Data - MRR

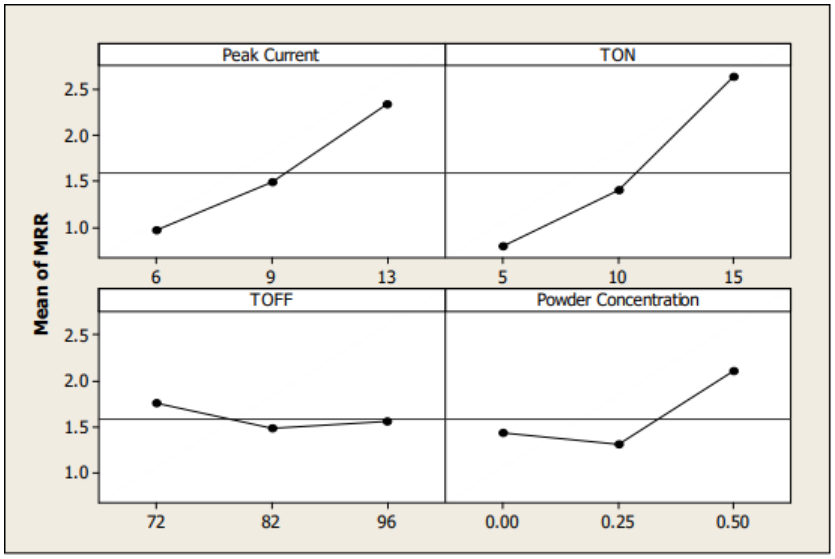

FIGURE 4.2 Main Effect Plots – MRR

4.2.2 Tool Wear Rate (TWR) Analysis

The TWR findings were analyzed using ANOVA to pinpoint the crucial elements influencing the procedure' effectiveness. The ANOVA table with the 95% confidence interval for the mean TWR is shown in Table 4.3. Under the experimental conditions, it was determined that Input Current (F value: 27.42), Pulse ON Time (F value: 6.83), and Powder Concentration (F value: 7.23) were significant. It has been discovered that TWR is significantly influenced by Pulse ON Time, Powder Concentration, and Input Current.

TABLE 4.2 Analysis of Variance (General Linear Model) for TWR

Source	DOF	Seq SS	Adj SS	Adj MS	F	P
Ip	2	0.267188	0.229122	0.114561	27.42	0.000
TON	2	0.043631	0.057092	0.028546	6.83	0.005
TOFF	2	0.000097	0.004187	0.002094	0.50	0.613
P.C.	2	0.060423	0.060423	0.030212	7.23	0.004
Error	21	0.087728	0.087728	0.004178		
Total	29	0.459067				

S				0.0646336		
R^2				80.89%		
R^2 (Adj.)				73.61%		

In Fig. 4.3, various residual plots for an ANOVA of tool wear rate are displayed. The Normal Probability curve for residuals is shown in Fig. 4.3 (a). The shown residual values show that the error terms have a normal distribution. Residuals versus fits plot is shown in Fig. 4.3 (b). The residuals' assumption of random distribution and constant variance is confirmed by the figure. The distribution of the residuals for all experimental observations may be seen in the residuals histogram. The residuals' histogram, shown in Fig. 4.3(c), indicates that the residuals (and consequently the error terms) are regularly distributed. A plot of residuals vs sequence of data collection is shown in Fig. 4.3 (d). The residuals are dispersed randomly around the middle line and the plot displays no discernible pattern. Fig.
4.4 presents the TWR principal effect graphic. The graph demonstrates that when the pulse current and pulse ON time increases, the TWR also rises.

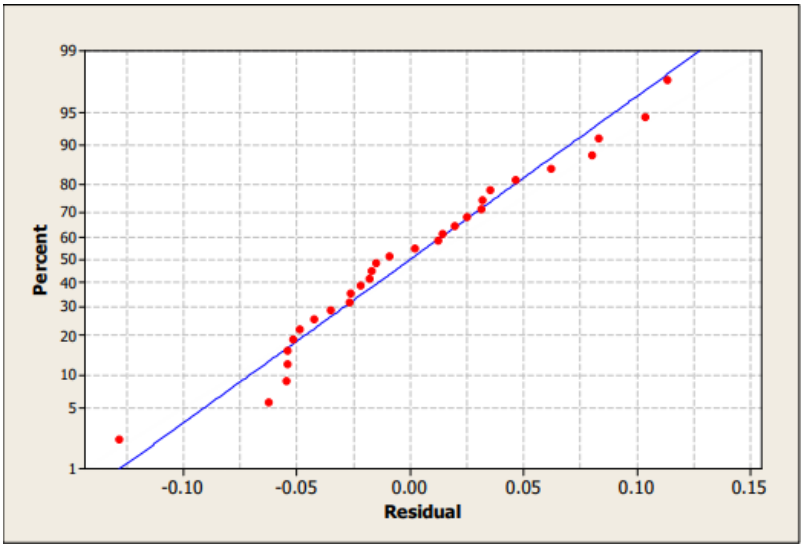

FIGURE 4.3 (a) Normal Probability Plot for Residuals – TWR

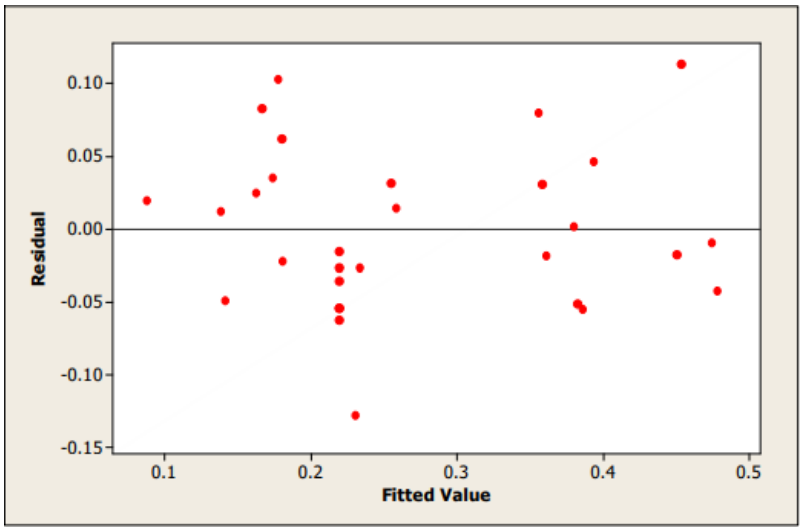

FIGURE 4.3 (b) Residuals Vs Fitted Values – TWR

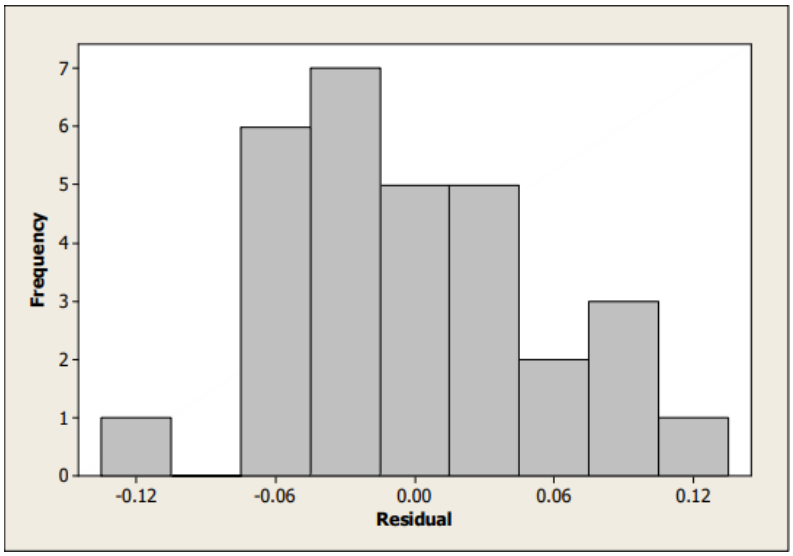

FIGURE 4.3 (c) Histogram of Residuals – TWR

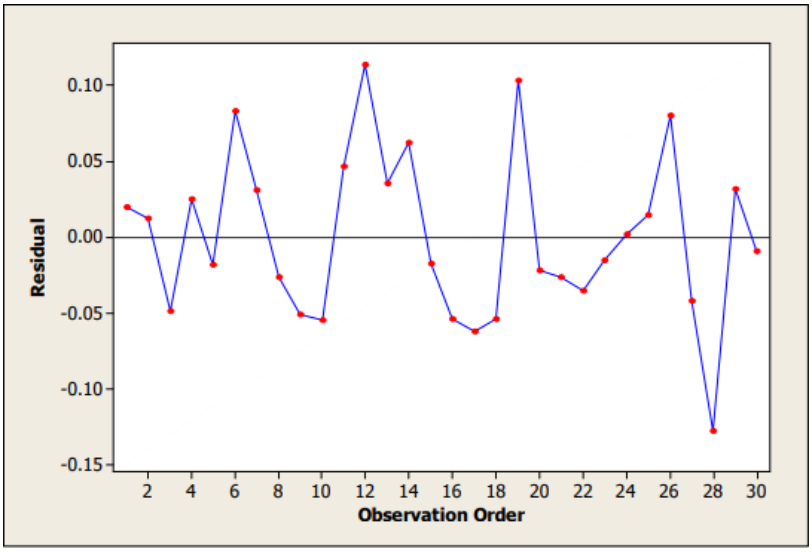

FIGURE 4.3 (d) Residuals Vs Order of Data – TWR

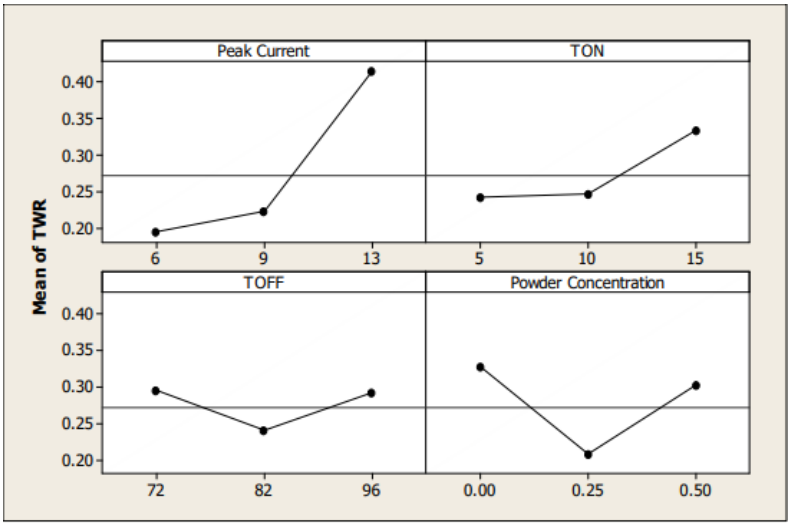

FIGURE 4.4 Main Effect Plots – TWR

4.2.3 Analysis of Surface Roughness (SR)

ANOVA was used to examine the findings for SR and find the important variables influencing the performance metrics. The ANOVA table for the mean SR with a 95% confidence interval is shown in Table 4.4. Input Current (F value: 18.45), Pulse ON Time (F value: 7.17) and Pulse OFF Time (F value: 10.44) were shown to be significant under the experimental circumstances. It has been shown that Input Current, Pulse OFF Time, and Pulse ON Time all have the greatest impact on SR. Additionally, it has been found that Powder Concentration has little impact on SR. Different residual plots for the ANOVA of Surface Roughness are shown in Fig. 4.5. The Normal Probability curve for residuals is shown in Fig. 4.5 (a). The shown residual values show that the error terms have a normal distribution. Residuals versus fits plot is shown in Fig. 4.5(b). The residuals' assumption of random distribution and constant variance is confirmed by the figure. The distribution of the residuals for all experimental observations may be seen in the residuals histogram. The residuals' histogram, shown in Fig. 4.5(c), indicates that the residuals (and consequently the error terms) are regularly distributed. The plot of residuals vs order of data collection is shown in Figure 4.5(d). The residuals are dispersed randomly around the middle line and the plot displays no discernible pattern. The primary effect plot for TWR is displayed in Fig. 4.6. The graph shows that the SR rises as the pulse current and pulse ON time increase.

TABLE 4.3 Analysis of Variance (General Linear Model) for SR

Source	DOF	Seq SS	Adj SS	Adj MS	F	P
Ip	2	6.1174	7.2141	3.6070	18.45	0.000
TON	2	3.3678	2.8057	1.4029	7.17	0.004
TOFF	2	4.1576	4.0831	2.0416	10.44	0.001
P.C.	2	0.3017	0.3017	0.1508	0.77	0.475
Error	21	4.1065	4.1065	0.1955		
Total	29	18.0510				
S				0.442207		
R^2				77.25%		
R^2 (Adj.)				68.58%		

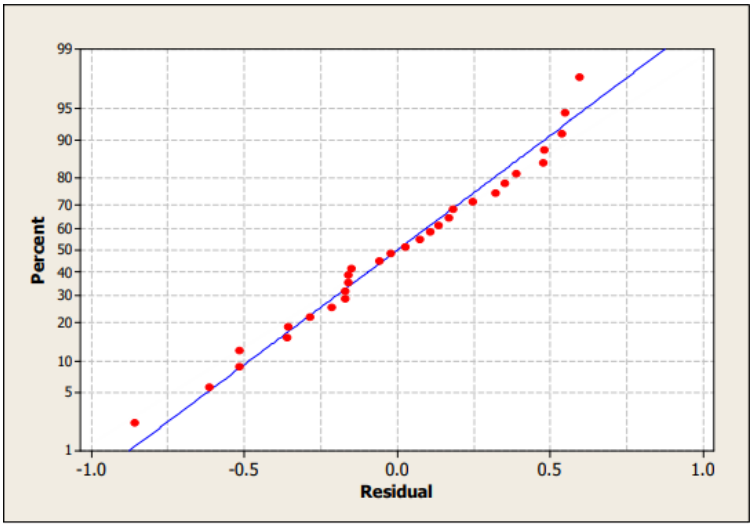

FIGURE 4.5 (a) Normal Probability Plot for Residuals – SR

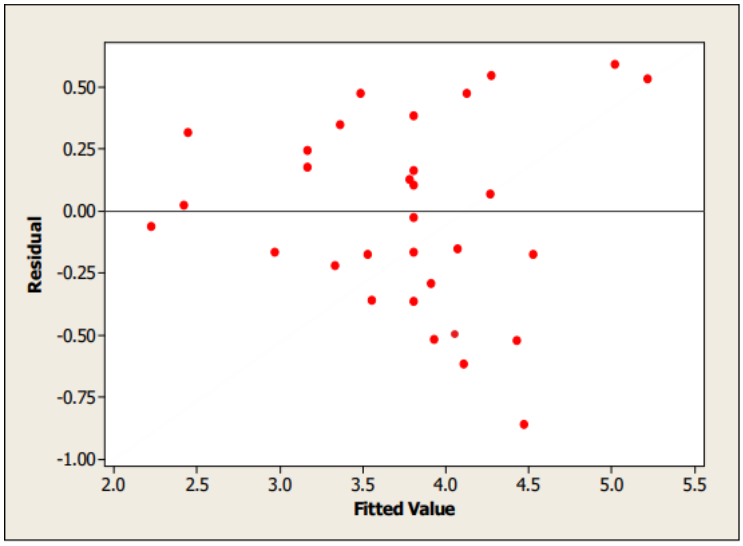

FIGURE 4.5 (b) Residuals Vs Fitted Values – SR

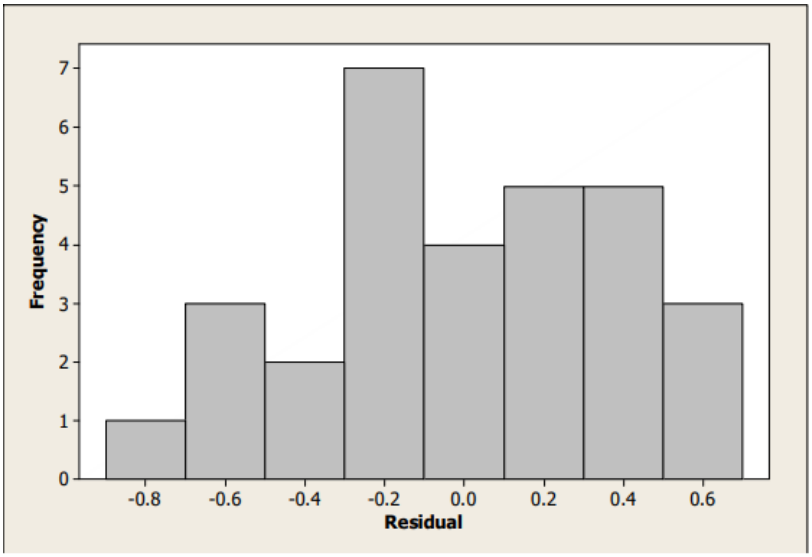

FIGURE 4.5 (c) Histogram of Residuals – SR

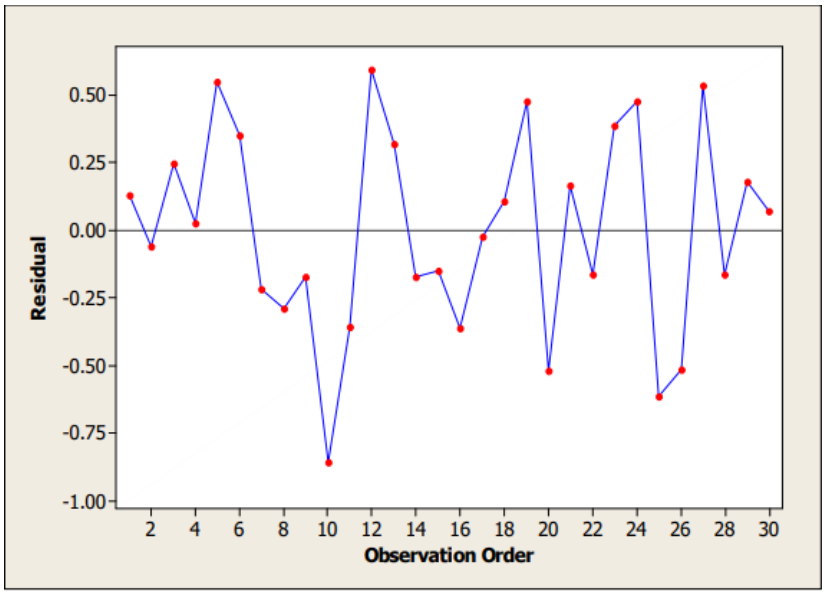

FIGURE 4.5 (d) Residuals Vs Order of Data – SR

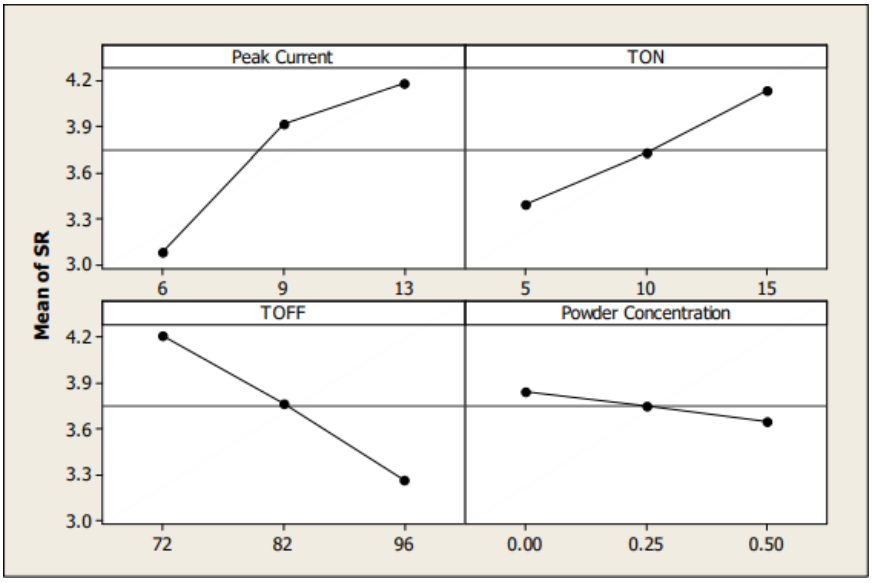

FIGURE 4.6 Main Effect Plots – SR

4.3 Regression Modeling and RSM Analysis

In the current study, RSM analysis is employed to determine how the process parameters and responses relate to one another. Design Expert 12 is used to do the analysis. The experiment's independent variables are assumed by the design to be continuous and subject

to testing with low margins of error. The experimental design had to be optimized for the response variables (Y). To accurately represent the real correlation between independent variables and response surfaces, an appropriate approximation must be found. Randomization was used during the experimental run to reduce error and the impact of uncontrollable factors. The answer was used to create an empirical model that, using a second-degree polynomial equation, Eqn (4.11) corresponds to the experimental variables.

$$Y = \beta 0 + \sum_{i=1}^{n} \beta iXi + \sum_{i=1}^{n} \beta iiXi^2 + \sum_{i=1}^{n} \beta ijXiXj \pm \xi \qquad (4.11)$$

Y is the predicted response, 0 is the constant coefficient, i is the linear coefficients, ii is the quadratic coefficients, ij is the interaction coefficients, and n is the number of factors examined and optimized in the experiments. Xi and Xj are the coded values of the variable parameters for the leaching process, and is the random error. As was discussed earlier for the screening stage, an ANOVA analysis is used to determine the significance of the coefficients. The fitted model should accurately reflect the data connection inside the experimental region in order to provide a precise forecast. To assess the relevance of the second order model while fitting linear models, an ANOVA test should be used. The latter may be deemed sufficient if the regression is significant and a non-significant lack of fit is discovered for the selected confidence level (=0.05).A substantial model does not, however, imply that the data's volatility is well explained. Additionally, it is necessary to analyze the residual plots and evaluate the coefficient of determination (R2) and adjusted coefficient of determination (Adj R2), which show the proportion of variance that is explained by the model. One of the fundamental presumptions for the validity of ANOVA is that the residuals follow a normal distribution, which is shown by the normal probability plot. The plot of residuals vs the ascending projected response values may be used to assess the homogeneity of the variance, which is another ANOVA assumption. The outcome of the optimization of two elements can be seen as a solid surface in three dimensions. When there are more than two components, the graphical representation is generated for two of them while keeping the values of the additional elements constant. Another choice is to show the response surface using a contour plot, which consists of lines of constant response that correspond to a certain height of the response surface.

Using Design Expert 12,Regression analysis was done on the RSM-CCD runs' experimental results. A sequential sum of squares test based on an analysis of variance was

carried out before selecting the best model to be fitted. Linear, two-factor interaction, and quadratic models were examined to see if adding more terms enhanced the fitting as shown by the F value in the Fischer's F test. The F values may be converted into p values using the F probability distribution curve. To assess the model's relevance, one might compare the F value to a threshold F value or the accompanying p value to a threshold p value. The significance level that was chosen, in this case 5%, will determine the threshold p value. The model was not aliased, and the highest order polynomial for which the new terms were significant was chosen. The two factor interaction model was selected for fitting based on the test outcome. For MRR, TWR, and SR, models were created with notable factor effects.

4.3.1 Analysis of Material Removal Rate (MRR) : Analysis of Variance (ANOVA) is used to examine the response data for MRR and to verify the sufficiency of the created model using a regression model significance test. Using Design Expert 12, regression analysis was performed on the experimental findings from the RSM-CCD runs. For MRR, a quadratic model was chosen to account for the curvature impact. Table 4.5 displays the ANOVA and regression statistics for the entire two factor interaction model as well as the findings of the quadratic model for MRR. The combined R2 and corrected R2 score is over 90%. This shows that the regression model does a great job of explaining the relationship between the independent variables (factors) and the response (MRR). A model is considered statistically significant when the related p-value is less than 0.05 (i.e., = 0.05, or 95% confidence). Other important variables are Pulse ON Time (F value: 146.68), Powder Concentration (F value: 20.22), the interaction between Pulse Current and Pulse ON Time, Pulse Current and Powder Concentration, and the Second order term of Pulse Current.

TABLE 4.4 Response Surface Analysis for MRR

Source	Sum of Squares	DOF	Mean Square	F Value	P Value	Significance
Model	33.8	14	2.41	22.79	0.0001	Significant
Ip	8.41	1	8.41	79.42	0.0001	Significant
TON	15.54	1	15.54	146.68	0.0001	Significant

TOFF	0.1841	1	0.1841	1.74	0.2072	
P.C.	2.14	1	2.14	20.22	0.0004	Significant
Ip * TON	1.13	1	1.13	10.63	0.0053	Significant
Ip * TOFF	0.0641	1	0.0641	0.605	0.4488	
Ip * P.C.	3.48	1	3.48	32.89	0.0001	Significant
TON * TOFF	0.4102	1	0.4102	3.87	0.0679	
TON * P.C.	0.0004	1	0.0004	0.004	0.9504	
TOFF * P.C.	0.3515	1	0.3515	3.32	0.0885	
Ip^2	0.4883	1	0.4883	4.61	0.0486	Significant
TON^2	0.1391	1	0.1391	1.31	0.2698	
TOFF^2	0.1989	1	0.1989	1.88	0.1908	
P.C^2	1.45	1	1.45	13.7	0.0021	Significant
Residuals	1.59	15	0.1059			
Lack of Fit	1.59	10	0.1588	1155.21	0.0001	Significant
Pure Error	0.0007	5	0.0001			
Total	35.39	29				

Std. Dev.	0.3255					
R^2	95.51%					
R^2 (Adj.)	91.32%					

TABLE 4.5 Estimated Regression Co-efficient for MRR

Source	Coefficient Estimate	Coefficient Terms of Actual Factors
Constant	1.48	-14.76927
Ip	0.6838	0.47291
TON	0.9294	0.081528
TOFF	-0.1012	0.324741
P.C.	0.3451	-13.7714
Ip * TON	0.2649	0.01514
Ip * TOFF	0.0631	0.001503
Ip * P.C.	0.4662	0.532743
TON * TOFF	-0.1599	-0.002665
TON * P.C.	-0.0051	-0.004115
TOFF * P.C.	0.148	0.049328
Ip^2	-0.4438	-0.03623

TON^2	0.2317	0.009269
TOFF^2	-0.2855	-0.001983
P.C^2	0.7485	11.97642

The estimated regression coefficients for the factors, interaction with other factor and second order factors are shown in Table 4.5. The RSM-based mathematical models for MRR is represented in Eqn. 4.12 as;

MRR = (-14.7693)+(0.4729 * Peak Current) + (0.0815 * TON) + (0.3247 * TOFF) - (13.7714 * Powder Concentration) - (0.0362 * Peak Current * Peak Current)+(0.0093 * TON * TON)-(0.002 * TOFF * TOFF)+(11.9764 * Powder Concentration * Powder Concentration) + (0.0151 * Peak Current * TON) + (0.0015 * Peak Current * TOFF) + (0.5327 * Peak Current * Powder Concentration) - (0.0027 * TON * TOFF) - (0.0041 * TON * Powder Concentration) + (0.0493 * TOFF * Powder Concentration)

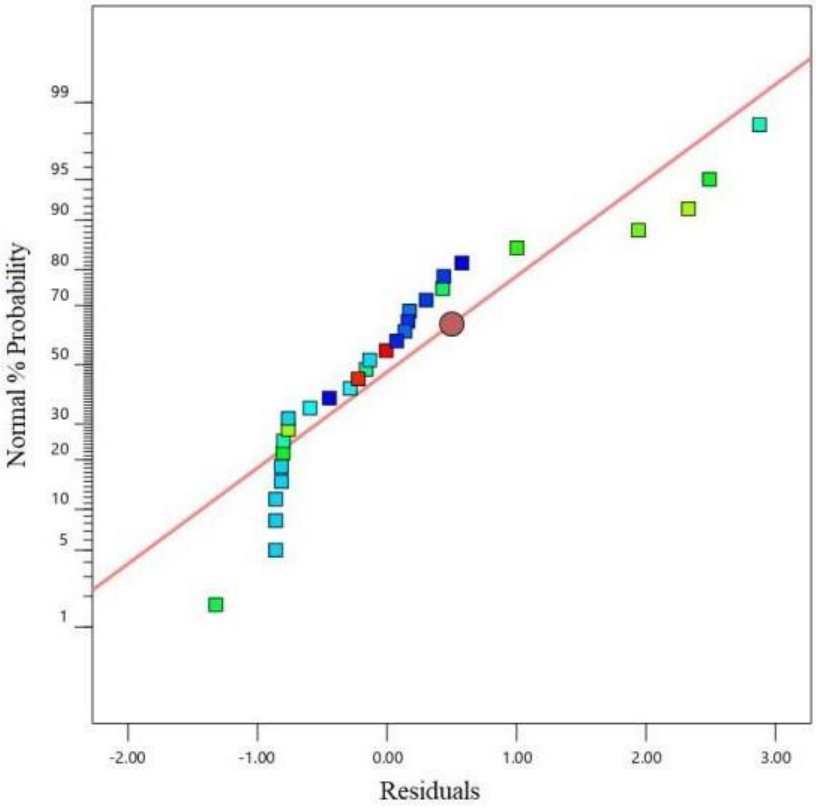

FIGURE 4.7 (a) Normal Probability Plot for Residuals – MRR

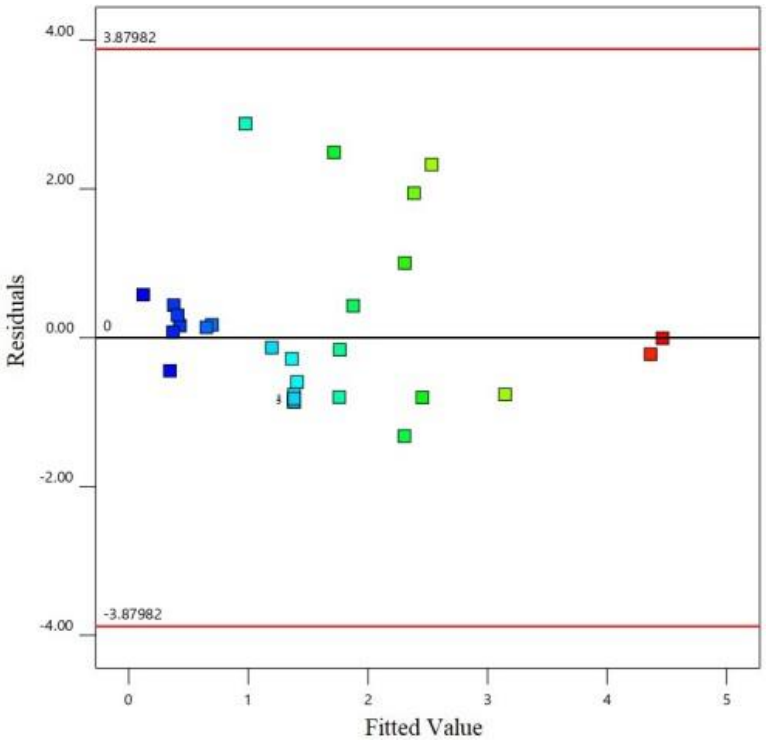

FIGURE 4.7 (b) Residuals Vs Fitted Values – MRR

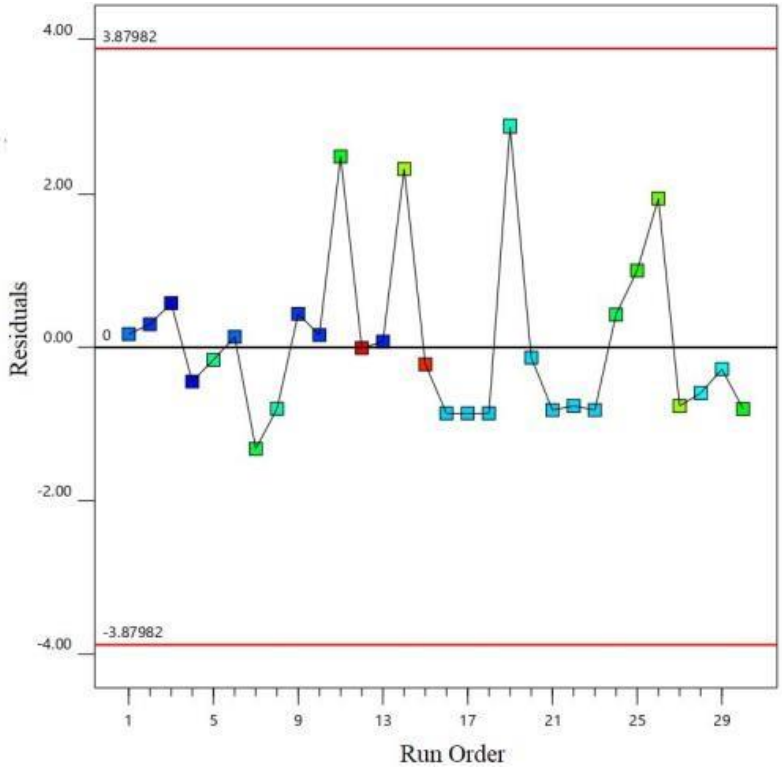

FIGURE 4.7 (c) Residuals Vs Run Order of Data - MRR

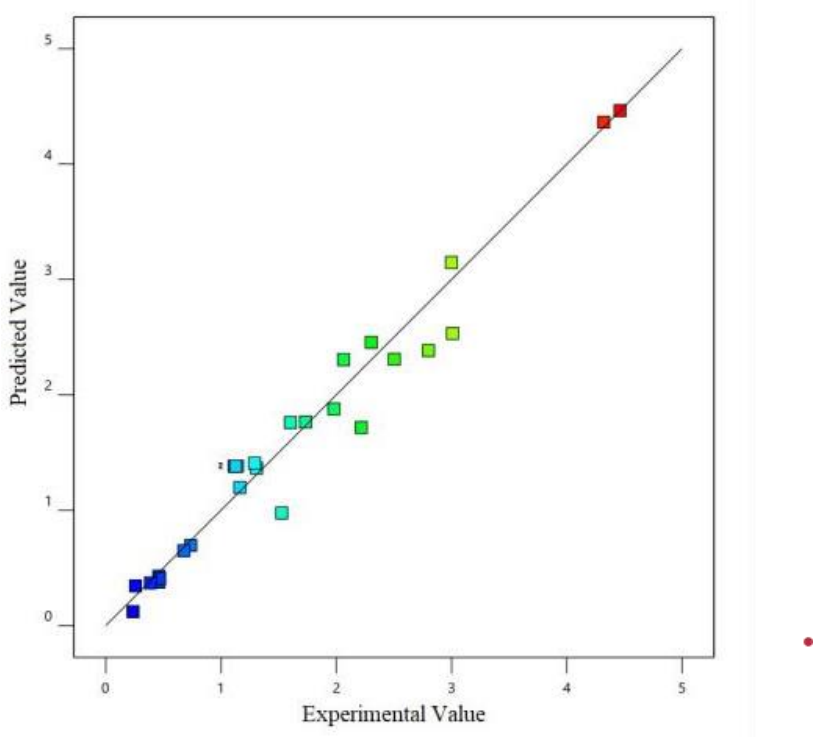

FIGURE 4.8 Experimental Value Vs Predicted Value – MRR

The ANOVA table (Table 4.5) clearly shows how Ip - TON and Ip - PC have an interaction effect on MRR. Figure 4.9 displays the interaction plot for Pulse (Peak) Current and Pulse ON Time with MRR. Figure 4.10 displays the interaction plot for Pulse ON Time and Powder Concentration with MRR. Peak (pulse) Current increased due to an increase in discharge energy, which led to an increase in MRR. Low pulse ON times resulted in a workpiece's heating period being so brief that just a tiny portion of the material melted, giving the MRR a lower value. As more peak current density and appropriate discharge energy were achieved with a longer pulse signal (bigger Pulse ON Time), the MRR increases. As operating with high pulse current and longer pulse ON times the energy intensity going into the workpeice increases and hence results in higher melting of material and thereby increases the rate of removal of material. It can also be seen from Fig. 4.10 that increase in the powder concentration along with Pulse ON Time improves MRR as high density, widens the plasma channel and covers a larger area.

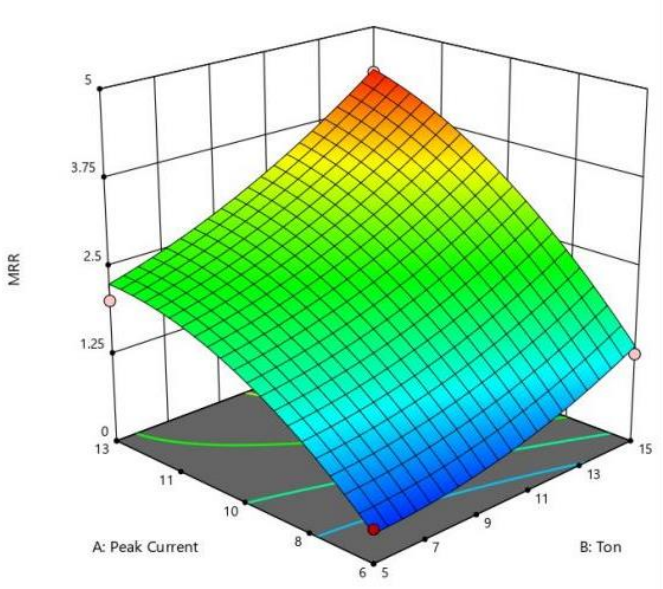

FIGURE 4.9 Interaction Plot Ip, TON vs MRR

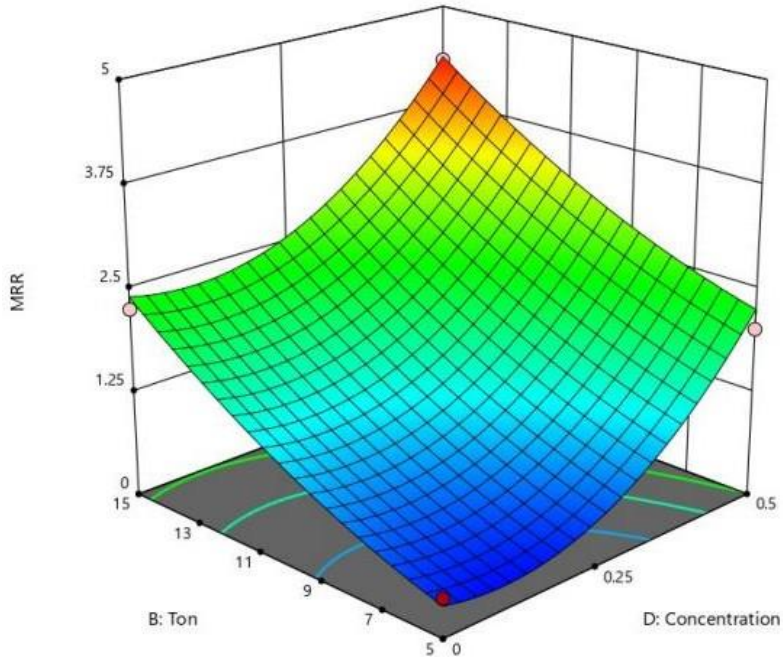

FIGURE 4.10 Interaction Plot TON, Powder Concentration vs MRR

4.3.2 Analysis of Tool Wear Rate (TWR)

The results of the entire two component interaction model, which used the quadratic model for MRR, are shown in Table 4.7 as ANOVA and regression statistics. According to the value of R2, which is 88.21%, the regression model best explains the association between the independent variables (factors) and the response (TWR). A model is considered statistically significant when the related p-value is less than 0.05 (i.e., = 0.05, or 95% confidence).

TABLE 4.6 Response Surface Analysis for TWR

Source	Sum of Squares	DOF	Mean Square	F Value	P Value
Model	0.4049	14	0.0289	8.01	0.0001
Ip	0.2181	1	0.2181	60.44	0.0001
TON	0.0383	1	0.0383	10.62	0.0053
TOFF	0	1	0	0.0133	0.9096
P.C.	0.0025	1	0.0025	0.7001	0.4159
Ip * TON	0.0061	1	0.0061	1.69	0.2137
Ip * TOFF	0	1	0	0.0037	0.9522
Ip * P.C.	0.0227	1	0.0227	6.28	0.0242
TON * TOFF	0.0037	1	0.0037	1.04	0.3251
TON * P.C.	0	1	0	0.0134	0.9094
TOFF * P.C.	0.0011	1	0.0011	0.3054	0.5886
Ip^2	0.0063	1	0.0063	1.75	0.2059
TON^2	0.0188	1	0.0188	5.21	0.0375
TOFF^2	0.0041	1	0.0041	1.13	0.3055

Source	Sum of Squares	DOF	Mean Square	F Value	P Value

Model	0.4049	14	0.0289	8.01	0.0001
Ip	0.2181	1	0.2181	60.44	0.0001
P.C^2	0.0577	1	0.0577	15.99	0.0012
Residuals	0.0541	15	0.0036		
Lack of Fit	0.0524	10	0.0052	15.1	0.0039
Pure Error	0.0017	5	0.0003		
Total	0.4591	29			
Std. Dev. = 0.0601	R^2 = 88.21%		R^2 (Adj.) =	77.20%	

TABLE 4.7 Estimated Regression Co-efficient for TWR

Source	Coefficient Estimate	Coefficient Terms of Actual Factors
Constant	0.2342	-2.00304
Ip	0.1101	-0.070491
TON	0.0462	0.088499
TOFF	-0.0016	0.050503
P.C.	-0.0119	-1.40341
Ip * TON	0.0195	0.001113
Ip * TOFF	0.0009	0.000022
Ip * P.C.	0.0376	0.042959
TON * TOFF	-0.0153	-0.000254
TON * P.C.	-0.0017	-0.00139
TOFF * P.C.	-0.0083	-0.002762

Ip^2	0.0505	0.004119
TON^2	-0.0852	-0.003407
TOFF^2	-0.0408	-0.000283
P.C^2	0.1492	2.38766

The regression coefficients (estimated) for the factors, interaction with other factor and second order factors are shown in Table 4.8. The generated mathematical models (RSM-based) for TWR is represented in Eqn. 4.13 as;

TWR = (-2.003) - (0.0705 * Peak Current) + (0.0885 * TON) + (0.0505 * TOFF) - (1.4034 * Powder Concentration) + (0.0041 * Peak Current * Peak Current) - (0.0034 * TON * TON) - (0.0003 * TOFF * TOFF) + (2.3877 * Powder Concentration * Powder Concentration) + (0.0011 * Peak Current * TON) + (0.043 * Peak Current * Powder Concentration) - (0.0003 * TON * TOFF) - (0.0014 * TON * Powder Concentration) - (0.0002 * TOFF * Powder Concentration)

Fig. 4.11 (a) and Fig. 4.11 (b)depicts the residuals' normal probability plot and the residuals' graph against the fitted value, respectively. It is shown that the errors have a normal distribution and that the regression model accurately predicts the values that were observed. A graph of residuals vs order of data collection is shown in Fig. 4.11 (c). According to the figure, the residuals are distributed at random around the center line. The experimental value versus predicted value graph for MRR is shown in Figure 4.12. The data values are evenly distributed around the mean, which reflects the model's effective prediction skills.

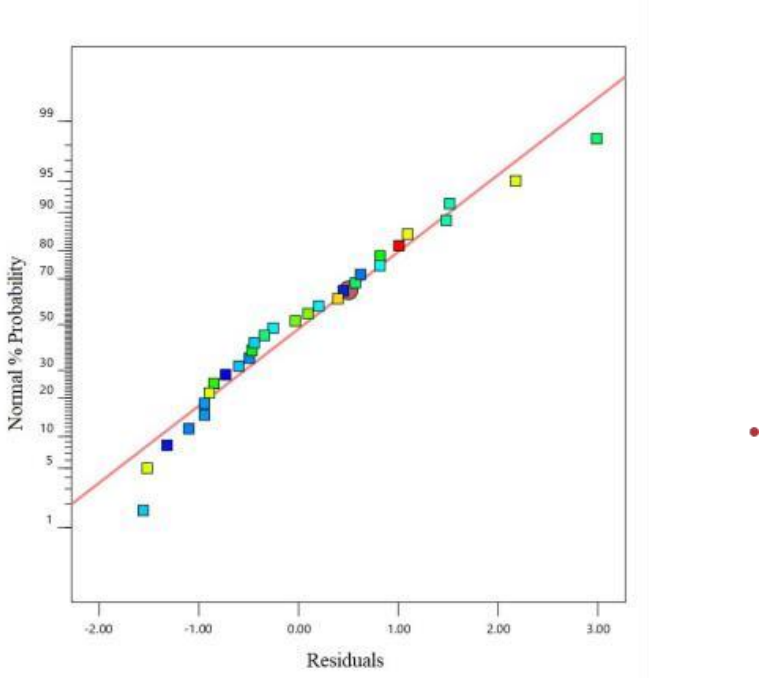

FIGURE 4.11 (a) Normal Probability Plot for Residuals – TWR

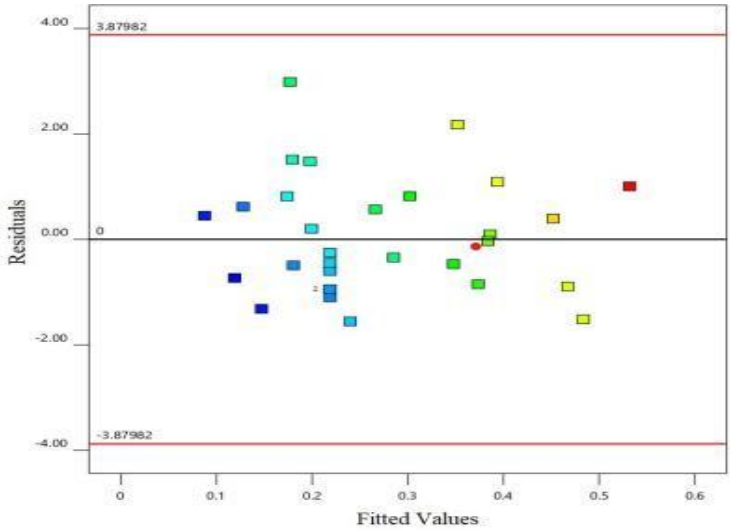

FIGURE 4.11 (b) Residuals Vs Fitted Values – TWR

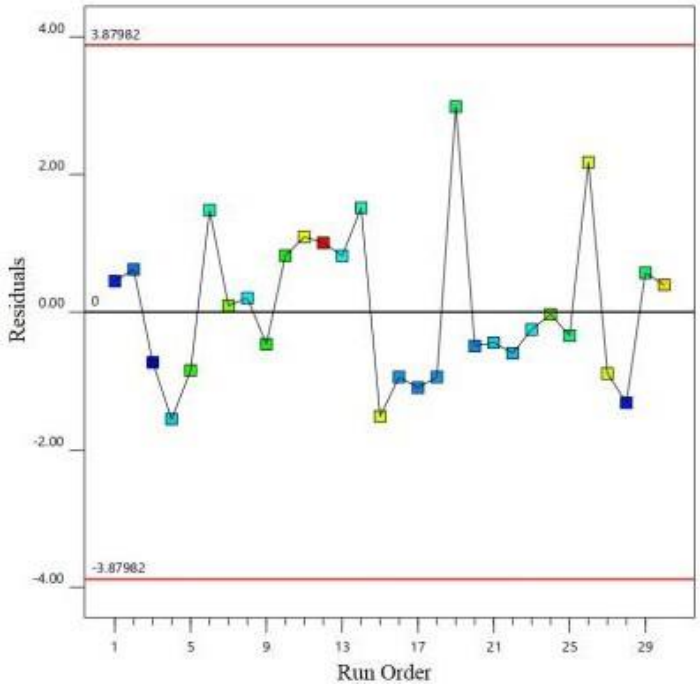

FIGURE 4.11 (c) Residuals Vs Run Order of Data – TWR

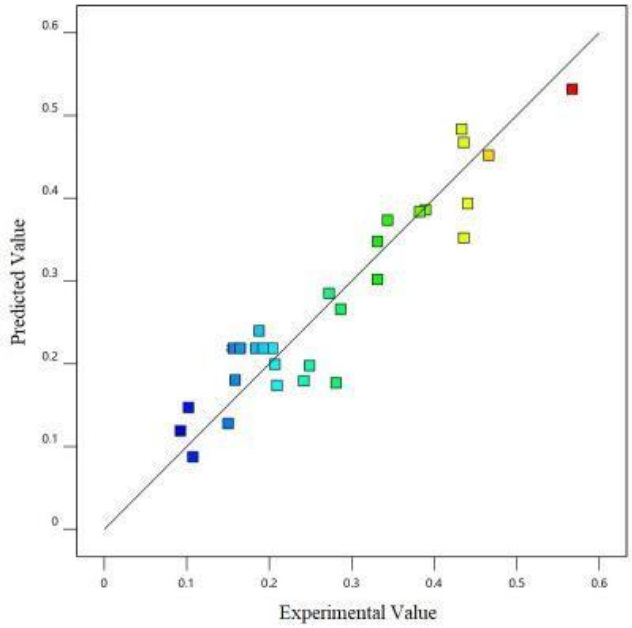

FIGURE 4.12 Experimental Value Vs Predicted Value – TWR

Fig. 4.13 represents an interaction plot of Pulse (Peak) Current and Powder Concentration with TWR. It can be seen that for a moderate value of Powder Concentration (0.25

grams./ltrs.) the tool wear is minimum. With an increase in Peak Current value, the TWR rises. Additionally, Table 4.7 demonstrates the importance of the relationship between Peak Current (Ip) and Powder Concentration (P.C).

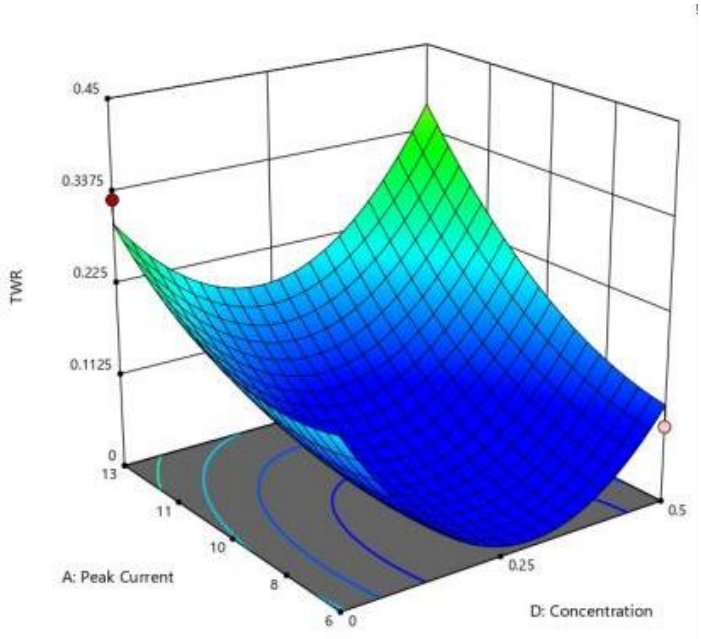

FIGURE 4.13 Interaction Plot Ip, Powder Concentration Vs TWR

4.3.3 Analysis of Surface Roughness (SR)

Table 4.9 displays the ANOVA and regression data for the whole two factor interaction model (quadratic) for SR. The R2 result is 85.01%,demonstrating that the regression model does a good job of explaining how the independent components relate to SR. A model is considered statistically significant when the related p-value is less than 0.05 (i.e., = 0.05, or 95% confidence). The expression "lack of fit" is meaningless because it is desired.

TABLE 4.8 Response Surface Analysis for SR

Source	Sum of Squares	DOF	Mean Square	F Value	P Value	Significant
Model	15.35	14	1.1	6.08	0.0006	Yes
Ip	5.48	1	5.48	30.4	0.0001	Yes
TON	2.54	1	2.54	14.1	0.0019	Yes
TOFF	4.05	1	4.05	22.45	0.0003	Yes
P.C.	0.1776	1	0.1776	0.9845	0.3368	No
Ip * TON	0.6555	1	0.6555	3.63	0.076	No
Ip * TOFF	0.1608	1	0.1608	0.8915	0.36	No
Ip * P.C.	0.1494	1	0.1494	0.8281	0.3772	No
TON * TOFF	0.0133	1	0.0133	0.0738	0.7896	No
TON * P.C.	0.1156	1	0.1156	0.6408	0.4359	No
TOFF * P.C.	0.3067	1	0.3067	1.7	0.2119	No
Ip^2	2.04	1	2.04	11.31	0.0043	Yes
TON^2	0.313	1	0.313	1.74	0.2075	No
TOFF^2	0.1357	1	0.1357	0.752	0.3995	No
P.C^2	0.1284	1	0.1284	0.7117	0.4121	No

Residuals	2.71	15	0.1804			
Lack of Fit	2.36	10	0.236	3.41	0.094	No
Pure Error	0.3459	5	0.0692			
Total	18.05	29				
Std. Dev.	= 0.4247		R2 = 85.01%			
R2 (Adj.)	= 71.02%					

TABLE 4.9 Estimated Regression Co-efficient for SR

Source	Coefficient Estimate
Constant	3.82
Ip	0.552
TON	0.376
TOFF	-0.4744
P.C.	-0.0994
Ip * TON	0.2022
Ip * TOFF	-0.1
Ip * P.C.	0.0965
TON * TOFF	0.0288

TON * P.C.	-0.085
TOFF * P.C.	-0.1382
Ip^2	-0.9072
TON^2	0.3476
TOFF^2	0.2358
P.C^2	0.2226

The regression coefficients (estimated) for the factors, interaction with other factor and second order factors are shown in Table 4.10. Eqn. 4.14 represents the generated mathematical model (RSM-based) for SR;

SR = (10.1964) + (1.6216 * Peak Current) - (0.336 * TON) - (0.2853 * TOFF) + (1.3244 * Powder Concentration) - (0.0741 * Peak Current * Peak Current) + (0.0139 * TON * TON) + (0.0016 * TOFF * TOFF) + (3.5616 * Powder Concentration * Powder Concentration) + (0.0116 * Peak Current * TON) - (0.0024 * Peak Current * TOFF) + (0.1103 * Peak Current * Powder Concentration) + (0.0005 * TON * TOFF) - (0.068 * TON * Powder Concentration) - (0.0461 * TOFF * Powder Concentration)

Fig. 4.14 (a)Fig. 4.14 (a) depicts the residual vs fitted value graph, whereas Fig. 4.14 (b) displays the normal probability plot. The plots show whether or not the residuals have a normal distribution. If they do, the bulk of the dots will follow a straight line, with some minor dispersion even for normal data. The residuals are shown to typically follow a straight line in the figure, indicating that the mistakes are distributed regularly. Fig. 4.14 (c) represents a graph of Residuals versus order of data collected. The represents that the

residuals are falling randomly around the center line. Fig. 4.15 represents the Experimental Value Vs Predicted Value graph for MRR. The graph represents a comparison between predicted and experimented values

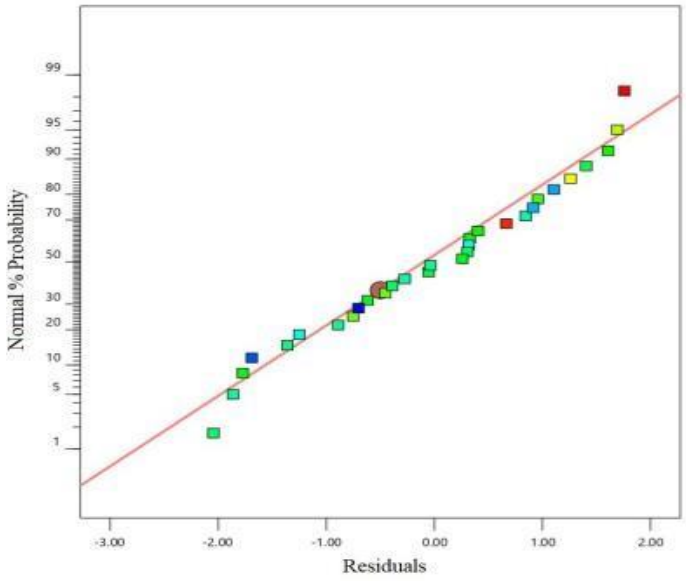

FIGURE 4.14 (a) Normal Probability Plot for Residuals – SR

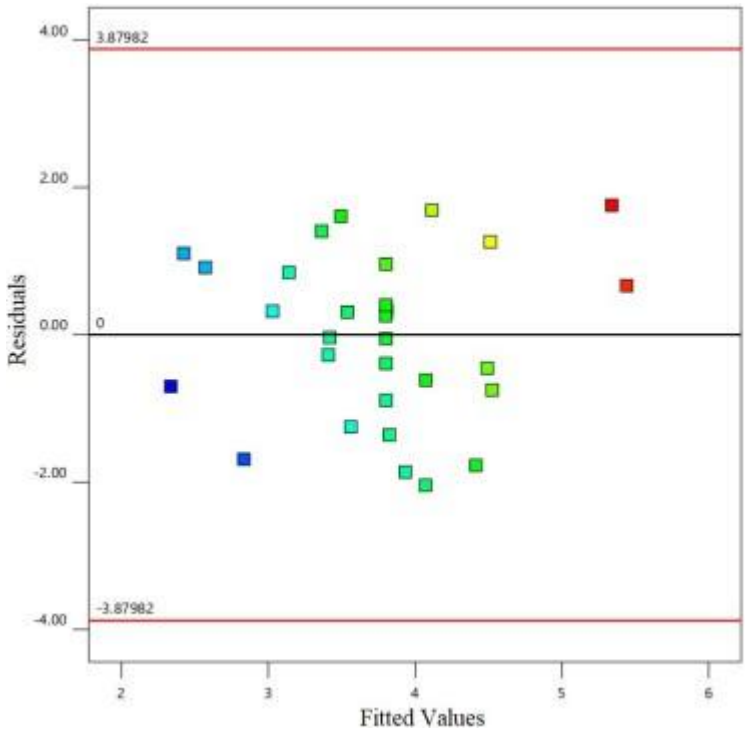

FIGURE 4.14 (b) Residuals Vs Fitted Values – SR

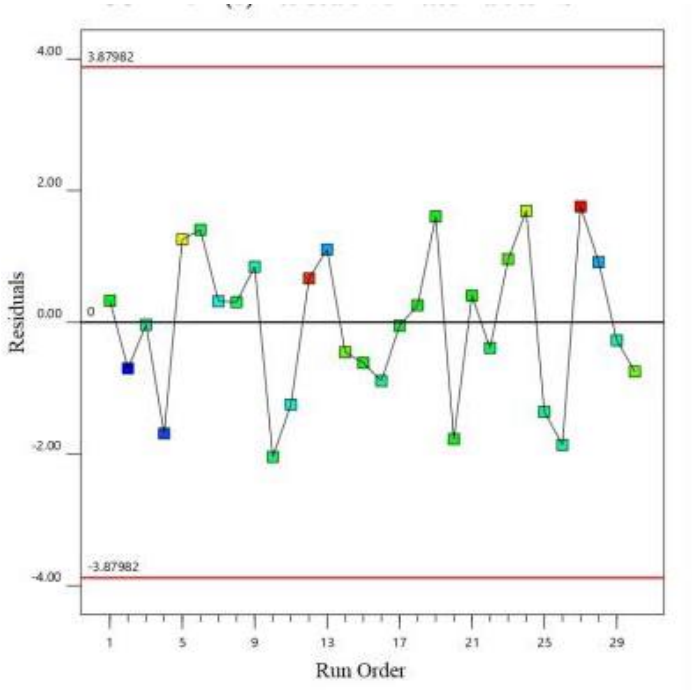

FIGURE 4.14 (c) Residuals Vs Run Order of Data – SR

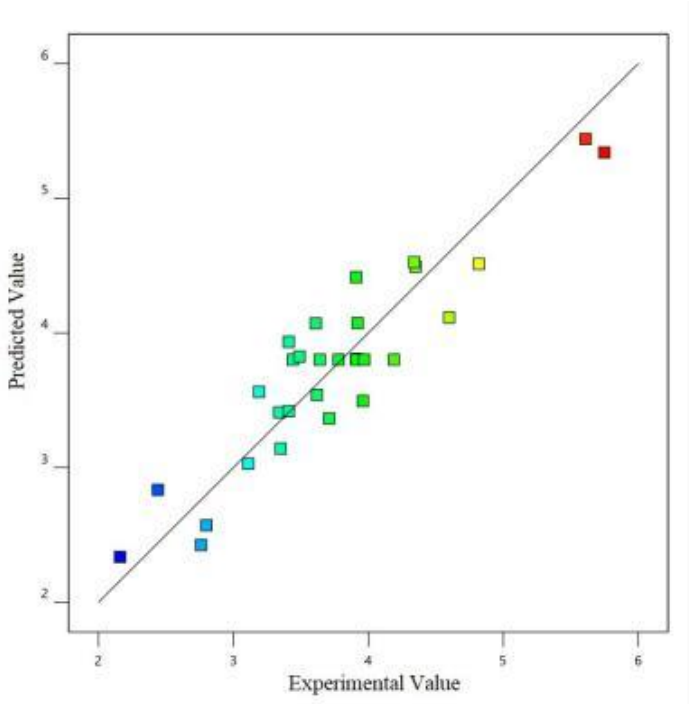

FIGURE 4.15 Experimental Value Vs Predicted Value – SR

4.4 Multi-Objective Analysis Using GRA: When the process is being optimized for several purposes, single objective optimization may not always be enough to produce the optimal combination of machining parameters. The best combination of parameters for one particular reaction may not be complementary to other answers. Therefore, multi-objective optimization is necessary. One of the most potent and useful soft-tools for analyzing numerous processes with multiple performance parameters is the gray relational analysis (GRA). Grey Relational Technique, a multi objective optimization method, provides a sequential strategy for incomplete, undecided, and ambiguous systems. Typically, GRA is used to resolve challenging issues when the targeted performance indicators are interconnected. The multi-objective issue has been reduced to a single objective optimization for the purposes of gray relational analysis. The GRA is a substitute for conventional statistical approaches that may be used to optimize a variety of quality attributes while dealing with limited sample sizes and uncertainty situations. The creation of Grey Relational is the first step in the GRA process. The experimentally determined response values are normalized in this phase to lie between 0 and 1. The Grey relational co-efficient (GRC) is then calculated. The process performance characteristics are calculated using the GRG - Grey relational grade, which reduces the multi-objective optimization problem to a single-objective optimization problem. The set of parameters with the highest GRG value is thought to be the best set. The association between sequences and the degree of total data value variance (among the sequences) may be easily determined using GRA. The stepwise procedure for the calculation of GRA is as follows;

- Averaging across all performance facets of experimental findings.
- Calculation of grey relational coefficient (GRC).
- Grey relational grade (GRG) calculation employing performance characteristic weighted factor.
- Analysis of experimental results using GRG.
- choosing the best process parameter values.

4.4.1 Normalization of experimental results

If the response optimization goals change (maximization for some replies and minimization for others), the analysis of the experimental outcomes will not fit. As a result, it is important to use a method akin to normalization to arrange performances for each distinct

choice into a comparative series. Grey Relational Generation is the name given to it. All responses should employ either the "Larger-the-better (LBT)" or "Smaller-the-better (SBT)" condition depending on the objective function. SBT criteria for surface roughness and tool wear rate and LBT criteria for material removal rate were both applied in the current investigation. For gray relational generation, the normalized values of MRR, TWR, and SR are acquired and shown in Table 4.11.Normalization equation (Eqn. 4.15) for LBT is;

$$\mathbf{Yi(k)} = \frac{[Xi(k) - min\ Xi(k)]}{max\ Xi\ (k) - min\ Xi(k)} \qquad (4.15)$$

For SBT, Normalization equation (Eqn. 4.16) is;

$$\mathbf{Yi(k)} = \frac{[maxXi(k) - Xi(k)]}{max\ Xi\ (k) - min\ Xi(k)} \qquad (4.16)$$

Wherein, Yi(k) - ith response value (normalized) and Xi(k) – observed value of ith run for kth response.

TABLE 4.10 Normalized Data MRR, TWR, SR

Sr. No.	MRR (mm^3/min)	TWR (mm^3/min)	Ra
1	0.1186	0.9684	0.5125
2	0.0548	0.8785	1.0000
3	0.0000	1.0000	0.6518
4	0.0050	0.7993	0.9220
5	0.3542	0.4713	0.2591
6	0.1043	0.6705	0.5682
7	0.4324	0.3744	0.7354
8	0.3234	0.7589	0.5933
9	0.0530	0.4972	0.6685

10	0.0582	0.3681	0.5961
11	0.4687	0.2670	0.7131
12	1.0000	0.0000	0.0390
13	0.0360	0.7536	0.8329
14	0.6560	0.6852	0.3900
15	0.9665	0.2824	0.5097
16	0.2076	0.8480	0.6435
17	0.2076	0.8654	0.5487
18	0.2076	0.8480	0.5125
19	0.3053	0.6029	0.4986
20	0.2195	0.8604	0.5125
21	0.2107	0.7890	0.4958
22	0.2145	0.8077	0.5877
23	0.2107	0.7656	0.4345
24	0.4125	0.3896	0.3203
25	0.5364	0.6208	0.6295
26	0.6066	0.2769	0.6518
27	0.6539	0.2771	0.0000
28	0.2498	0.9796	0.8217
29	0.2537	0.5911	0.6713
30	0.4892	0.2133	0.3928

4.4.2 Grey Relational Coefficient calculation (GRC)

The preprocessed order of response characteristics are used to determine the GRC once the data has been processed. GRC (i(k)) is determined using a formula.(Eqn. 4.17) ;

$$\xi i\,(k) = \frac{\Delta \min + £\, i\, \Delta max}{\Delta i\,(k) + £ i\, \Delta max} \qquad (4.17)$$

Where, to compress or enlarge the GRC range, there is a distinguishing factor, whose value ranges from 0 to 1. The value of used in this study is 0.5. The global maximum and minimum values of the kth response's normalized values are max and min, respectively. The values of the estimated Grey-Relational Coefficient are shown in Table 4.12.

TABLE 4.11 Grey Relational Coefficient

Sr. No.	Reference Sequence	Weighted Grey-Relational Coefficient	MRR (mm^3/min)	TWR (mm^3/min)	Ra
1	0.8814	0.0316	0.4875	0.3619	0.9406
2	0.9452	0.1215	0.0000	0.3460	0.8045
3	1.0000	0.0000	0.3482	0.3333	1.0000
4	0.9950	0.2007	0.0780	0.3345	0.7136
5	0.6458	0.5287	0.7409	0.4364	0.4860
6	0.8957	0.3295	0.4318	0.3583	0.6027
7	0.5676	0.6256	0.2646	0.4683	0.4442
8	0.6766	0.2411	0.4067	0.4249	0.6747
9	0.9470	0.5028	0.3315	0.3455	0.4986
10	0.9418	0.6319	0.4039	0.3468	0.4417
11	0.5313	0.7330	0.2869	0.4848	0.4055
12	0.0000	1.0000	0.9610	1.0000	0.3333
13	0.9640	0.2464	0.1671	0.3415	0.6699
14	0.3440	0.3148	0.6100	0.5924	0.6136

15	0.0335	0.7176	0.4903	0.9372	0.4106
16	0.7924	0.1520	0.3565	0.3869	0.7668
17	0.7924	0.1346	0.4513	0.3869	0.7880
18	0.7924	0.1520	0.4875	0.3869	0.7668
19	0.6947	0.3971	0.5014	0.4185	0.5573
20	0.7805	0.1396	0.4875	0.3905	0.7817
21	0.7893	0.2110	0.5042	0.3878	0.7032
22	0.7855	0.1923	0.4123	0.3889	0.7223
23	0.7893	0.2344	0.5655	0.3878	0.6809
24	0.5875	0.6104	0.6797	0.4598	0.4503
25	0.4636	0.3792	0.3705	0.5189	0.5687
26	0.3934	0.7231	0.3482	0.5597	0.4088
27	0.3461	0.7229	1.0000	0.5910	0.4089
28	0.7502	0.0204	0.1783	0.3999	0.9608
29	0.7463	0.4089	0.3287	0.4012	0.5501
30	0.5108	0.7867	0.6072	0.4946	0.3886

4.4.3 Grey Relation Grade calculation (GRG)

GRG stands for the correlation strength between the reference sequence and the comparability sequence. GRG is a performance metric for problems with multi-response optimization. It is the weighted total of every GRC. The comparative sequences' performance for each response is all inferior to that of the reference sequence. As a result, the comparability sequence for an alternative is most comparable to the reference sequence if it receives the highest GRG with the reference sequence, making that alternative the best choice. In Table 4.13, the Grey Relational Grade is calculated and shown. Using a formula, GRG is computed.(Eqn. 4.18) ;

$$\gamma = (1/n) \sum_{i=1}^{n} \xi\, i\, (k) \qquad (4.18)$$

The greatest GRG is seen in experimental run #02 (GRG Value: 0.8105), as can be shown. Pulse Current (Ip) - 06 Amps, Pulse ON Time (TON) - 05 Sec, Pulse OFF Time (TOFF) - 96 Sec, and Powder Concentration (P.C) - 0.5 grms/ltrs are the appropriate values for Experimental Run #2.

TABLE 4.12 Grey Relational Grade

Sr. No.	Grey-Relational Grade	Rank
1	0.6077	6
2	0.8105	1
3	0.6614	4
4	0.7135	3
5	0.4345	29
6	0.5208	21
7	0.5539	15
8	0.5631	11
9	0.5194	22

Sr. No.	Grey-Relational Grade	Rank

10	0.4785	25
11	0.5363	18
12	0.4711	26
13	0.6440	15
14	0.5278	20
15	0.5631	12
16	0.5993	7
17	0.5766	8
18	0.5606	14
19	0.5006	24
20	0.5658	10
21	0.5375	17
22	0.5685	9
23	0.5165	23
24	0.4390	28
25	0.5616	13
26	0.5293	19
27	0.4075	30
28	0.7368	2
29	0.5469	16

Sr. No.	**Grey-Relational Grade**	**Rank**
30	0.4413	27

4.4.4 Analysis and Optimization of GRG

It is possible to differentiate between the effects of each parameter at different levels in the case of an orthogonal experimental design. It is feasible to determine the mean GRG for each level of input parameter by extrapolating the average GRG for a certain level setting from the observed experimental data. For all levels, the mean GRG may be determined in a similar manner. Average GRG is shown by factor level in Table 4.14. From this table, it can be deduced that the "*" indicates the ideal parameter values. Higher grey relational grades from each level of component in this table show the optimal level because higher grey relational grades are taken into account after taking the maxim "higher-the-better" into consideration. It is determined that Pulse Current - 06 Amps, Pulse ON Time - 05 Sec, Pulse OFF Time - 96 Sec, and Powder Concentration - 0.5 grms./ltrs. are the ideal parameter settings. One interpretation of it is Table 4.14 shows that when many responses are taken into account concurrently, the pulse current (Ip) has the most dominant influence. Fig. 4.16 represents the Main Effect Plot of Grey Relational Grade. It can be stated using the plot that Ip and P.C has higher significance on responses when multi variable optimization is required.

TABLE 4.13 Response Table for Grey Relational Grade

Process Parameters	Average grey relational grade by factor level	Mean Effect
Pulse Current (Ip)	Level 1: 0.6399 Level 2: 0.5329 Level 3: 0.4895	0.1503
Pulse ON Time (TON)	Level 1: 0.5889 Level 2: 0.5393 Level 3: 0.5355	0.0534
Pulse OFF Time (TOFF)	Level 1: 0.5183 Level 2: 0.5491 Level 3:	0.0802
	0.5984	
Powder Concentration (PC)	Level 1: 0.5143 Level 2: 0.5631 Level 3: 0.5915	0.0773

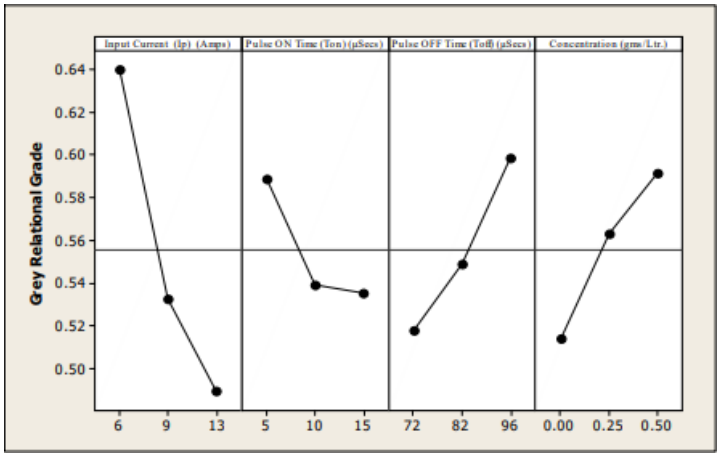

FIGURE 4.16 Main Effect Plot – Grey Relational Grade

An ANOVA was conducted for the Grey Relational Grade at a 95% confidence level to examine the significance and percentage impact of each component on the numerous response characteristics. The ANOVA table for GRGs is shown in Table 4.15. The table shows that the most important parameter for multi response optimization is pulse current (Ip) (F value - 23), which is followed by powder concentration (P.C) (F value - 7.54), pulse OFF time (TOFF) (F value - 6.21), and pulse on time (TON) (F value - 3.13). The proportional contribution of each element to GRA is shown in Fig. 4.17.

TABLE 4.15 ANOVA Table for Grey Relational Grade

Process Parameters	DOF	SS	MS	F	% CONTRIBUTION
Pulse Current (Ip)	2	0.104749	0.053932	23.00	44.98
Pulse ON Time (TON)	2	0.012857	0.007328	3.13	5.52
Pulse OFF Time (TOFF)	2	0.030723	0.014555	6.21	13.19
Powder Concentration (PC)	2	0.035336	0.017668	7.54	15.17
Error	21	0.049232	0.002344	21.14	-

Total	29	0.232898	100	-	-

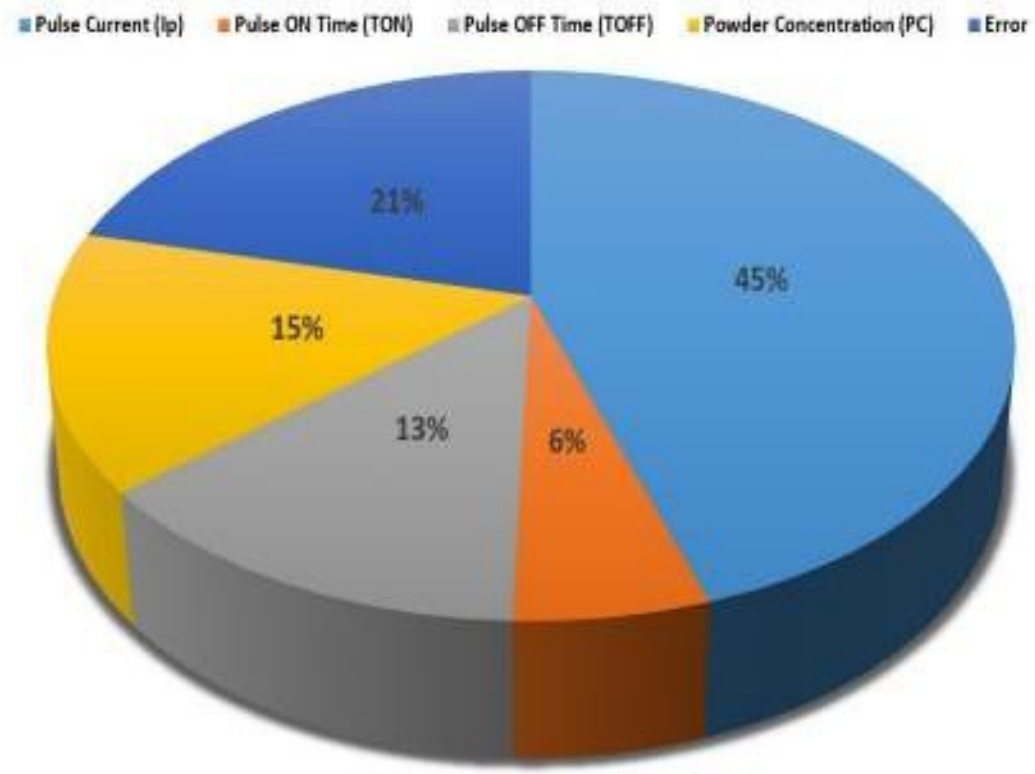

FIGURE 4.17 % Contribution – Process Parameters – GRA

.5 Surface Characterization

In the present research, Surface modifications due to the effect of process parameters and the addition of power additives in the dielectric fluid have been investigated. The EDM process surface characteristics gets altered due to formation of surface cracks, resolidified layers, deposition of debris, etc. The generated sparks vaporize the dielectric fluid quickly and generates pressure impulse around tool. These pressure impulse and the generated high thermal stresses produces the craters and micro-cracks on the EDMed surface. The haphazard erosion of the surface sources poor surface finish due to frequent cracking. The surface micrographs of the machined samples were analyzed using SEM. The SEM micrographs were analyzed for machining without addition of powder particles and also for powder mixed EDM using Al2O3 and SiC powders. While machining with pure dielectric (without addition of powder particles), most cracks, pores and surface pits were found to befall with a non-uniform surfaces having higher Surface Roughness

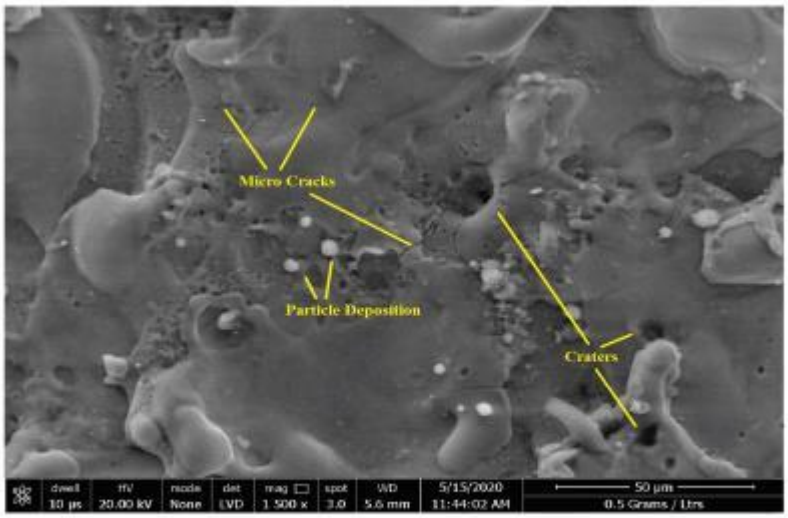

FIGURE 4.18 EDMed surface SEM micrograph in (a)
(Ip = 06 Amps, TON = 05 sec, TOFF = 96 sec).

Surface micrographs shows formation of uneven surface patterns and thick cracks which may be due to the higher value of pulse current and Pulse ON Time that leads to upsurge heat concentration and thus making the surfaces prone to cracking.The photo-micrograph of surfaces that were machined without the addition of powder particles to deionized water

(dielectric) is shown in Figure 4.18 (a). It was discovered that the surface characteristics improve as the surface roughness decreases during machining when Al2O3 and SiC powder mixed with dielectric fluid is used, as opposed to machining done without powder particles.Fewer and smaller cracks were formed compared to that observed while EDMing without powder particles. It was also observed that EDMing with powder added dielectric resulted in to almost no ridges and very low density of craters

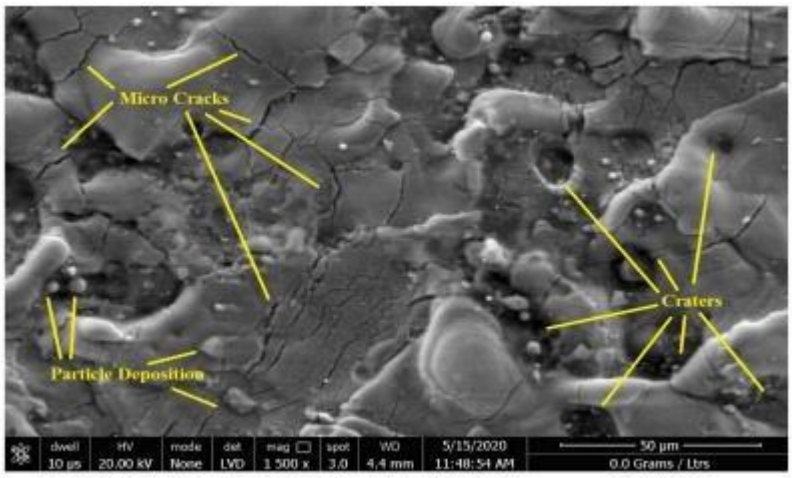

FIGURE 4.18 (b) SEM micrograph of the PMEDMed surface

(Ip = 06 Amps, TON = 05 µsec, TOFF = 96 µsec and P.C. = 0.5 grms./ltrs.)

Figure. 4.18 (b) show SEM micrograph of surfaces machined with Al2O3 and SiC powders mixed dielectric at the optimum set of process parameters obtained using GRA.

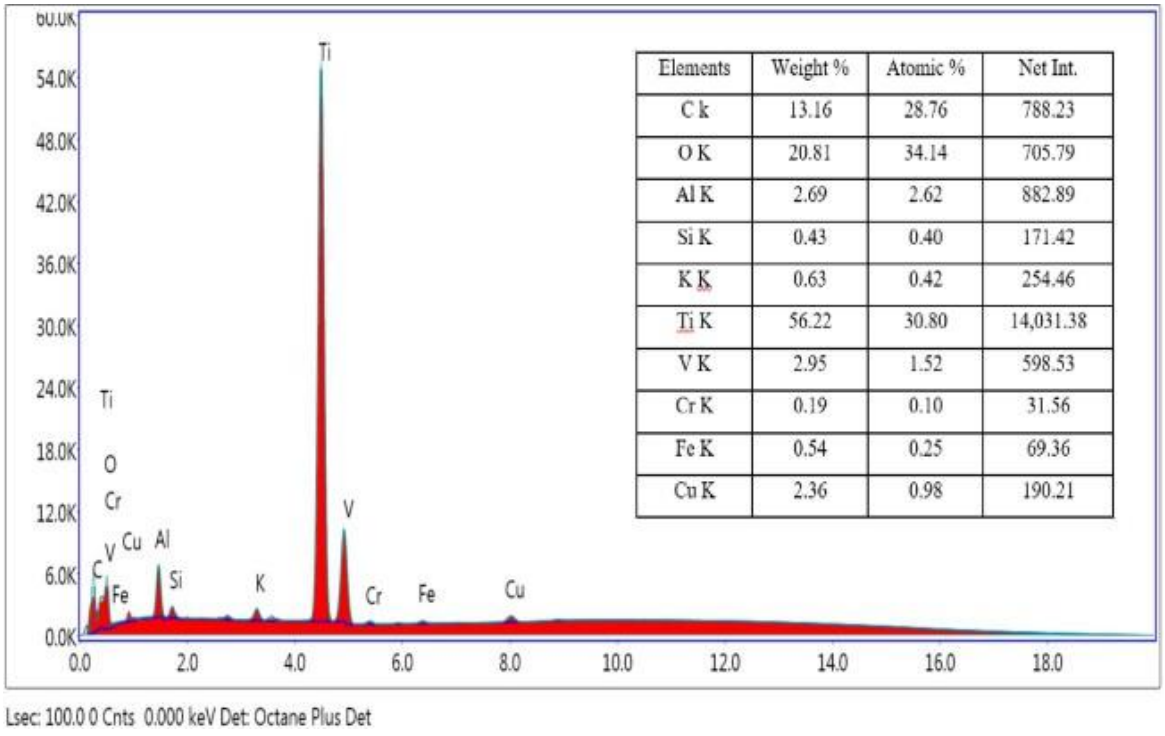

Elements	Weight %	Atomic %	Net Int.
C k	13.16	28.76	788.23
O K	20.81	34.14	705.79
Al K	2.69	2.62	882.89
Si K	0.43	0.40	171.42
K K	0.63	0.42	254.46
Ti K	56.22	30.80	14,031.38
V K	2.95	1.52	598.53
Cr K	0.19	0.10	31.56
Fe K	0.54	0.25	69.36
Cu K	2.36	0.98	190.21

FIGURE 4.19 EDAX Spectrograph of the PMEDMed surface

(Ip = 06 Amps, TON = 05 µsec, TOFF = 96 µsec and P.C. = 0.5 g/ltrs)

Energy Dispersive Spectroscopy (EDS) is a quantitative and qualitative analytical technique used for elemental analysis - surfaces characterization. Figure. 4.19 shows EDAX spectra of PMEDMed surface at the optimum set of process parameters which represents the elemental qualitative analysis.

4.6 Confirmation test: Confirmation testing is the experiment's last phase. Confirmation runs are performed in order to verify the results of the analytical phases. Additionally, confirmation tests must be run to determine whether or not the anticipated parameter combination for the software's best outcomes is appropriate. The confirmatory trials were conducted at the ideal level proposed by Grey Relational Analysis, which was at a pulse current (Ip) of 06 amps, a pulse on time (TON) of 05 sec, a pulse off time (TOFF) of 96 sec, and a powder concentration (PC) of 0.5 grams per liter.

TABLE 4.15 Comparison of Results of GRA and Confirmatory Experiment

Response	Optimized Responses (Using GRA)	Responses of the Confirmatory Experiments
Material Removal Rate (mm^3/min)	0.4678	0.4680
Tool Wear Rate (mm^3/min)	0.1501	0.1503
Surface Roughness (Ra)	2.16	2.15

Table 4.15 compares the input parameters with the calculated parameters under ideal circumstances, showing a fair degree of agreement.

CHAPTER-5

CONCLUSIONS AND FUTURE SCOPE

Powder Mixed EDM of Titanium Alloy - Ti-6Al-4V with Al2O3 and SiC Powder Mixed Deionized Water as the dielectric fluid is investigated in this study to determine the impact of various process parameters on Material Removal Rate (MRR), Tool Wear Rate (TWR), and Surface Roughness (SR). The Central Composite Design-Response Surface Method was used to plan the experiments. The relevance and importance of the parameters, as well as the impact and interaction effects of the parameters, have been determined by ANOVA analysis of the experimental results. Regression models have been created to predict the performance characteristics. The PMEDM process responses were analyzed for the simultaneous influence of many process parameters using Grey Relational Analysis (Multi- objective optimization), and the optimal set of process (input) parameters were identified. Samples (machined with the best possible settings) were analyzed for surface integrity and surface change by scanning electron microscopy. Machining using a dielectric composed of Al2O3 and SiC Powder showed considerable improvements in performance parameters during the experiments. The powder substance (combined with dielectric) and its concentration determine the enhancement of the properties. The primary takeaways from this study may be summed up as follows:

5.1 Conclusion

5.1.1 Effect of Selected Process Parameters on MRR

- According to the analysis of variance performed on MRR, the variables with the greatest impact on the removal rate are the pulse ON time (TON) and the pulse current (Ip). When both the pulse current and the pulse ON time are increased, the MRR rises. When the pulse current (Ip) is 13 Amps and the pulse on time (TON) is 15 Sec, the maximum achievable MRR is achieved.
- As the input current rises, so does the energy of the pulse discharge. The greater energy discharge pulse will enhance the intensity of the plasma channel resulting in to bigger and deeper craters and consequently raises MRR.
- By prolonging the period of time during which heat flux is generated, as the Pulse ON Time is increased, the Material Removal Rate is also increased.

- When powder particles are added to dielectric, the MR rate rises. The MRR improves because the extra particles act as a "bridging effect" between the electrodes, allowing the discharge to spread out into many, smaller increments. EDMing may be performed with greater discharge currents because powder increases the inter-electrodial gap.Powder concentration of 0.5 grams./ltrs. yields the highest MRR.
- It is also shown that the interaction between the pulse current and the powder concentration has a major impact.

5.1.2 The Outcome of Changing a Few Process Variables on TWR

- According to the analysis of variance, Tool Wear Rate is largely affected by the Pulse Current (Ip) and the Pulse ON Time (TON).
- Pulse current has a direct correlation to the rate of tool wear since an increase in current means an increase in discharge energy input. At the moment when the Input current develops, a higher heat vitality is exposed to both workpiece and tool. Because of this effect, more thermal energy is generated at the interface between the work piece and the tool electrode, which causes more melting and evaporation of the tool and hence more TWR.
- With increased Pulse ON Time the quantity of positively charged particles impacting the negatively charged instrument is more. As a result, the TWR rises as a greater quantity of tool electrode melts. The best TWR was achieved with a pulse current of 13 A and a on time of 15 microseconds.
- Pulse (Peak) Current and Powder Concentration interact with TWR in a way that suggests the optimal Powder Concentration is 0.25 grams./ltrs., resulting in minimal tool wear.

5.1.3 Effect of Selected Process Parameters on SR

- The larger and more hotter the pool of molten material became, the greater the observed resulting Surface Roughness (Ra) value was. At this high temperatures production and burst of gas bubbles happens leading into deeper craters. Surface quality is improved with low Ip values (0.6 amps) and short ON times (0.5 microseconds).

- The powder reduces the insulating properties of the dielectric, which in turn widens the spark gap between the electrodes. By widening the spark gap, debris may be more easily flushed out, leading to greater process stability. Better surface polish after thorough cleansing. Powder Concentration level of 0.5 grams./ltrs. produces the finest surface finish.
- The powder reduces the insulating properties of the dielectric, which in turn widens the spark gap between the electrodes. By widening the spark gap, debris may be more easily flushed out, leading to greater process stability. Better surface polish after thorough cleansing. Powder Concentration level of 0.5 grams./ltrs. produces the finest surface finish.

5.1.4 Multi-Objective Analysis

- Grey Relational Analysis interpretation indicates that the maximum Grey Relational Grade (GRG) value is found for experiment # 2. The corresponding GRG value for experiment # 2 is 0.8105 and the parameter levels are Pulse Current (Ip) – 06 Amps., Pulse ON Time (TON) – 05 µSec, Pulse OFF Time (TOFF) – 96 µSec, Powder Concentration (P.C) – 0.5 grms./ltrs. These are the optimum set of parameters values that maximizes rate of material removal and surface finish with lower rate of tool wear simultaneously.
- According to GRG's response analysis, Pulse Current (Ip) has the greatest average impact. This suggests that, of all the factors thought about for multi response optimization, Pulse Current is seen as the most dominant. Pulse Current and Powder Concentration are shown to have approximately a 45% and 15% impact contribution, respectively, in the GRG main effects plot.

5.1.5 Surface Characterization

- EDMing with dielectric (without the inclusion of powder particles) leads to degraded surface characteristics with a high concentration of cracks and voids, as seen by scanning electron microscopy. The surface quality suffers as a result of these irregularities.
- According to the scanning electron microscopy (SEM) data, the surface polish is greatly enhanced by PMEDMing with the following parameters: Input Current (Ip)

- 06 Amps; Pulse ON Time (TON) - 05 sec; Pulse OFF Time (TOFF) - 96 sec; Powder concentration - 0.50 g/ltrs. Powder mixing increases discharge energy dispersion, leading to less surface cracking and shallower craters.

5.2 Future Scope of Work

The present research presents a systematic investigation of PMEDM in the Titanium Alloy Ti-6Al-4V. These is still a scope for more investigation. Here are some ideas that might be useful going forward:

- With the hope of discovering if PMEDMing Nanocomposites is ever possible.
- The purpose of this study is to determine the average size of the debris generated by the PMEDM process and to develop a filtering mechanism to effectively separate the debris from the powder particles.
- Aiming for the best possible dielectric storage tank dimensions for the PMEDM procedure.
- With the use of numerical modeling and simulation, we may learn the effect that adjusting various process parameters has on PMEDM's behavior.
- To further understand the cost effectiveness and sustainability of the PMEDM process, researchers should conduct a comprehensive Life-Cycle study.

References

1. Donachie MJ. Titanium: a technical guide. Geauga County, OH: ASM International, 2000.
2. P.J. Bridges, B. Magnus. ―Manufacture of Titanium Alloy Components for Aerospace and Military Applications,‖ Cost Effective Application of Titanium Alloys in Military Platforms, RTO-MP-069(II)
3. J.R. Myers, H.B. Bomberger, F.H. Froes, J. Mater, Titanium alloys and their machinability a review. 36 (10) (1984) 50-60.
4. A.R. Machado,J Wallbank. ―Machining of titanium and its alloys-a review,‖ Journal of Engineering Man. Proc. Inatn. Mech. Engrs. Vol.204.
5. Durul Ulutan, Tugrul Ozel, ―Machining induced surface integrity in titanium and nickel alloys: A review,‖ International Journal of Machine Tools & Manufacture, 2011, vol. 51, pp. 250–280.
6. Titanium Alloy Guide, RMI Titanium Co., Niles, OH,2000. (www.titanium.com)
7. Titanium Machining Guide, Kennametal, pp. A18 A23
8. R.M. Duncan, P.A. Blenkinsop, R.E. Goosey, "IMI Titanium," P.O. Box 216, Witton, Birmingham B6 7BA, UK, pp. 63-87.
9. D. Eylon, S. Fulishiro, P.J. Postans, F.H. Froes, "High Temperature Titanium Alloys: A Review," Journal of Metallurgy, Vol. 36, No. 11 (1984), pp. 55-62.
10. Kishawy H.A., Hosseini A. (2019) "Titanium and Titanium Alloys." In: Machining Difficult-to-Cut Materials. Materials Forming, Machining and Tribology. Springer, Cham.
11. Barriobero-Vila, Pere (2015). "Phase Transformation Kinetics during Continuous Heating of α+β and Metastable β Titanium Alloys." doi: 10.13140/RG.2.1.2466.3529.
12. M. J. Donachie Jr., "Introduction to Titanium and Titanium Alloys," in "Titanium and Titanium Alloys - Source Book: A Collection of Outstanding Articles from the Technical Literature," American Society for Metals (1982), pp. 3-9.
13. Ezugwu, E.O., and Z.M. Wang. "Titanium Alloys and Their Machinability – A Review." Journal of Materials Processing Technology (1997).

14. M. C. Shaw, "Metal Cutting Principles," Oxford Series on Advanced Manufacturing, Oxford University Press Inc., New York (1984).
15. H.J. Siekmann, "Tool Engineering," Vol. 34 (1955), pp. 78-82.
16. Production Technology by P.C Sharma, pp. 565-572.
17. Liu, Qingyu, et al. "Review of Size Effects in Micro Electrical Discharge Machining." Precision Engineering, Vol. 44 (2016), pp. 29-40.
18. M. Kunieda, M. Yoshida, N. Taniguchi, "Electrical Discharge Machining in Gas," CIRP Annals - Manufacturing Technology, Vol. 46 (1997), pp. 143-146.
19. EDM Technical Manual, Poco Graphite, Inc., www.edmtechman.com/about.cfm.
20. Seyed Ali Niknam, Raid Khettabi, and Victor Songmene, "Machinability and Machining of Titanium Alloys: A Review," Materials Forming, Machining, and Tribology, pp. 1-29 (2014).
21. B. Jabbaripour, M. H. Sadeghi, Sh. Faridvand, and M. R. Shabgard, "Investigating the Effects Of EDM Parameters On Surface Integrity, MRR and TWR In Machining Of Ti–6Al–4V," Machining Science and Technology: An International Journal, Vol. 16, No. 3, pp. 419-444, 2012.
22. Sivakoteswararao Katta and G. Chaitanya, "Key Improvements in Machining of Ti6Al4V Alloy: A Review," AIP Conference Proceedings 1859, 2017.
23. Mahros Darsin, Hari Arbiantara Basuki, "Development Machining of Titanium Alloys: A Review," Applied Mechanics and Materials, Vol. 493, pp. 492-500, 2014.
24. P.-J. Arrazolaa, A. Garaya, L.-M. Iriarte, M. Armendia, S. Marya, F. Le Maître, "Machinability of titanium alloys (Ti6Al4V and Ti555.3)," Journal Of Materials Processing Technology, Vol. 209, pp. 2223-2230, 2009.
25. C. Veiga, J. P. Davim, and A.J.R. Loureiro, "Review on Machinability of Titanium Alloys: The Process Perspective," Rev. Adv. Mater. Sci., Vol. 34, pp. 148-164, 2013.
26. Rihova, Z., Saksl, K., Siemers, C., Ostroushko, D. (2012). "Analyses of Wear Mechanisms Occurring During Machining of the Titanium Alloy Ti-6Al-2Sn-4Zr-6Mo". World Academy of Science, Engineering and Technology, pp. 1515-1518.

27. Alokesh Pramanik and Guy Littlefair (2015). "Machining of Titanium Alloy (Ti-6Al-4V) - Theory to Application." Machining Science and Technology, Vol. 19, pp. 1-49.
28. Coromant S (1994). "Modern Metal Cutting: A Practical Handbook." Sandvik Coromant, Sweden.
29. Komanduri R, Von Turkovich B (1981). "New Observations on the Mechanism of Chip Formation when Machining Titanium Alloys." Journal of Wear, 69, 179-188. doi: 10.1016/0043-1648(81)90242-8.
30. Barry J, Byrne G, Lennon D (2001). "Observations on Chip Formation and Acoustic Emission in Machining Ti-6Al-4V Alloy." International Journal of Machine Tools and Manufacture, 41, 1055-1070. doi: 10.1016/S0890- 6955(00)00096-1.
31. Vyas A, Shaw M (1999). "Mechanics of Saw-Tooth Chip Formation in Metal Cutting." Journal of Manufacturing Science and Engineering, 121, 163-172. doi: 10.1115/1.2831200.
32. Obikawa T, Usui E (1996). "Computational Machining of Titanium Alloy - Finite Element Modeling and a Few Results." Journal of Manufacturing Science and Engineering, 118, 208-215. doi: 10.1115/1.2831013.
33. Gente A, Hoffmeister HW, Evans C (2001). "Chip Formation in Machining Ti6Al4V at Extremely High Cutting Speeds." CIRP Annals - Manufacturing Technology, 50, 49-52. doi: 10.1016/S0007-8506(07)62068-X.
34. A.R. Machado and J. Wallbank (1990). "Machining of Titanium and its Alloys - A Review." Journal of Mechanical Engineering, pp. 53-60.
35. Ashwin Polishetty, Manikanda Shunumugavel, Moshe Goldberg, Guy Littlefair, Raj Kumar Singh (2016). "Cutting Force and Surface Finish Analysis of Machining Additive Manufactured Titanium Alloy Ti-6Al-4V." Procedia Manufacturing, Vol. 7, pp. 284-289.
36. Amit S. Patil (2015). "Machining Challenges in Ti-6Al-4V - A Review." International Journal of Innovations in Engineering and Technology (IJIET), Vol. 4, Issue 5, pp. 6-23.

37. Ginta, L.T., Lajis, M.A., and Nurul Amin, AKM. (2009). "The Performance of Uncoated Tungsten Carbide Insert in End Milling Titanium Alloy Ti-6Al-4V through Work Piece Preheating." American Journal of Engineering and Applied Sciences, 2 (1), 147-153.
38. Che-Haron, C.H., and Jawaid, A (2005). "The Effect of Machining on Surface Integrity of Titanium Alloy Ti–6% Al–4% V." Journal of Materials Processing Technology, 166, 188–192.
39. Ginting, A., Nouari, M. (2009). "Surface Integrity of Dry Machined Titanium Alloys." International Journal of Machine Tools & Manufacture, 49, 325–332.
40. Nabhani, F. (2001). "Machining of Aerospace Titanium Alloys." Robotics and Computer Integrated Manufacturing, 17, 99-106.
41. Nazmi, A. (2010). "Performance of Diamond Tool in Machining Titanium." Thesis: Universiti Malaysia Pahang.
42. Sharif, S., Jawaid, A., Koksal, S. "Effect of Edge Geometry on Coated Carbide Tools when Face Milling Titanium Alloy."
43. Zareena AR, Veldhuis SC (2012). "Tool Wear Mechanisms and Tool Life Enhancement in Ultraprecision Machining of Titanium." Journal of Materials Processing Technology, 212, 560–570. doi:10.1016/j.jmatprotec.2011.10.014.
44. Machado A, Wallbank J, Pashby I, Ezugwu E. "Tool Performance and Chip Control when Machining Ti6a14v and Inconel 901 using High-Pressure Coolant Supply." Machining Science and Technology, 2(1), 1–12 (1998).
45. Singh S, Maheshwari S, Pandey PC (2004). "Some Investigations into the Electric Discharge Machining of Hardened Tool Steel Using Different Electrode Materials." Journal of Materials Processing Technology, 149, 272–277.
46. K. H. Ho, S.T. Newman. "State of the Art Electrical Discharge Machining (EDM)." International Journal of Machine Tools & Manufacture, 43, 1287–1300 (2003).
47. H. Ramasawmy, L. Blunt. "Effect of EDM Process Parameters on 3D Surface Topography." Journal of Materials Processing Technology, 148, 155–164 (2004).
48. Mohri, N., Fukuzawa, Y., Tani, T., Saito, N., & Furutani, K. (1996). "Assisting Electrode Method for Machining Insulating Ceramics." Annals of the CIRP, 45, 201-204.

49. Mohri, N., Fukusima, Y., Fukuzawa, Y., Tani, T., & Sato, N. (2003). "Layer Generation Process on Work-Piece in Electrical Discharge Machining." CIRP Annals – Manufacturing Technology, 52 (1), 157-160. DOI: 10.1016/S0007-8506(07)60554-X.
50. Mahardika, M., Tsujimoto, T., & Mitsui, K. (2008). "A New Approach on the Determination of Ease of Machining by EDM Processes." International Journal of Machine Tools and Manufacture, 48, 746-760. DOI: 10.1016/j.ijmachtools.2007.12.012.
51. Jahan, M. P., Wong, Y. S., & Rahman, M. (2009). "A Study on the Quality Micro-Hole Machining of Tungsten Carbide by Micro-EDM Process Using Transistor and RC-Type Pulse Generator." Journal of Materials Processing Technology, 209, 1706-1716. DOI: 10.1016/j.jmatprotec.2008.04.029.
52. Masuzawa, T. (2000). "State of the Art of Micromachining." CIRP Annals – Manufacturing Technology, 49(2), 473-488. DOI: 10.1016/S0007-8506(07)63451-9.
53. Schubert, A., Zeidler, H., Hackert, M., Schneider, J., & Hahn, M. (2013). "Enhancing Micro-EDM Using Ultrasonic Vibration and Approaches for Machining of Nonconducting Ceramics." Journal of Mechanical Engineering, 59(3), 156-164. DOI: 10.5545/sv-jme.2012.442.
54. Mohd Abbas N, Solomon DG, Fuad Bahari M. "A Review on Current Research Trends in Electrical Discharge Machining (EDM)." International Journal of Machine Tools and Manufacture, 47, 1214-1228 (2007).
55. Zahiruddin M, Kunieda M. "Comparison of Energy and Removal Efficiencies between Micro and Macro EDM." CIRP Annals - Manufacturing Technology, 61, 187-190 (2012).
56. Alting L, Kimura F, Hansen HN, Bissacco G. "Micro Engineering." CIRP Annals - Manufacturing Technology, 52, 635-657 (2003).
57. Rajurkar KP, Levy G, Malshe A., Sundaram MM, McGeough J, Hu X, et al. "Micro and Nano Machining by Electro-Physical and Chemical Processes." CIRP Annals - Manufacturing Technology, 55, 643-666 (2006).

58. K.P. Rajurkar, "Handbook of Design, Manufacturing and Automation," Chapter 13: Nontraditional Manufacturing Processes, Wiley, USA (1994).
59. F. Han, S. Wachi, M. Kunieda, "Improvement of Machining Characteristics of Micro-EDM Using Transistor Type ISO Pulse Generator and Servo Feed Control." Precision Engineering, 28, 378-385 (2004).
60. R. Casanueva, F.J. Azcondo, S. Bracho, "Series-Parallel Resonant Converter for an EDM Power Supply." Journal of Materials Processing Technology, 149, 172-177 (2004).
61. M. Ghoreishi, C. Tabari, "Investigation into the Effect of Voltage Excitation of Pre-Ignition Spark Pulse on the Electro Discharge Machining Process." Materials and Manufacturing Processes, 22, 833-841 (2007).
62. Y.Y. Tsai, C.T. Lu, "Influence of Current Impulse on Machining Characteristics in EDM." Journal of Mechanical Science and Technology, 21, 1617-1621 (2007).
63. T. Muthuramalingam, B. Mohan, "Influence of Discharge Current Pulse on Machinability in Electrical Discharge Machining." Materials and Manufacturing Processes, 28, 375-380 (2013).
64. S. M. Son, H.S. Lim, A.S. Kumar, M. Rahman, "Influences of Pulsed Power Condition on the Machining Properties in Micro EDM." Journal of Materials Processing Technology, 190, 73-76 (2007).
65. K. Liu, D. Reynaerts, B. Lauwers, "Influence of the Pulse Shape on the EDM Performance of Si3N4–TiN Ceramic Composite." CIRP Annals – Manufacturing Technology, 58, 217-220 (2009).
66. V. Janardhan, G.L. Samuel. "Pulse Train Data Analysis to Investigate the Effect of Machining Parameters on the Performance of Wire Electro Discharge Turning Process." International Journal of Machine Tools and Manufacture, 50 (2010), 775–788.
67. S.H. Yeo, E. Aligiri, P.C. Tan, H. Zarepour. "A New Pulse Discriminating System for Micro-EDM." Materials and Manufacturing Processes, 24 (2009), 1297–1305.
68. M. Gostimirovic, P. Kovac, B. Skoric, M. Sekulic. "Effect of Electrical Process Parameters on the Machining Performance in EDM." Indian Journal of Engineering and Materials Sciences, 18 (2012), 411–415.

69. B. Nowicki, A. Dmowska, A.P. Lejtas. "Morphology of Traces Made by Individual Electric Discharge in the EDM." Advances in Manufacturing Science and Technology, 33 (2009), 5–24.
70. B. Mohan, A. Rajadurai, K.G. Satyanarayana. "Effect of SiC and Rotation of Electrode on Electric Discharge Machining of Al–SiC Composite." Journal of Materials Processing Technology, 124 (2002), 297–304.
71. Puertas, I., Lusis, C.J. (2003). "A Study on the Machining Parameters Optimization of Electrical Discharge Machining." Journal of Materials Processing Technology, 521-526.
72. El-Taweel, T. A. (2009). "Multi-Response Optimization of EDM with Al-Cu-Si- TiC P/M Composite Electrode." International Journal of Advanced Manufacturing Technology, 44, 100-113.
73. Tomadi, S.H., Hassan, M.A., Hamedon, Z (2009). "Analysis of the Influence of EDM Parameters on Surface Quality, Material Removal Rate, and Electrode Wear of Tungsten Carbide." International Multi Conference of Engineers and Computer Scientists, 2.
74. Singh, Herpreet, Singh, Amandeep (2013). "Effect of Pulse on / Pulse off on Machining of Steel Using Cryogenically Treated Copper Electrode." International Journal of Engineering Research and Development, 5(12), 29-34.
75. Ali Ozgedik and Can Cogun (2006). "An Experimental Investigation of Tool Wear in Electric Discharge Machining." International National Journal of Advanced Manufacturing Technology, 27, 488-500.
76. Ahmet Hascalık and Ulas Caydas (2007). "Electrical Discharge Machining of Titanium Alloy (Ti–6Al–4V)." Applied Surface Science, 253, 9007-9016.
77. J. Strasky, M. Janecek, P. Harcuba (2011). "Electric Discharge Machining of Ti-6Al-4V Alloy for Biomedical Use." WDS'11 Proceedings of Contributed Papers, Part 3, 127-131.
78. Lin Gu, Lei Li, Wansheng Zhao, K.P. Rajurkar (2012). "Electrical Discharge Machining of Ti6Al4V with a Bundled Electrode." International Journal of Machine Tools & Manufacture, 53, 100-106.

79. Mohammed Baba Ndaliman, Ahsan Ali Khan, Ruth Anayimi Lafia-Araga (2017). "Electro-Discharge Machining of Ti-6AI-4V Alloy Using Cu-TaC Compact Electrode with Urea Dielectric: Reactions and Their Effects on the Machined Surface." 8th International Conference on Mechanical and Intelligent Manufacturing Technologies (ICMIMT), 32-37.
80. Dignesh Thesiya, Avadhoot Rajurkar, Sagar Patel. "Heat-Affected Zone and Recast Layer of Ti-6Al-4V Alloy in the EDM Process through Scanning Electron Microscopy (SEM)." Journal of Manufacturing Technology Research, 6(1-2), 41-47.
81. Yan Cherng Lin, Biing Hwa Yan, Yong Song Chang. "Machining Characteristics of Titanium Alloy (Ti-6Al-4V) Using a Combination Process of EDM with USM." Journal of Materials Processing Technology, 104, 171-177.
82. M. R. Shabgard & H. Alenabi (2014). "Ultrasonic Assisted Electrical Discharge Machining of Ti-6Al-4V Alloy." Materials and Manufacturing Processes.
83. Sunil Gaikwad, S.N. Teli, L.M. Gaikwad (2014). "Optimization of EDM Parameters on Machining Ti-6Al-4V with a Core Electrode Using Grey Relational Analysis." International Journal of Research in Aeronautical and Mechanical Engineering, 2, 24-31.
84. M. Ghoreishi, J. Atkinson. "A Comparative Experimental Study of Machining Characteristics in Vibratory." Journal of Materials Processing Technology, 120, 374–384 (2002).
85. Gunawan Setia Prihandana, M. Hamdi, Y.S. Wong, Kimiyuki Mitsui. "Effect of Vibrated Electrode in Electrical Discharge Machining." Proceedings of the First International Conference and Seventh AUN/SEED-Net Fieldwise Seminar on Manufacturing and Material Processing, 133–138 (2006).
86. M. Yoshida, M. Kunieda. "Study on Mechanism for Minute Tool Electrode Wear in Dry EDM." Seimitsu Kogaku Kaishi/Journal of the Japan Society for Precision Engineering, 65, 689–693 (1999).
87. Q.H. Zhang, R. Du, J.H. Zhang, Q. Zhang. "An Investigation of Ultrasonic-Assisted Electrical Discharge Machining in Gas." International Journal of Machine Tools & Manufacture.

88. Jeswani, M. L. (1981). "Electrical Discharge Machining in Distilled Water." Journal of Wear, 72, 81–88.
89. Erden, A., & Temel, D. (1981). "Investigation on the Use of Water as a Dielectric Liquid in Electric Discharge Machining." Proceedings of the 22nd Machine Tool Design and Research Conference, 437–440.
90. S. Tariq Jilani, P.C. Pandey. "Experimental Investigations into the Performance of Water as Dielectric in EDM." International Journal of Machine Tool Design and Research, 24, 31–43.
91. Koenig, W., & Joerres, L. (1987). "An Aqueous Solution." CIRP Annals—Manufacturing Technology, 36, 105–109.
92. Koenig, W., & Siebers, F. J. (1993). "Influence of the Working Medium on the Removal Process in EDM Sinking." ASME PED, 64, 649–656.
93. Koenig, W., Klocke, F., & Sparrer, M. (1995). "EDM-Sinking Using Water-Based Dielectrics and Electropolishing—A New Manufacturing Sequence in Tool-Making." In Proceedings of the 11th International Symposium on Electro Machining (ISEM XI) (pp. 225–234).
94. Masuzawa, T. (1981). "Machining Characteristics of EDM Using Water as Dielectric Fluid." In Proceedings of the 22nd Machine Tool Design and Research Conference (pp. 441–447). Manchester.
95. Masuzawa, T., Tanaka, K., & Nakamura, Y. (1983). "Water-Based Dielectric Solution for EDM." CIRP Annals – Manufacturing Technology, 32, 119–122. http://dx.doi.org/10.1016/S0007-8506(07)63374-5
96. Zhang, Y., Liu, Y., Shen, Y., Ji, R., Wang, X., & Li, Z. (2013). "Diesinking Electrical Discharge Machining with Oxygen-Mixed Water-in-Oil Emulsion Working Fluid." Proceedings of the Institution of Mechanical Engineers, Part B: Journal of Engineering Manufacture, 227, 109–118.
97. Liu, Y., Zhang, Y., Ji, R., Cai, B., Wang, F., Tian, X., & Dong, X. (2013). "Experimental Characterization of Sinking Electrical Discharge Machining Using Water-in-Oil Emulsion as Dielectric." Materials and Manufacturing Processes, 28, 355–363. http://dx.doi.org/10.1080/10426914.2012.700162.

98. Tsunekawa, Y., Okumiya, M., Mohri, N., Takahashi, I. (1994). "Surface Modification of Aluminum by Electrical Discharge Alloying." Materials Science and Engineering A, 174, 193–198.
99. J.P. Kruth, L. Stevens, L. Froyen, B. Lauwers. "Study of the White Layer of a Surface Machined by Die-Sinking Electro-Discharge Machining." CIRP Annals—Manufacturing Technology, 44, 169–172 (1995).
100. S.L. Chen, B.H. Yan, F.Y. Huang. "Influence of Kerosene and Distilled Water as Dielectric on the Electric Discharge Machining Characteristics of Ti-6Al-4V." Journal of Materials Processing Technology, 87, 107–111 (1999).
101. B. Ekmekci, O. Elkoca. "A Comparative Study on the Surface Integrity of Plastic Mold Steel Due to Electric Discharge Machining." Metallurgical and Materials Transactions B: Process Metallurgy and Materials Processing Science, 36, 117–124 (2005).
102. A. Sharma, M. Iwai, K. Suzuki, T. Uematsu. "Potential of Electrically Conductive Chemical Vapor Deposited Diamond as an Electrode for Micro-Electrical Discharge Machining in Oil and Water." New Diamond and Frontier Carbon Technology, 15, 181–194 (2005).
103. Leao, F.N., Pashby, I.R. (2004). "A Review on the Use of Environmentally Friendly Dielectric Fluids in Electrical Discharge Machining." Journal of Materials Processing Technology, 149, 341–346.
104. A. Erden and S. Bilgin. "Proceedings of 21st International Machine Tool Design and Research Conference." MacMillan, London, p. 345, 1980.
105. M.L. Jeswani. "Effects of the Addition of Graphite Powder to Kerosene Used as the Dielectric Fluid in Electrical Discharge Machining." Wear, 70, 133–139, 1981.
106. H. Narumiya, ―EDM by Powder Suspended Working Fluid,‖ in: Proceedings of the 9th ISEM, pp. 5–8, 1989.
107. Mohri, N.; Saito, N.; and Higash, M. (1991). ―A New Process of Finish Machining on Free Surface by EDM Methods.‖ Annals of the CIRP, Vol. 40, No. 1, pp. 207-210.

108. Kobayashi, K.; Magara, T.; Ozaki, Y.; and Yatomi, T. (1992). ―The Present and Future Developments of Electrical Discharge Machining.‖ Proceedings of the 2nd International Conference on Die and Mould Technology, Singapore, pp. 35-47.
109. Singh, S., Yeh, M. F. (2012). "Optimization of Abrasive Powder Mixed EDM of Aluminum Matrix Composites with Multiple Responses Using Gray Relational Analysis." Journal of Materials Engineering and Performance, Vol. 21, No. 4, pp. 481–491.
110. Kumar, S., Singh, R. (2010). "Investigating Surface Properties of OHNS Die Steel after Electrical Discharge Machining with Manganese Powder Mixed in the Dielectric." International Journal of Advanced Manufacturing Technology, Vol. 50, No. 5-8, pp. 625–633.
111. Y. Uno, A. Okada, and S. Cetin (2001). "Formation of Hard Layer by EDM with Carbon Powder Mixed Fluid Using Titanium Electrode." In Proceedings of the International Conference on Progress of Machining Technology, pp. 464–469.
112. Pecas, P., Henriques, E. (2003). "Influence of Silicon Powder-Mixed Dielectric on Conventional Electrical Discharge Machining." International Journal of Machine Tool Manufacture, Vol. 43, No. 14, pp. 1465–1471.
113. Y.F. Tzeng, C.Y. Lee (2001). "Effects of Powder Characteristics on Electro-Discharge Machining Efficiency." International Journal of Advanced Manufacturing Technology, Vol. 17, pp. 586–592.
114. Wong, Y.S., Lim, L.C., Rahuman, I. (1998). "Near-Mirror-Finish Phenomenon in EDM Using Powder-Mixed Dielectric." Journal of Materials Processing Technology, Vol. 79, No. 1-3, pp. 30–40.
115. Ming, Q.Y., He, L.Y. (1995). "Powder-Suspension Dielectric Fluid for EDM." Journal of Materials Processing Technology, Vol. 52, pp. 44–54.
116. Cogun, C., Ozerkan, B., Karacay, T. (2006). "An Experimental Investigation on the Effect of Powder Mixed Dielectric on Machining Performance in Electric Discharge Machining." Proceedings of the Institution of Mechanical Engineers, Part B: Journal of Engineering Manufacture, Vol. 220, No. 7, pp. 1035–1050.

117. Okada, A., Uno, Y., Hirao, K. (2000). "Formation of Hard Layer by EDM with Carbon Powder Mixed Fluid Using Titanium Electrode." In Proceedings of the International Conference on Progress of Machining Technology, pp. 464–469.
118. Chow, Han-Ming, Yang, Lieh-Dai, Lin, Ching-Tien, Chen, Yuan-Feng (2008). "The Use of SiC Powder in Water as Dielectric for Micro-Slit EDM Machining." Journal of Materials Processing Technology, Vol. 195, pp. 160–170.
119. Furutani, K., Saneto, A., Takezawa, H., Mohri, N., Miyake, H. (2001). "Accretion of Titanium Carbide by Electrical Discharge Machining with Powder Suspended in Working Fluid." Precision Engineering, Vol. 25, pp. 138–144.
120. Yan, B.H., Lin, Y.C., Huang, F.Y., Wang, C.H. (2001). "Surface Modification of SKD 61 during EDM with Metal Powder Mixed in the Dielectric." Materials Transactions, Vol. 42, No. 12, pp. 2597-2604.
121. Kozak, J., Rozenek, M., Dabrowski, L. (2003). "Study of Electrical Discharge Machining Using Powder-Suspended Working Media." Proceedings of the Institution of Mechanical Engineers, Part B: Journal of Engineering Manufacture, Vol. 217, No. 11, pp. 1597-1602.
122. F. Klocke, D. Lung, G. Antonoglou, D. Thomaidis (2004). "The Effects of Powder Suspended Dielectrics on the Thermal Influenced Zone by Electrodischarge Machining with Small Discharge Energies." Journal of Materials Processing Technology, Vol. 149, No. 1-3, pp. 191-197.
123. Yan, B.H., Tsa, H.C., Huang, F.Y. (2005). "The Effect in EDM of a Dielectric of a Urea Solution in Water on Modifying the Surface of Titanium." International Journal of Machine Tools & Manufacture, Vol. 45, No. 1, pp. 194–200.
124. Wu, K.L., Yan, B.H., Huang, F.Y., Chen, S.C. (2005). "Improvement of Surface Finish on SKD Steel Using Electro-Discharge Machining with Aluminum and Surfactant Added Dielectric." International Journal of Machine Tools & Manufacture, Vol. 45, pp. 1195–1201.
125. Anil Kumar, Sachin Maheshwari, Chitra Sharma & Naveen Beri (2010). "Effect of Aluminum Powder Characteristics in Additive Electric Discharge Machining of Nickel-Based Super Alloy Inconel." Journal of Material and Manufacturing Processes, Vol. 25, pp. 1166-1180.

126. Gurule N. B., Nandurkar K. N (2012). "Effect of Tool Rotation on Material Removal Rate during Powder Mixed Electric Discharge Machining of Die Steel." International Journal of Emerging Technology and Advanced Engineering, Vol. 2, Issue 8, pp. 328-332, August 2012.
127. Khalid Hussain Syed, Kuppan Palaniyandi (2012). "Performance of Electrical Discharge Machining Using Aluminum Powder Suspended Distilled Water." Turkish Journal of Engineering and Environmental Sciences, pp. 1-13.
128. Kuang-Yuan Kung, Jenn-Tsong Horng, Ko-Ta Chiang (2009). "Material Removal Rate and Electrode Wear Ratio Study on the Powder Mixed Electrical Discharge Machining of Cobalt-Bonded Tungsten Carbide." International Journal of Advanced Manufacturing Technology, pp. 95-104.
129. Paramjit Singh, Anil Kumar, Naveen Beri, Vijay Kumar (2010). "Some Experimental Investigation on Aluminum Powder Mixed EDM on Machining Performance of Hastelloy Steel." International Journal of Advanced Engineering Technology (IJAET), Vol. 1, Issue 2, pp. 28-45, July-Sept., 2010.
130. Shitij Sood (2008). "Effect of Powder Mixed Dielectric on Material Removal Rate, Tool Wear Rate, and Surface Properties in Electric Discharge Machining."
131. Gurtej Singh, Paramjit Singh, Gaurav Tejpal & Baljinder Singh (2012). "Effect of Machining Parameters on Surface Roughness of H13 Steel in EDM Process Using Powder Mixed Fluid." International Journal of Advanced Engineering Research and Studies, Vol. 2, No. 1, pp. 148-150.
132. Mathapathi U., Jeevraj S., Kumar S., Ramola I.C. (2013). "Analysis of Material Removal Rate with Powder Mixed Dielectric." International Journal of Computer Applications in Engineering, Vol. 4, No. 3, pp. 316-332.
133. Kumar A., Maheshwari S., Sharma C., Beri N. (2011). "Analysis of Machining Characteristics in Additive Mixed Electrical Discharge Machining of Nickel-Based Super Alloy Inconel 718." Materials and Manufacturing Processes, Vol. 26, pp. 1011–1018.
134. Bhattacharya A., Batish A., Singh G., Singla V.K. (2012). "Optimal Parameter Settings for Rough and Finish Machining of Die Steels in Powder-Mixed EDM."

International Journal of Advanced Manufacturing Technology, Vol. 61, pp. 537–548.

135. Tan P.C., Yeo S.H. (2013). "Simulation of Surface Integrity for Nano Powder-Mixed Dielectric in Micro Electrical Discharge Machining." The Minerals, Metallurgical and Materials Transactions B. DOI: 10.1007/s11663-013-9819-7.
136. Goyal S. & Singh R. K. (2014). "Parametric Study of Powder Mixed EDM and Optimization of MRR & Surface Roughness." International Journal of Scientific Engineering and Technology, Vol. 3, No. 1, pp. 56-62.
137. G. Kucukturk, C. Cogun (2010). "A New Method for Machining of Electrically Nonconductive Workpieces Using Electric Discharge Machining Technique." Machining Science and Technology, Vol. 14, pp. 189–207.
138. M.P. Jahan, M. Rahman, Y.S. Wong (2011). "Study on the Nano-Powder-Mixed Sinking and Milling Micro-EDM of WC-Co." International Journal of Advanced Manufacturing Technology, Vol. 53, pp. 167–180.
139. S.L. Chen, M.H. Lin, G.X. Huang, C.C. Wang (2014). "Research of the Recast Layer on Implant Surface Modified by Micro-Current Electrical Discharge Machining Using Deionized Water Mixed with Titanium Powder as Dielectric Solvent." Applied Surface Science, Vol. 311, pp. 47–53.
140. Y.Y. Tsai, C.K. Chang (2010). "Effects of Polymer Particles Suspending in Dielectric Fluid on Surface Roughness of EDM." Advanced Materials Research, Vols. 97-101, pp. 4146–4149.
141. Jabbaripour, Behzad & Sadeghi, Mohammad & Shabgard, Mohammad & Faraji, Hossein (2013). "Investigating Surface Roughness, Material Removal Rate and Corrosion Resistance in PMEDM of γ-TiAl Intermetallic." Journal of Manufacturing Processes, Vol. 15, pp. 56–68. DOI: 10.1016/j.jmapro.2012.09.016.
142. Ojha, Kuldeep, R. K. Garg, and K. K. Singh (2012). "An Investigation into the Effect of Nickel Micro Powder Suspended Dielectric and Varying Triangular Shape Electrodes on EDM Performance Measures of EN-19 Steel." International Journal of Mechatronics and Manufacturing Systems, Vol. 5, No. 1, pp. 66-92.

143. M. Kolli, A. Kumar (2014). "Effect of Boron Carbide Powder Mixed in Dielectric Liquid on Titanium Compound Electrical Release Machining." Procedia Materials Science, Vol. 5, pp. 1957–1965.
144. Shabgard, Mohammadreza, and Behnam Khosrozadeh (2017). "Investigation of Carbon Nanotube Added Dielectric on the Surface Characteristics and Machining Performance of Ti–6Al–4V Alloy in EDM Process." Journal of Manufacturing Processes, Vol. 25, pp. 212-219.
145. S. Ramesh, M.P. Jenarthanan, A.S. Bhuvanesh Kanna (2017). "Powder-Blended Electrical Release Machining of AISI P20 Steel Using Multiple Powders and Apparatus Components." DOI: 10.1108/MMS-04-2017-0025.
146. A. Sugunakar, A. Kumar, R. Markandeya (2017). "Effect of Powder Mixed Dielectric Liquid on Surface Integrity by Electrical Discharge Machining RENE 80." Materials Today: Proceedings, Vol. 5, pp. 43-50. p-ISSN: 2320-334X.
147. Santosh Kumar Sahu, Saurav Datta (2018). "Experimental Investigations into Inconel 718 Supercompounds Graphite Powder-Blended Electro-Release Machining." DOI: 10.1177/0954408918787104.
148. Amit Kumar, Amitava Mandal, Amit Rai Dixit, Alok Kumar (2018). "The Performance Evaluation of Al2O3 Nano Powder Mixed Dielectric for Electric Discharge Machining of Inconel 825." DOI: 10.1080/10426914.2017.1376081.
149. Divia Rana, Ajay Kr. Buddy, Pooja Tiwari (2015). "Study of Powder Mixed Dielectric in EDM – A Review." International Journal of Engineering Science and Advanced Research, Vol. 1, No. 2, pp. 69–74.
150. Sravankumar Gudur, V. Potdar (2015). "Effect of Silicon Carbide Powder Mixed EDM Machining Characteristics of SS 316L Material – Experimentation." DOI: 10.15680/IJIRSET.2015.0409017.
151. B. Kuriachen & J. Mathew (2015). "Effect of Powder Mixed Dielectric on Material Removal and Surface Modification in Micro Electric Discharge Machining of Ti-6Al-4V." Materials and Manufacturing Processes. DOI: 10.1080/10426914.2015.1004705.
152. Harmesh Kumar (2015). "Development of Mirror-Like Surface Characteristics Using Nano Powder Mixed Electric Discharge Machining (NPMEDM)."

International Journal of Advanced Manufacturing Technology. DOI: 10.1007/s00170-014-5965-6.

153. Zakaria Mohd Zain, Mohammed Baba Ndaliman, Ahsan Ali Khan, and Mohammad Yeakub Ali (2014). "Improving Micro-Hardness of Stainless Steel through Powder-Mixed Electrical Discharge Machining." DOI: 10.1177/0954406214530872.
154. Paul, B.K., Sahu, S.K., Jadam, T., Datta, S., Dhupal, D., Mahapatra, S.S. (2018). "Effects of Addition of Copper Powder in the Dielectric Media (EDM Oil) on Electro-Discharge Machining Performance of Inconel 718 Super Alloys." Materials Today: Proceedings, Vol. 5, pp. 17618–17626.
155. Patel, S.; Thesiya, D.; Rajurkar, A. (2018). "Aluminium Powder Mixed Rotary Electric Discharge Machining (PMEDM) on Inconel 718." Australian Journal of Mechanical Engineering, Vol. 16, pp. 21–30.
156. Khan, A.A.; Mohiuddin, A.K.M.; Latif, M.A.A. (2018). "Improvement of MRR and Surface Roughness during Electrical Discharge Machining (EDM) using Aluminum Oxide Powder Mixed Dielectric Fluid." IOP Conference Series: Materials Science and Engineering, Vol. 290, p. 012063.
157. Kansal, H.K.; Singh, S.; Kumar, P. (2008). "Numerical Simulation of Powder Mixed Electric Discharge Machining (PMEDM) using Finite Element Method." Mathematics and Computers in Simulation, Vol. 47, pp. 1217–1237.
158. Sethuramalingam, P.; Vinayagam, B.K. (2015). "Adaptive Neuro Fuzzy Inference System Modelling of Multi-Objective Optimization of Electrical Discharge Machining Process using Single-Wall Carbon Nanotubes." Australian Journal of Mechanical Engineering, Vol. 13, pp. 97–117.
159. Cogun, C.; Savsar, M. (1990). "Statistical Modelling of Properties of Discharge Pulses in Electric Discharge Machining." International Journal of Machine Tools and Manufacture, Vol. 30, pp. 467–474.
160. Salah, N.B.; Ghanem, F.; Atig, K.B. (2006). "Numerical Study of Thermal Aspects of Electric Discharge Machining Process." International Journal of Machine Tools and Manufacture, Vol. 46, pp. 908–911.

161. B. Bhattacharyya, S. Gangopadhyay, B.R. Sarkar (2007). "Modelling and Analysis of EDMed Job Surface Integrity." Journal of Materials Processing Technology, Vol. 189, pp. 169–177.

162. M.P. Jahan, M. Rahman, Y.S. Wong (2010). "Modelling and Experimental Investigation on the Effect of Nanopowder-Mixed Dielectric in Micro-Electrodischarge Machining of Tungsten Carbide." Proceedings of the Institution of Mechanical Engineers, Part B: Journal of Engineering Manufacture, Vol. 224, pp. 1725–1739.

163. S. Prabhu, M. Uma, B.K. Vinayagam (2013). "Adaptive Neuro-Fuzzy Inference System Modelling of Carbon Nanotube-Based Electrical Discharge Machining Process." Journal of the Brazilian Society of Mechanical Sciences and Engineering, Vol. 35, pp. 505–516.

164. M.K. Pradhan (2010). "Experimental Investigation and Modelling of Surface Integrity, Accuracy, and Productivity Aspects in EDM of AISI D2 Steel."

165. V. Vikram Reddy, P. Madar valli (2014). "Mathematical Modeling of Process Parameters on Material Removal Rate in EDM of EN31 Steel Using RSM Approach." International Journal of Research and Innovations in Science and Technology, Vol. 1, Issue 1.

166. A. Behrens, J. Ginzel (2003). "Neuro-Fuzzy Process Control System for Sinking EDM." Journal of Manufacturing Processes, Vol. 5, pp. 33–39.

167. M.S. Popa, G. Contiu, G. Pop, P. Dan (2009). "New Technologies and Applications of EDM Process." The International Journal of Material Forming, Vol. 2, pp. 633–636.

168. C. Fenggou, Y. Dayong (2004). "The Study of High Efficiency and Intelligent Optimization System in EDM Sinking Process." Journal of Materials Processing Technology, Vol. 149, pp. 83–87.

169. U. Caydas, A. Hascalik (2008). "Modeling and Analysis of Electrode Wear and White Layer Thickness in Die-Sinking EDM Process through Response Surface Methodology." International Journal of Advanced Manufacturing Technology, Vol. 38, pp. 1148–1156.

170. S. Parsana, N. Radadia, M. Sheth, N. Sheth, V. Savsani, N.E. Prasad, T. Ramprabhu (2018). "Machining Parameter Optimization for EDM Machining of Mg-RE-Zn-Zr Alloy using Multi-Objective Passing Vehicle Search Algorithm." Archives of Civil and Mechanical Engineering, Vol. 18, pp. 799–817.
171. C. Prakash, S. Singh, M. Singh, K. Verma, B. Chaudhary, S. Singh (2018). "Multi-Objective Particle Swarm Optimization of EDM Parameters to Deposit HA- Coating on Biodegradable Mg-Alloy." Vacuum, Vol. 158, pp. 180–190.
172. G. Ramanan, J.E.R. Dhas (2018). "Multi-Objective Optimization of Wire EDM Machining Parameters for AA7075-PAC Composite using Grey-Fuzzy Technique." Materials Today, Vol. 5, pp. 8280–8289.
173. K.R. Aharwal, C.M. Krishna (2018). "Optimization of Material Removal Rate and Surface Roughness in EDM Machining of Metal Matrix Composite using Genetic Algorithm." Materials Today, Vol. 5, pp. 5391–5397.
174. Sengottuvel.Pa, Satishkumar.Sb, Dinakaran.Dc (2013). "Optimization of Multiple Characteristics of EDM Parameters Based on Desirability Approach and Fuzzy Modeling." Procedia Engineering, Vol. 64, pp. 1069–1078.
175. Shailesh Dewangan, Soumya Gangopadhyay, Chandan Kumar Biswas (2015). "Multi-Response Optimization of Surface Integrity Characteristics of EDM Process using Grey-Fuzzy Logic-Based Hybrid Approach." Engineering Science and Technology, an International Journal, Vol. 18, pp. 1-8.
176. S. Tripathy, D.K. Tripathy (2015). "Multi-Attribute Optimization of Machining Process Parameters in Powder Mixed Electro-Discharge Machining using TOPSIS and Grey Relational Analysis." Engineering Science and Technology, an International Journal.
177. M Manohara, T Selvarajb , D Sivakumara (2014). "Experimental Study to Assess the Effect of Electrode Bottom Profiles while Machining Inconel 718 through EDM Process." 3rd International Conference on Materials Processing and Characterization (ICMPC 2014), Procedia Materials Science, Vol. 6, pp. 92–104.
178. N.Y. Tantra, F. Leao, I.R. Pashby (2006). "Evaluating Theoretical Equations to Predict Wear in Electro-Discharge Machining." Proceedings of the First

International Conference and Seventh AUN/SEED-Net Fieldwise Seminar on Manufacturing and Material Processing.

179. Huu, Phan Nguyen (2020). "Multi-Objective Optimization in Titanium Powder Mixed Electrical Discharge Machining Process Parameters for Die Steels."
180. Niamat, Misbah (2020). "Parametric Modeling and Multi-Objective Optimization of Electro Discharge Machining Process Parameters for Sustainable Production." Energies, Vol. 13, Issue 1, p. 38.
181. D.C. Montgomery (2001). "Design and Analysis of Experiments." Wiley, New York.
182. G. Cochran, G.M. Cox, "Experimental Design," Asia Publishing House, New Delhi, 1962.
183. M.K. Pradhan, "Experimental Investigation and Modeling of Surface Integrity, Accuracy, and Productivity Aspects in EDM of AISI D2 Steel," 2010.
184. M.K. Pradhan, "Determination of Optimal Parameters with Multi-Response Characteristics of EDM by Response Surface Methodology, Grey Relational Analysis, and Principal Component Analysis," International Journal of Manufacturing Technology and Management, Vol. 26, 2012, pp. 56–80.
185. J. Xu, G.P. Sheng, H.W. Luo, F. Fang, W.W. Li, R.J. Zeng, et al., "Evaluating the Influence of Process Parameters on Soluble Microbial Products Formation using Response Surface Methodology Coupled with Grey Relational Analysis," Water Research, Vol. 45, 2011, pp. 674–680.
186. Sampath Kumar, T. S., "Chapter 2 - Physical and Chemical Characterization of Biomaterials," in "Characterization of Biomaterials," 2013, pp. 11-47.
187. Zhou, W., and Wang, Z.L., "Scanning Microscopy for Nanotechnology," Springer, USA, 2007.
188. Rajani Vijayaraghavan, K., "Ph.D. Thesis," School of Electronic Engineering, Dublin City University, 2011.
189. Rama Rao. S, Padmanabhan. G, "Application Of Taguchi Methods And ANOVA In Optimization Of Process Parameters For Metal Removal Rate In Electrochemical Machining Of Al/5%Sic Composites," International Journal of

Engineering Research and Applications (IJERA), Vol. 2, Issue 3, May-Jun 2012, pp. 192-197.

190. Fisher, R.A., "Statistical Methods for Research Worker," London: Oliver and Boyd, 1925.
191. Julong, Deng, "Introduction to Grey System Theory," The Journal of Grey System, Vol. 1, No. 1, 1989, pp. 1-24.
192. S. Tripathy & D. K. Tripathy, "Multi-Response Optimization of Machining Process Parameters for Powder Mixed Electro-Discharge Machining of H-11 Die Steel using Grey Relational Analysis and TOPSIS," Machining Science and Technology, Volume 21, Issue 3, 2017, pp. 362-384.
193. G. Rajyalakshmi, Dr. P. Venkata Ramaiah, "Simulation, Modeling and Optimization of Process Parameters of Wire EDM using Taguchi –Grey Relational Analysis" in 2012 IJAIR.
194. S. Datta, A. Bandyopadhyay, P.K. Pal, "Solving Multi-Criteria Optimization Problem in Submerged Arc Welding Consuming a Mixture of Fresh Flux and Fused Slag," International Journal of Advanced Manufacturing Technology, Vol. 35, 2008, pp. 935–942.
195. Singh, S.; Yeh, M.F., "Optimization of Abrasive Powder Mixed EDM of Aluminum Matrix Composites with Multiple Responses using Gray Relational Analysis," Journal of Materials Engineering and Performance, 2012, Vol. 21, Issue 4, pp. 481–491.
196. Huang, J.T. and Liao, Y.S., "Optimization of Machining Parameters of Wire EDM based on Grey Relational and Statistical Analyses," International Journal of Production Research, 2003, Vol. 41, Issue 8, pp. 1707–1720.

THANKS